Relay Technology in Cellular Networks

Von der Fakultät für Ingenieurwissenschaften
Abteilung Elektrotechnik und Informationstechnik
der Universität Duisburg-Essen

zur Erlangung des akademischen Grades

Doktor der Ingenieurwissenschaften

genehmigte Dissertation

von

Tao Tao
aus
Jiangsu, China

1. Gutachter: Prof. Dr.-Ing. Andreas Czylwik
2. Gutachter: Prof. Dr.-Ing. habil. Volker Kühn
Tag der mündlichen Prüfung: 10.09.2014

Abstract

Relay technology has been explored and studied for decades, ranging from generic multi-hop mobile ad hoc networks to most recent collaborative multiple-input multiple-output (MIMO) cellular networks. Deploying low cost relays reduces the infrastructure cost of establishing new base stations in order to improve the cell coverage and system capacity of next generation cellular networks. For efficient heterogeneous network planning, fixed relays are considered as one of the main enhancing technologies in 3rd Generation Partnership Project (3GPP) Long Term Evolution Advanced (LTE-A).

The function of the relay station can be described simply as a device which assists in transmissions between the local base station and the mobile station. Since the performance of relay transmissions is strongly affected by the collaborative strategy in dense wireless networks, the relay selection always attracts research attentions. In this thesis, the symbol error probability of the selective decode-and-forward (DF) relaying strategy is derived to explore the selection diversity. Furthermore, an effective joint beamforming vector design and relay selection scheme for a MIMO relay system are proposed.

In addition, two main relay deployment scenarios are addressed in this thesis: the fixed relay and the mobile relay.

The LTE relay is a fixed relay which is located near the cell edge. A dynamic system level simulator is developed to evaluate the downlink transmission performance of fixed relay-enhanced LTE-A systems. With deployment of a high number of relay nodes inter-cell interference and resource management problems increase. An adaptive beamforming strategy with limited feedback is proposed to reduce inter-cell interference. The proposed algorithm has been applied in relay-enhanced LTE-A cellular networks to show its advantage. Furthermore, we study the concept of shared relays, in which a relay station is deployed at the intersection of neighboring macro cells. An efficient resource allocation and scheduling scheme based on the sub-frame structure of LTE-A is proposed to maximize the benefit of shared relays.

As the penetration rate of mobile phones, especially smart phones keeps increasing, users in public transportation expect high speed wireless services. Recently, the mobile relay for high speed railways has gained significant interest. A system level simulator is developed to investigate the capacity and handover performance of the mobile relay in a high speed railway scenario. Furthermore, a coordinated mobile relay node (MRN) strategy is proposed to combat co-channel interference and handover delay problems in a conventional mobile relay system.

Acknowledgments

I would like to express my gratitude to all those who helped me during my study in Germany.

My sincere gratitude goes first and foremost to my supervisor Prof. Dr.-Ing. Andreas Czylwik, for his patience, motivation, enthusiasm, and immense knowledge. He offered me the opportunity to start this interesting topic, and gave me great help during my research and writing of this thesis. I am extremely grateful for his support in the accomplishment of my study in Germany. I could not have imagined having a better advisor and mentor for my Ph.D study.

Besides my supervisor, I would like to thank the rest of my thesis committee: Prof. Dr. V. Kühn, Prof. Dr. I Erlich, Prof. Dr. M. Kraft, and PD Dr. A. Stöhr, for their encouragement, insightful comments, and hard questions.

I am also deeply indebted to all my colleagues and student assistants in the chair of Communication Systems, University of Duisburg-Essen. Special thanks should go to M.Sc B. Zhao, Dr. M. Simsek, and M.Sc. N. Obaid for stimulating discussions about our simulator, and for the sleepless nights we were working together.

Last but not the least, my gratitude also extends to my family who has been assisting, supporting and caring for me throughout my life.

Contents

Notation

The used mathematical symbols, abbreviations and operations are listed here. These symbols and abbreviations are sorted in alphabetical order.

Symbols		Page
α	the pathloss exponent	74
$B_{i,i}$	the number of feedback bits for quantizing $\mathbf{h}_{i,i}$	70
$\mathbf{f}_i$	the beamforming vector at the i-th base station	68
γ_{eff}	effective SINR	54
$\gamma_{i,n}$	post-processing SINR of the user i on the n-th subcarrier	53
$h_{\text{S,D}}$	the source-destination channel coefficient	7
$h_{\text{S,R}}$	the source-relay channel coefficient	7
$h_{\text{R,D}}$	the relay-destination channel coefficient	7
$\mathbf{h}_{i,j}$	the channel gain from j-th base station to the i-th UE	68
I	instantaneous mutual information	9
L_{LOS}	the LOS path loss	50
L_{NLOS}	the NLOS path loss	50
$\mathcal{N}_0$	variance of complex Gaussian random variables	7
n_{BE}	the average bandwidth efficiency	22
$\eta_{\text{S,D}}$	additive noise on source-destination link	7
$\eta_{\text{S,R}}$	additive noise on source-relay link	7
$\eta_{\text{R,D}}$	additive noise on relay-destination link	7
N_{t}	number of transmit antennas	67
Ω	the decoding set	17

Symbols		Page
P_{S}	the transmitted power at the source	7
P_m	the transmitted power at the macro base station	68
P_r	the transmitted power at the relay station	68
P^{out}	outage probability	9
P_e	average symbol error rate	19
$\gamma_{\mathrm{S,D}}$	the received SNR of the direct link	10
$\gamma_{\mathrm{S,R}}$	the received SNR of the relay back-haul link	11
$\gamma_{\mathrm{R,D}}$	the received SNR of the access link	11
R	the average normalized achievable rate of UE	68
σ	relay amplifier factor	27
$\mathbf{S}_{\mathrm{R}}$	the relay beamforming vector	27
$\mathbf{S}_{\mathrm{S}}$	the source beamforming vector	26
x_i	transmitted information symbol for the i-th UE	68
$\xi_{i,i}$	the degradation factor of the desired signal power due to quantization	70
$y_{\mathrm{S,D}}$	the received signal at the destination from the source	6
$y_{\mathrm{S,R}}$	the received signal at the relay from the source	6
$y_{\mathrm{R,D}}$	the received signal at the destination from the relay	7
$\boldsymbol{Z}$	Chi-squared random variable	70

Abbreviations		Page
3GPP	3rd generation partnership project	2
AF	amplify-and-forward	6
AoA	angle of arrival	49
AoD	angle of departure	49
BLER	block error rate	54
BS	base station	39
CA	carrier aggregation	36
CDI	channel direction information	69
CF	compress-and-forward	6
CoMP	coordinated multipoint processing	36
CQI	channel quality indicator	41
CRS	cell-specific reference signal	41
CSI	channel state information	25
DeNB	donor eNB	39
DF	decode-and-forward	3
DFS	doppler frequency shift	89
E-RAB	LTE radio access bearer	115
EESM	exponential effective SNR mapping	54
eICIC	enhanced inter-cell interference coordination	36
eMBMS	evolved multimedia broadcast and multicast service	35
FDD	frequency division duplex	35
GPS	global positioning system	95
GSM	global system for mobile communications	90
GSM-R	GSM for railway	90
HARQ	hybrid automatic repeat request	55
HeNB	home eNodeB	35
HO	handover	90
ICI	inter-cell interference	78
INR	interference-to-noise ratio	72
ISD	inter-site distance	44
ISR	interference-to-signal ratio	74
LOS	line of sight	41
LTE	long term evolution	35

Abbreviations		Page
LTE-A	long term evolution advanced	2
MAC	medium access control	39
MCS	modulation and coding scheme	59
MIESM	mutual information effective SINR mapping	54
MIMO	multiple-input multiple-output	3
MISO	multiple-input single-output	6
MME	mobility management entity	115
MMSE	minimum mean square error	53
MRC	maximal ratio combining	8
MRN	mobile relay node	91
MRT	maximum ratio transmission	66
MS	mobile station	48
NLOS	non line of sight	42
OCI	other-cell interference	65
OFDM	orthogonal frequency domain multiple	35
OFDMA	orthogonal frequency domain multiple access	35
PDCCH	physical downlink control channel	41
PDSCH	physical downlink shared channel	41
PDF	probability density function	16
P-GW	packet data network gateway	93
PHY	physical layer	39
PWS	public warning system	35
RAU	radio access unit	91
RAN	radio access network	118
RawBER	raw or uncoded bit error rate mapping	54
RCC	relay central controller	98
RLC	radio link control	39
RN	relay node	39
RoF	radio-over-fiber	91
RRP	radio resource control	115
RS	relay station	67
RSRP	reference signal received power	58
RVQ	random vector quantization	67

Abbreviations		Page
SC-FDMA	single-carrier frequency domain multiple access	35
SCM	spatial channel model	49
SINR	signal-to-interference-plus-noise ratio	42
SISO	single-input single-output	53
SLS	System-level simulation	43
SM	spatial multiplexing	53
SNR	signal-to-noise ratio	8
SON	self-organizing network	35
SPCU	symbols per channel use	22
S-DeNB	source DeNB	93
S-DF	selective DF	16
S-GW	serving gateway	93
TDD	time division duplex	35
TTI	transmit time interval	45
T-DeNB	target DeNB	93
UE	user equipment	38
ZF	zero forcing	66

Operations, Functions

$\mathcal{CN}(\mu, \mathbf{C})$	complex Gaussian distribution with mean μ and covariance matrix $\mathbf{C}$
$\Pr[\cdot]$	the probability operator
$\mathrm{Q}(u)$	the Gaussian Q-function
$\delta(x)$	the delta function
$\beta(\cdot)$	the Beta function
$\psi(\cdot)$	the Euler's psi function
$\lceil z \rceil$	ceiling function
$\lfloor z \rfloor$	floor function
$(\mathbf{A})^{\mathbf{T}}$	transpose of matrix $\mathbf{A}$
$(\mathbf{A})^{\mathbf{H}}$	Hermitian transpose of matrix $\mathbf{A}$
$\mathbb{E}\{\boldsymbol{Z}\}$	expectation of random variable $\boldsymbol{Z}$
$\|\|\cdot\|\|^2$	norm function

Chapter 1

Introduction

1.1 Background and motivation

The concept of relaying can be traced back to the work of E. C. van der Meulen in the 1970's [104], which models a three nodes communication scenario consisting of a source, a destination and a relay node. From then on, a large body of research is geared to explore potential gains of relaying by information theory [22][84]. The most groundbreaking work on relaying to date is the work by Cover and El Gamal [32], in which capacity theorems for the relay channel are analyzed. With significant technology advances over the last two decades, more and more researchers are focus on developing practical relay cooperation schemes that attempt to exploit the promised gains predicted by information theory [86][94].

The relay technology is firstly implemented extensively in wireless ad-hoc networks to assist the transmission between neighboring nodes [28][93]. Wu et al. propose an integrated cellular and ad hoc relaying system (iCAR), which is a new wireless system architecture based on the integration of cellular and modern ad hoc relaying technologies [105]. It addresses the congestion problem due to unbalanced traffic in a cellular system and provides interoperability for heterogeneous networks. Based on iCAR, the relay technology attracts more research attention in cellular systems.

Nowadays with a rapid growth in the number of cellular subscribers, the data rate requirement in 2020 is predicted to be 100 to 1000 times as large as the currently served data rate. With the increase in data traffic, operators have to think about a new solution that could improve the data rate in certain areas. However, increasing the number of base stations entails a cost that operators cannot afford. A solution being employed in next generation cellular systems [95] is to deploy low-cost cellular relay stations in each cell to improve coverage in hotspots, communication services in public transportation vehicles and transmission capacity on the cell edge.

The relay technology is introduced in cellular networks to achieve improvement in several aspects:

- **Coverage extension**:

  A user at the cell edge or in a coverage hole may experience poor received signal-to-noise power ratio for the signal received from the base station. With dedicated relay nodes, the user receives stronger signals from the relay nodes. The relay deployment thus is able to provide coverage extension and maintain good communication [19]. The infrastructure cost can be reduced by deploying lower cost relay stations instead of base stations. To extend the communication service coverage, relay nodes are typically deployed near the cell edge. Considering the long distance between the relay node and the base station, the received signal power at the relay node is usually low, which requires an optimized relay backhual link resource allocation strategy.

- **Increase network capacity**:

  To deploy a relay node inside the base station service coverage could obtain higher network capacity while providing coverage enhancement. And relay stations are easy to install as they do not require a wireline backhaul. However, with deployment of a high number of relay nodes, interference scenarios become very complex and difficult to predict. Hence, good interference cancellation and relay selection schemes are desired in relay enhanced cellular networks.

- **Rapid network roll-out**:

  Because of the natural self-backhaul functionality, the relay technology can be used to provide temporary wireless communication services. Self-organizing network mechanisms should support the network roll-out and operation.

- **Mobile relay**:

  Higher throughput and lower handover outage for on-board users can be expected by installing relay nodes on the top of the moving vehicles. However, due to high speed mobility, the delay of the group handover procedure becomes the bottleneck of on-board user performance. New contributions should be proposed to overcome such limitations.

As a hot research topic with great application potential, the relay technology has been considered as one of the key features in the standard of 3rd Generation Partnership Project (3GPP) 4G Long Term Evolution Advanced (LTE-Advanced) [9]. LTE-Advanced extends LTE Release 8 with support for relaying as an efficient way to improve e.g. the coverage for high data rates, group mobility, temporary network deployment, the cell-edge throughput and/or to provide coverage in new areas [12].

1.2 Contribution and outline

In this thesis, we aim to evaluate and enhance the performance of the existing cellular networks assisted by the relay technology. The thesis is organized as follows.

Chapter 2 starts with a brief overview of cooperative communications. Then the outage performance of different cooperative strategies is analyzed in a single relay scenario. In the multiple-relay network, the performance of relay transmissions is greatly affected by the collaborative strategy, which includes the selection of relay types and relay partners (i.e., to decide when, how, and with whom to collaborate). We have two main contributions on this topic:

- We propose a selective decode-and-forward (DF) relaying strategy and derive an exact closed-form expression for the symbol error probability of the given strategy. Numerical results show the significant advantages of the relay selection in a cooperative communication system and can be considered as a performance lower bound for the future research.

- We propose an effective joint beamforming vector design and relay selection scheme for a multiple input multiple output (MIMO) relay system. Most of existing literature assumes that the channel state information is available at all nodes. We employ a new channel quantization strategy to jointly design beamforming vectors and perform relay selection with limited feedback. The results of this part are published in

  T. Tao and A. Czylwik, "**Beamforming Design and Relay Selection for Multiple MIMO AF Relay Systems with Limited Feedback**", IEEE 77th Vehicular Technology Conference 2013 Spring (VTC2013Spring), Dresden, Germany, June. 2013.

With proposals for optimizing relay technology at the link level, **Chapter 3** will focus on the system level aspect for relay technology in cellular systems. In Chapter 3, baseline assumptions for relay technology in LTE-A are introduced. We develop a dynamic system level simulator to evaluate the downlink transmission performance of relay-enhanced LTE-A systems. An efficient architecture for relay-assisted cellular networks is designed based on the results of a system level simulation. Simulation results will illustrate the relay deployment can further improve the quality and coverage of original cellular networks.

With deployment of a high number of relay nodes inter-cell interference and resource management problems increase. **Chapter 4** gives our proposals for interference management in relay-enhanced LTE-A cellular networks. Two potential solutions are proposed

to mitigate inter-cell interference in relay-enhanced cellular systems: one is beamforming design for cooperative communication and the other is the deployment of shared relays.

- An adaptive beamforming strategy with limited feedback is proposed to suppress other cell interference problem in a two-cell scenario. The algorithm is subsequently extended to general multi-cell networks. The throughput performance is evaluated by our dynamic system level simulator. Some of given results are published in

  Tao Tao, Bo Zhao, Andreas Czylwik, "**Beamforming design for a cooperative relay system with limited feedback**", IEEE 24th International Symposium on Personal, Indoor and Mobile Radio Communications: Mobile and Wireless Networks, London, UK, Sep. 2013.

- An efficient and effective resource allocation and scheduling scheme based on the sub-frame structure of LTE-A is proposed to maximize the benefit of shared relays. Corresponding results are published in

  T. Tao and A. Czylwik, "**System Performance of an LTE-A Cellular Network with Shared Relays under Different Resource Demands**", IEEE 79th Vehicular Technology Conference 2014 Spring (VTC2014Spring), Seoul, Korea, May. 2014.

The mobile relay, which is a hot research topic in LTE-A systems, is addressed in **Chapter 5**. The LTE-A fixed relay nodes are used for providing enhanced cell edge coverage and capacity. The mobile relay is proposed to offer high quality services for high speed train passengers (on-board users). We develop a system level simulator to investigate the capacity and handover performance gain of the mobile relay. Furthermore, a coordinated MRN strategy is proposed to combat the co-channel interference and handover delay challenge in the conventional mobile relay system.

In the **last Chapter** of this thesis, a conclusion and outlook are presented.

Chapter 2

Cooperative communication with relays

2.1 Cooperative communication: The overview

Cooperative communication is currently one of the intensive research areas in wireless communication and has recently been included to one of the state-of-the-art features of 3GPP LTE-Advanced (LTE-A). The motivation to explore cooperative communications is to share the power and computation with neighboring nodes which can lead to more stable and higher data rate transmissions in the whole network. In traditional communication networks, the physical layer is only responsible for point-to-point communications. In contrast, cooperative communications, where the channel is not one link but the whole network, fundamentally change the abstraction of the traditional communication. Significant potential advantages can be achieved by the cooperation.

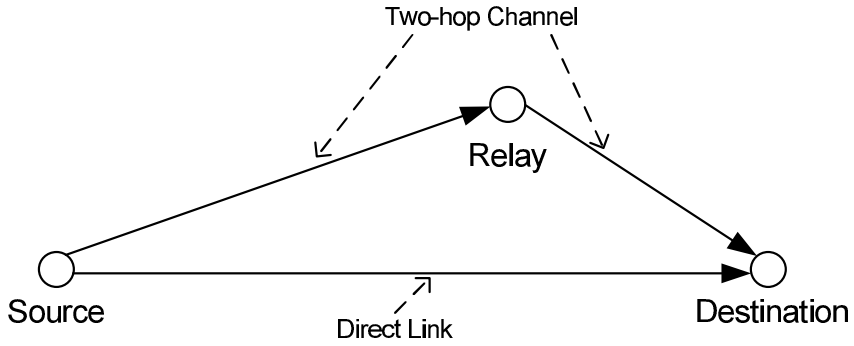

Figure 2.1: A simplified cooperative communication model.

In cooperative communications, an auxiliary path between the source and the destination is generated via the introduction of a relay channel as illustrated in Figure 2.1. The concept of relaying can be traced back to the work of E. C. van der Meulen in the 1970's [104], which models a three nodes communication scenario consisting of a source, a destination and a relay node. After that the capacity bounds discovered by van der Meulen were significantly improved by T. Cover and A.E. Gamal in the year 1979 [32]. Most of the results in this work have still not been superseded. In [37], the authors discovered the capacity of the relay channel in a fixed manner, where the received signal

at the relay is a deterministic function of the source and relay transmissions. In the year 1998, a new form of realizing spatial diversity has been introduced called cooperative diversity by Andrew Sendonaris, Elza Erkip and Behnaam Aazhang [85]. In such network, several nodes serve as relays for one active source-destination pair. This idea can be characterized as a specific application of the traditional relay model.

The relay protocol differs according to signal processing capabilities of the relay. In the amplify-and-forward (AF) relaying protocol, the relay simply scales the signal and transmits an amplified version of it to the destination. Thus, the AF relaying leads to low-complexity function and lower power consumption since the signal processing for decoding is not required, but it suffers from the additional noise amplified by the relay. Another idea involves decoding of the signal from the source at the relay. The relay then re-encodes and re-transmits the decoded signal after possibly compressing or adding redundancy. This strategy is known as the decode-and-forward protocol. The decode-and-forward protocol is close to optimal when the source and relay are physically near each other. Because the relay channel becomes a multiple-input single-output (MISO) system in the such situation. A third relay protocol, which is known as the compress-and-forward (CF) (also known as estimate-and-forward or quantize-and-forward) protocol, is introduced in [32]. In this case, the relay sends a compressed version of the source transmission to the destination. Although the CF relay achieves promising advantage in [57][56], to the best of our knowledge there is no physical implementation that can be found up to now.

2.2 Single relay scenario: When to cooperate

In this section, we only consider a single relay node willing to aid in communication. The multiple relays case will be discussed in a later section.

The communication system of a single relay cooperative scheme is shown in Figure 2.2. It consists of a source S, its destination D, and a relay R. A typical cooperative communication strategy is considered with two mutually orthogonal phases, separated either in time, space or frequency domain, to avoid the self interference between the two phases.

In Phase 1, the source broadcasts its information to its destination, and the information is also received by the relay. The received signals $y_{\mathrm{S,D}}$ and $y_{\mathrm{S,R}}$ at the destination and the relay, respectively, can be written as

$$y_{\mathrm{S,D}} = \sqrt{P_{\mathrm{S}}} h_{\mathrm{S,D}} x + \eta_{\mathrm{S,D}}, \tag{2.1}$$

$$y_{\mathrm{S,R}} = \sqrt{P_{\mathrm{S}}} h_{\mathrm{S,R}} x + \eta_{\mathrm{S,R}}, \tag{2.2}$$

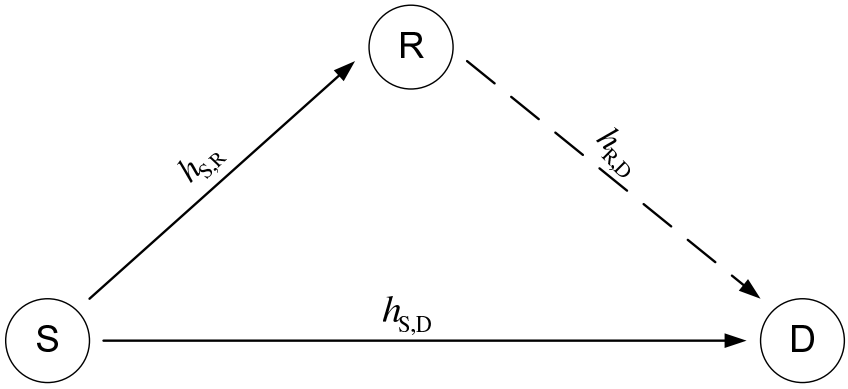

Figure 2.2: A cooperative communication network with single relay.

in which P_S is the transmitted power at the source, x is the transmitted information symbol, and $\eta_{S,D}$ and $\eta_{S,R}$ are additive noise modeled as zero-mean complex Gaussian random variables with variance $\mathcal{N}_0$. Also, $h_{S,D}$ and $h_{S,R}$ are the source-destination and source-relay channel coefficients, respectively.

In Phase 2, the relay can help the source by retransmitting the information to the destination. The received signal $y_{R,D}$ at the destination in phase 2 can be formulated as

$$y_{R,D} = h_{R,D}q(y_{S,R}) + \eta_{R,D}, \tag{2.3}$$

where the function $q(\cdot)$ depends on the protocol which is implemented at the relay. $h_{R,D}$ is the channel coefficient for the relay-destination link and $\eta_{R,D}$ is the additive noise.

2.2.1 Cooperation strategies

In this section, we describe some general low-complexity cooperative diversity protocols that can be utilized in the single relay scenario, including fixed, selective and incremental relaying.

Fixed relaying

In fixed relaying, the channel resources at the source are divided between the relay and the destination in a deterministic manner. The cooperative processing at the relay node differs according to different types of employed relay protocols. The most common strategies are the fixed AF and fixed DF relaying protocol.

In the fixed AF relaying, the relay amplifies the received signal and forwards it to the destination with transmitted power P_R. The received signal $y_{R,D}$ at the destination in

phase 2 can be formulated as

$$y_{\mathrm{R,D}} = \frac{\sqrt{P_{\mathrm{R}}}}{\sqrt{P_{\mathrm{S}} |h_{\mathrm{S,R}}|^2 + \mathcal{N}_0}} h_{\mathrm{R,D}} y_{\mathrm{S,R}} + \eta_{\mathrm{R,D}}. \tag{2.4}$$

By (2.2), the received signal can be specified as

$$y_{\mathrm{R,D}} = \frac{\sqrt{P_{\mathrm{S}} P_{\mathrm{R}}}}{\sqrt{P_{\mathrm{S}} |h_{\mathrm{S,R}}|^2 + \mathcal{N}_0}} h_{\mathrm{R,D}} h_{\mathrm{S,R}} x + \eta'_{\mathrm{R,D}}, \tag{2.5}$$

where

$$\eta'_{\mathrm{R,D}} = \frac{\sqrt{P_{\mathrm{R}}}}{\sqrt{P_{\mathrm{S}} |h_{\mathrm{S,R}}|^2 + \mathcal{N}_0}} h_{\mathrm{R,D}} \eta_{\mathrm{S,R}} + \eta_{\mathrm{R,D}}. \tag{2.6}$$

The destination jointly combines two copies of received signal from the source in phase 1 and that from the relay in phase 2 by different techniques, e.g., maximal ratio combining (MRC) .

In the fixed DF relaying, the relay decodes the received information, re-encodes it, and then forwards it to the destination. Note that the decoded signal at the relay may be incorrect if the source-relay link is too weak. If an incorrect signal is forwarded to the destination, the decoding at the destination is meaningless. It is clear that for such scheme the diversity achieved is only 1, because the performance of the system is limited by the worst link from the source-relay and source-destination [59].

Selective relaying

Fixed DF relaying suffers that the performance is limited by the weakest link between the source-relay and relay-destination which reduces the diversity gain to one. To overcome this problem, selective DF relaying is developed. In such a scheme, if the relay is able to decode the transmitted information correctly, in phase 2 the relay forwards the decoded symbol with power P_{R} to the destination, otherwise the relay remains idle. Therefore, the received signal at the destination can be modeled as

$$y_{\mathrm{R,D}} = \sqrt{\tilde{P}_{\mathrm{R}}} h_{\mathrm{R,D}} x + \eta_{\mathrm{R,D}}, \tag{2.7}$$

$$\text{where } \tilde{P}_{\mathrm{R}} = \begin{cases} P_{\mathrm{R}} & \text{if the relay decodes successfully} \\ 0 & \text{otherwise} \end{cases}.$$

To model the relay is able to detect the transmitted symbol or not, we may apply a signal-to-noise ratio (SNR) threshold at the relay in practice. If the received SNR at the relay is higher than the threshold, then the symbol has a high possibility to be decoded correctly.

Incremental relaying

Although the conventional cooperative relay network can achieve spatial diversity gain, it makes inefficient use of the degrees of freedom of the channel because the relay forwards the signal all the time regardless of channel conditions. In [59], authors describe an incremental relaying protocol, which exploits a limited feedback from the destination node, e.g., a single bit indicating the success or failure of the direct transmission. If the source-destination SNR is higher than a pre-defined threshold, the feedback indicates success of the direct transmission, then the relay does nothing. If the source-destination SNR is not sufficiently high for successful direct transmission, the feedback requests that the relay forwards the signal received from the source to the destination. The destination then performs maximum ratio combining of the signals from the source and the relay to explore an accumulation of SNRs. Since the relay forwards the signal only when it is necessary, the incremental relaying protocol makes more efficient use of channel resources.

In general, the selective relaying applies a adaptive strategy based on the fixed relaying concept. Incremental relaying improves the spectral efficiency of both fixed and selective relaying by exploiting limited feedback from the destination and relaying only when necessary.

2.2.2 Outage probabilities of different cooperation strategies

In this section, the performance of different cooperation strategies of the single relay are characterized in terms of outage probabilities. We consider a single relay network depicted in Figure 2.2. The channel coefficients $h_i, i \in \{(\mathrm{S},\mathrm{D}), (\mathrm{S},\mathrm{R}), (\mathrm{R},\mathrm{D})\}$ are assumed to be described by flat Rayleigh fading, i.e. they are modeled as zero-mean, complex Gaussian random variables with variances $\delta^2_{\mathrm{S,D}}$, $\delta^2_{\mathrm{S,R}}$ and $\delta^2_{\mathrm{R,D}}$, respectively. The noise terms $\eta_{\mathrm{S,D}}$, $\eta_{\mathrm{S,R}}$ and $\eta_{\mathrm{R,D}}$ are modeled as zero-mean, complex Gaussian random variables with variance $\mathcal{N}_0$.

From an information theory point of view, an outage event is defined as the set of channel realizations that can not support reliable transmission at a target rate. As the channel fading coefficients are viewed as random variables, the instantaneous mutual information as a function of the fading coefficients is also a random variable denoted by I . Therefore, for a target rate R, $I < R$ denotes the outage event, and the outage probability can be denoted as:

$$P^{\mathrm{out}} = \Pr\left[I < R\right], \tag{2.8}$$

where $\Pr[\cdot]$ is the probability operator.

Direct transmission

We firstly only consider the direct transmission to establish baseline performance. From (2.1), the received SNR from direct link is given by

$$\gamma_{\mathrm{SD}} = P\left|h_{\mathrm{S,D}}\right|^2/\mathcal{N}_0. \tag{2.9}$$

Then the instantaneous mutual information can be formulated as

$$I_{\mathrm{D}} = \log\left(1+\gamma_{\mathrm{SD}}\right) = \log\left(1+P\left|h_{\mathrm{S,D}}\right|^2/\mathcal{N}_0\right). \tag{2.10}$$

As the channel is Rayleigh fading, the random variables $\left|h_{\mathrm{S,D}}\right|^2$ will fulfill the exponential distribution. The outage probability can be written as:

$$\begin{aligned} P_{\mathrm{D}}^{\mathrm{out}} &= \Pr\left[I_{\mathrm{D}} < R\right] = \Pr\left[\left|h_{\mathrm{S,D}}\right|^2 < \frac{2^R-1}{P/\mathcal{N}_0}\right] \\ &= 1-\exp\left(-\frac{2^R-1}{\delta_{\mathrm{S,D}}^2 P/\mathcal{N}_0}\right) \\ &\approx \frac{1}{\delta_{\mathrm{S,D}}^2}\frac{2^R-1}{P/\mathcal{N}_0}. \end{aligned} \tag{2.11}$$

Fixed relaying

In the fixed relaying protocol, the destination will receive two copies of information: from the source in the 1st phase and from the relay in the 2nd phase. The optimal technique to combine these two signals is the MRC which maximizes the overall SNR. As shown in [24], the received signal at the output of the MRC will have an SNR which is equal to the sum of received SNRs from all paths:

$$\gamma_{\mathrm{tot}} = \gamma_{\mathrm{SD}} + \gamma_{\mathrm{SRD}}, \tag{2.12}$$

where $\gamma_{\mathrm{SD}} = P_{\mathrm{S}}\left|h_{\mathrm{S,D}}\right|^2/\mathcal{N}_0$ is the instantaneous SNR of the direct link and γ_{SRD} is the instantaneous SNR of the link aided by the relay.

As we mentioned before, fixed DF relaying suffers the problem of error propagation which reduces the diversity gain to one. Therefore, we only consider the AF protocol in the fixed relaying case. From (2.5), the instantaneous received SNR from the source-relay-destination link is:

$$\begin{aligned} \gamma_{\mathrm{SRD}} &= \frac{\left|\frac{\sqrt{P_{\mathrm{S}}P_{\mathrm{R}}}}{\sqrt{P_{\mathrm{S}}\left|h_{\mathrm{S,R}}\right|^2+\mathcal{N}_0}}h_{\mathrm{R,D}}h_{\mathrm{S,R}}\right|^2}{\left|\frac{\sqrt{P_{\mathrm{R}}}}{\sqrt{P_{\mathrm{S}}\left|h_{\mathrm{S,R}}\right|^2+\mathcal{N}_0}}h_{\mathrm{R,D}}\right|^2\mathcal{N}_0+\mathcal{N}_0} \\ &= \frac{\gamma_{\mathrm{SR}}\gamma_{\mathrm{RD}}}{\gamma_{\mathrm{SR}}+\gamma_{\mathrm{RD}}+1}, \end{aligned} \tag{2.13}$$

where $\gamma_{\mathrm{SR}} = P_{\mathrm{S}} \left|h_{\mathrm{S,R}}\right|^2 / \mathcal{N}_0$ and $\gamma_{\mathrm{RD}} = P_{\mathrm{R}} \left|h_{\mathrm{R,D}}\right|^2 / \mathcal{N}_0$ are the instantaneous SNRs for the relay back-haul link and the access link. The instantaneous mutual information between the input and two outputs for the fixed AF relaying is therefore given by

$$I_{\mathrm{AF}} = \frac{1}{2} \log \left(1 + \gamma_{\mathrm{SD}} + \gamma_{\mathrm{SRD}}\right), \tag{2.14}$$

where the factor of $\frac{1}{2}$ is because of the bandwidth loss by two hops transmission. In [82], the outage probability is obtained by averaging over the channel conditions:

$$P_{\mathrm{AF}}^{\mathrm{out}} = \Pr\left[I_{\mathrm{AF}} < R\right] \approx \left(\frac{\delta_{\mathrm{S,R}}^2 + \delta_{\mathrm{R,D}}^2}{2\delta_{\mathrm{S,D}}^2 \left(\delta_{\mathrm{S,R}}^2 \delta_{\mathrm{R,D}}^2\right)}\right) \left(\frac{2^{2R} - 1}{P/\mathcal{N}_0}\right)^2, \tag{2.15}$$

where the transmitted power of the source and the relay are the same $P_{\mathrm{S}} = P_{\mathrm{R}} = P$.

Selective relaying

In the selective DF relaying, we apply an SNR threshold at the relay in practice, i.e., if the SNR of the received signal at the relay exceeds a certain threshold, the relay is active to forward information. In the other case, the relay will remain idle. Thus, the instantaneous mutual information for the selective DF relaying can be written as

$$I_{\mathrm{SDF}} = \begin{cases} \frac{1}{2} \log \left(1 + 2\Gamma \left|h_{\mathrm{S,D}}\right|^2\right), & \left|h_{\mathrm{S,R}}\right|^2 < g(\Gamma) \\ \frac{1}{2} \log \left(1 + \Gamma \left|h_{\mathrm{S,D}}\right|^2 + \Gamma \left|h_{\mathrm{R,D}}\right|^2\right), & \left|h_{\mathrm{S,R}}\right|^2 \geq g(\Gamma) \end{cases}, \tag{2.16}$$

where $\Gamma = P/\mathcal{N}_0$ and $g(\Gamma) = (2^{2R} - 1)/\Gamma$. The first case in (2.16) is corresponding to that the relay is not able to decode the transmitted information correctly and the source should repeat its transmission. The multiplicative factor of 2 in $2\Gamma \left|h_{\mathrm{S,D}}\right|^2$ is hence because of this repeating transmission.

Next, the outage probability can be derived by using the law of conditional probability.

$$\begin{aligned} \Pr\left[I_{\mathrm{SDF}} < R\right] \;=\; & \Pr\left[I_{\mathrm{SDF}} < R \middle| \left|h_{\mathrm{S,R}}\right|^2 < g(\Gamma)\right] \Pr\left[\left|h_{\mathrm{S,R}}\right|^2 < g(\Gamma)\right] \\ & + \Pr\left[I_{\mathrm{SDF}} < R \middle| \left|h_{\mathrm{S,R}}\right|^2 \geq g(\Gamma)\right] \Pr\left[\left|h_{\mathrm{S,R}}\right|^2 \geq g(\Gamma)\right]. \end{aligned} \tag{2.17}$$

Substituting the mutual information of the selective DF relaying into the above formula

$$\begin{aligned} \Pr\left[I_{\mathrm{SDF}} < R\right] \;=\; & \Pr\left[\frac{1}{2} \log \left(1 + 2\Gamma \left|h_{\mathrm{S,D}}\right|^2\right) < R \mid \left|h_{\mathrm{S,R}}\right|^2 < g(\Gamma)\right] \Pr\left[\left|h_{\mathrm{S,R}}\right|^2 < g(\Gamma)\right] \\ & + \Pr\left[\frac{1}{2} \log \left(1 + \Gamma \left|h_{\mathrm{S,D}}\right|^2 + \Gamma \left|h_{\mathrm{R,D}}\right|^2\right) < R \mid \left|h_{\mathrm{S,R}}\right|^2 \geq g(\Gamma)\right] \\ & \Pr\left[\left|h_{\mathrm{S,R}}\right|^2 \geq g(\Gamma)\right]. \end{aligned} \tag{2.18}$$

We assume that all channels are Rayleigh fading channels and independent to each other, that means all random variables in (2.18) are independent exponential random variables.

The outage expression of the selective DF relaying at high SNR has been approximated in [82] as:

$$P_{\mathrm{SDF}}^{\mathrm{out}} = \Pr\left[I_{\mathrm{SDF}} < R\right] \approx \left(\frac{\delta_{\mathrm{S,R}}^2 + \delta_{\mathrm{R,D}}^2}{2\delta_{\mathrm{S,D}}^2\left(\delta_{\mathrm{S,R}}^2\delta_{\mathrm{R,D}}^2\right)}\right)\left(\frac{2^{2R}-1}{P/\mathcal{N}_0}\right)^2, \tag{2.19}$$

which has identical performance to that of the fixed AF relaying.

Incremental relaying

For incremental relaying, the destination sends a single bit acknowledgment to indicate the success or failure of the direct transmission. If the destination is able to decode the source information successfully, the relay will remain idle. In the other case, the relay forwards the source information to the destination. The destination then combine the two transmissions from the source and the relay. We will focus here on the relay node with AF protocol. Thus, the instantaneous mutual information of the incremental relaying can be summarize as

$$I_{\mathrm{IR}} = \begin{cases} I_{\mathrm{D}} = \log\left(1+\gamma_{\mathrm{SD}}\right), & |h_{\mathrm{S,D}}|^2 < (2^R-1)/\Gamma \\ I_{\mathrm{AF}} = \frac{1}{2}\log\left(1+\gamma_{\mathrm{SD}}+\gamma_{\mathrm{SRD}}\right), & |h_{\mathrm{S,D}}|^2 \geq (2^R-1)/\Gamma \end{cases}, \tag{2.20}$$

where $\Gamma = P/\mathcal{N}_0$. For the incremental AF relaying, the outage probability can be hence derived by using the law of conditional probability.

$$\Pr\left[I_{\mathrm{IR}} < R\right] \;=\; \Pr\left[I_{\mathrm{D}} < R\right]\Pr\left[I_{\mathrm{AF}} < R \middle|\; I_{\mathrm{D}} \geq R\right]. \tag{2.21}$$

The outage expression for the incremental relaying in large SNR region can be approximated straightforward by

$$P_{\mathrm{IR}}^{\mathrm{out}} = \Pr\left[I_{\mathrm{IR}} < R\right] \approx \left(\frac{\delta_{\mathrm{S,R}}^2 + \delta_{\mathrm{R,D}}^2}{\delta_{\mathrm{S,R}}^2\delta_{\mathrm{R,D}}^2}\right)\left(\frac{2^{2R}-1}{P/\mathcal{N}_0}\right)\left(\frac{1}{\delta_{\mathrm{S,D}}^2}\right)\left(\frac{2^{R}-1}{P/\mathcal{N}_0}\right). \tag{2.22}$$

2.2.3 Outage performance comparison

In this section, we will present the outage probability comparison among all before mentioned protocols. We consider a relatively simple scenario that the relay is located between the source and the destination. All channels are independent and identically distributed. Therefore, the channel variance of the direct link $\delta_{\mathrm{S,D}}$, the source-relay link $\delta_{\mathrm{S,R}}$ and the relay-destination link $\delta_{\mathrm{R,D}}$ are assumed to be 1 in our work. The noise variance $\mathcal{N}_0$ is 1.

Figure 2.3 shows outage probabilities of the various relaying protocols for a fixed rate of 1 bit/s/Hz. Both exact and high-SNR approximation results are presented. The exact outage probability is obtained via Monte Carlo simulations, which are shown as different

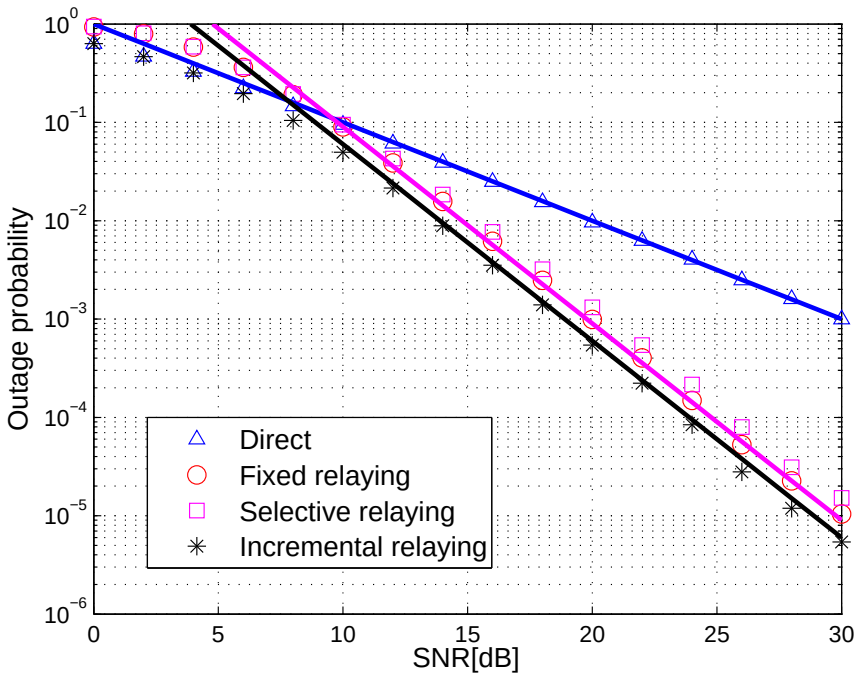

Figure 2.3: Outage probability versus SNR for different cooperation strategies.

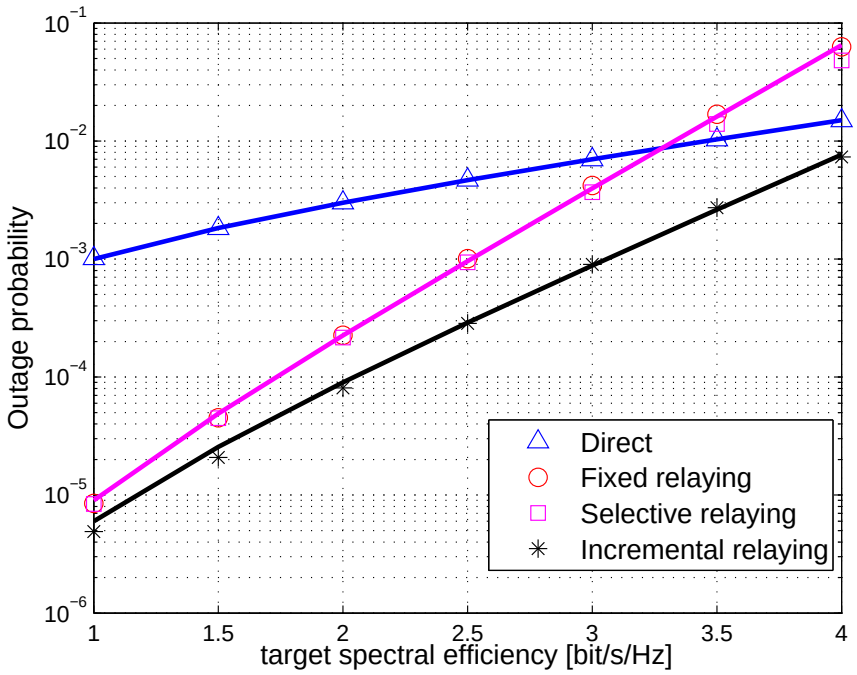

Figure 2.4: Outage probability versus target spectral efficiency for different cooperation strategies.

marks in the figure. While the solid curves correspond to the analytical result from high-SNR approximations. The diversity order two can be achieved by fixed, selective, and incremental relaying protocols as it can be read from the outage curve slopes. It is clear that the selective DF relaying has similar result as the fixed AF relaying, which has been proved in previous numerical result. The incremental relaying shows around 2 dB performance gain compared to the result from fixed AF relaying. In large SNR region, the analytical approximation is very close to the simulation result. Furthermore, cooperative protocols can achieve more than 10 dB improvement compared with the case of direct transmission for large SNR values.

In Figure 2.4, the outage probability is depicted versus target spectral efficiency for a fixed SNR value of 30 dB. The performance generally degrades with increasing spectral efficiency, but it degrades faster for fixed and selective relaying compared with incremental relaying because of the inherent loss in the spectral efficiency. For large values of the spectral efficiency, direct transmission becomes more efficient than cooperation.

2.3 Multiple relays scenario: Cooperate with whom

A natural extension of the single relay network is to the case of multiple relays, where the information is transmitted from a source to a destination with help of multiple relay nodes as depicted in Figure 2.5. Due to the broadcast nature of the wireless channel, the nodes other than destination can overhear the transmitted information and thus can cooperate with the source to forward the information.

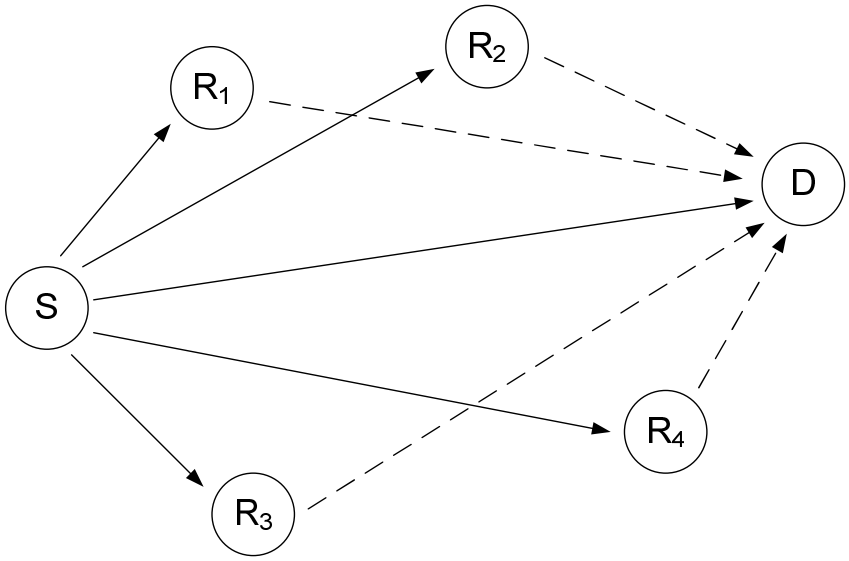

Figure 2.5: A cooperative communication network with multiple relays.

In the multiple relays scenario, there are some questions need to be answered:

- The first question is which stations should cooperate with each other. In a dense wireless network, there are typically several relay nodes in the region between the source and the destination. In [82], the considered scenario contains N relay nodes, the available channel resources are divided into $N+1$ orthogonal channels. All N relay nodes can help the source forward the signal to the destination. However, the throughput of such system is limited by the orthogonal partition of system resources, especially when the number of relay nodes is large. To overcome this drawback, a new cooperation structure called selection AF(S-AF) was introduced in [112]. In such a scheme, only the relay which contributes the most to the received SNR is selected to cooperate with. Various relay selection approaches have been explored for the relay selection in existing literature. However, to determine which of potential relays should be selected is still a difficult cross-layer problem. For example, a relay node has good channel quality to the destination, but it may has heavy traffic load. In our work we consider the relay selection using a novel criterion, i.e., the optimal relay is the relay which maximize the objective function among all candidate nodes.

- The second question is when to cooperate. The source should determine whether to cooperate with an additional node or additional nodes to assist the transmission. In reality, the channel gain is only available at the receiver side, hence the destination can evaluate the source-destination channel gain and then sends it back to the source node through a feedback channel. Thus, the source can calculate the metric among different links to decide whether requests for help from a relay node.

- Another question is who will control the cooperation. In most cases, the relay selection is assumed to be perfectly performed using a central controller without considering any incurred overhead. In practice, centralized implementation of relay selection requires extra control signals and information exchange, which will degrade the overall system performance, especially for systems with a large number of relays. Decentralized schemes, which only require local information, have been investigated for overcoming these implementation issues. However, the performance for decentralized scheme will be limited by such only locally optimal selections.

Since there exist such problems in the multiple relays scenario, the research of relay selection always attracts attention in multiple relays networks [83][92]. To evaluate different relay selection algorithms, it is better to firstly find the performance bound in the optimal case. The authors in [18] presented an exact closed form expression for the outage

probability of DF relaying in dissimilar Rayleigh fading channels. They consider a network with N relays, however, only C relays ($C < N$) with good channels are allowed to decode and forward the information from the source to the destination. Furthermore, some approximate performance analysis for DF systems can be found in [14][20]. The authors in [21] suggested that only the best relay among the decoding set shall forward the information to improve the outage probability performance, which is named as selective DF (S-DF) relaying. In [45], a closed-form expression for the outage probability in a cooperative communication system based on relay selection with low modulation order has been proposed. However, to the best of our knowledge, none of the authors derived an exact closed-form expression for the symbol error probability of S-DF cooperative networks which is valid for the whole SNR regime.

2.4 Selective DF relaying in multiple relays scenario

In this section, we focus on decode-and-forward dual-hop cooperative networks with the relay selection over independent non-identical Rayleigh fading channels. The main objective is giving a performance analysis of S-DF relay cooperative networks. We derive exact closed-form expressions for the probability density function (PDF) of the received SNR and symbol error probability at the destination of the S-DF cooperative network. The analytical expressions are validated by computer simulation results.

2.4.1 System model

Consider a wireless system where a source node transmits the information to a destination with the help of N relay nodes. A cooperative communication strategy with two phases is considered. Transmissions are orthogonal either through time or frequency division.

As shown in Figure 2.6, in Phase 1, the source broadcasts its information to the destination and relays. The received signals $y_{\mathrm{S,D}}$ and $y_{\mathrm{S,R}_i}$ at the destination and ith relay can be written as

$$y_{\mathrm{S,D}} = \sqrt{P_{\mathrm{S}}} h_{\mathrm{S,D}} x + \eta_{\mathrm{S,D}}, \tag{2.23}$$

$$y_{\mathrm{S,R}_i} = \sqrt{P_{\mathrm{S}}} h_{\mathrm{S,R}_i} x + \eta_{\mathrm{S,R}_i}, \tag{2.24}$$

respectively, in which P_{S} is the transmitted power at the source, x is the transmitted information symbol, and $\eta_{\mathrm{S,D}}$ and $\eta_{\mathrm{S,R}_i}$ are additive noise. The channel coefficients between S and D ($h_{\mathrm{S,D}}$) and between S and $\mathrm{R_i}$ ($h_{\mathrm{S,R}_i}$) are flat Rayleigh fading coefficients, i.e. they are modeled as zero-mean, complex Gaussian random variables with variances $\delta^2_{\mathrm{S,D}}$ and $\delta^2_{\mathrm{S,R}_i}$, respectively. The noise terms $\eta_{\mathrm{S,D}}$ and $\eta_{\mathrm{S,R}_i}$ are modeled as zero-mean, complex Gaussian random variables with variance $\mathcal{N}_0$.

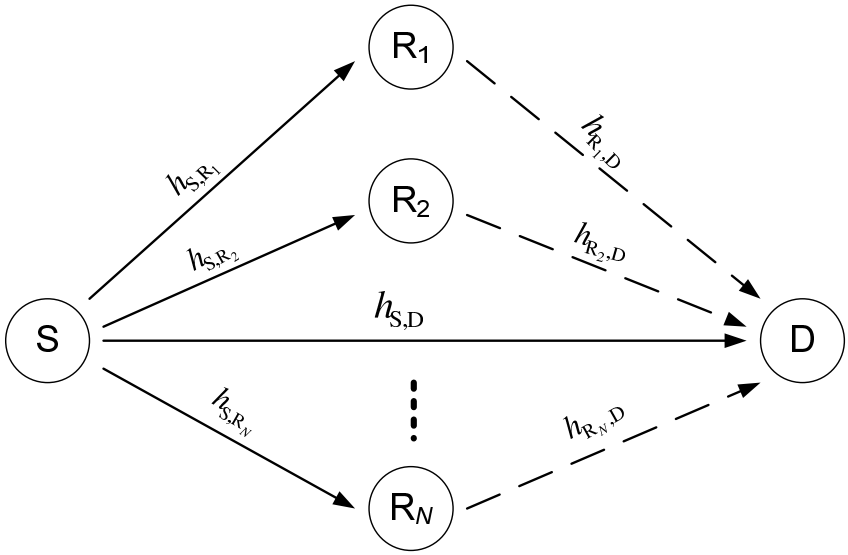

Figure 2.6: DF cooperative network with relay selection.

We define a decoding set Ω with relays which are able to decode the information from the source correctly. In Phase 2, we only activate the relay that offers the best instantaneous SNR at the destination among the relays in the decoding set Ω. This relay decodes, re-encodes and forwards the source information to the destination. The received signal at the destination from the best relay in this case can be modeled as

$$y_{\mathrm{R}_i,\mathrm{D}} = \sqrt{P_{\mathrm{R}}} h_{\mathrm{R}_i,\mathrm{D}} x + \eta_{\mathrm{R}_i,\mathrm{D}}, \tag{2.25}$$

where P_{R} is the transmitted power at the selected relay. The channel coefficient from the selected relay to the destination is $h_{\mathrm{R}_i,\mathrm{D}}$, which is modeled as a zero-mean, complex Gaussian random variable with variance $\delta^2_{\mathrm{R}_i,\mathrm{D}}$. The noise terms $\eta_{\mathrm{R}_i,\mathrm{D}}$ is also modeled as a zero-mean, complex Gaussian random variable with variance $\mathcal{N}_0$.

Two copies of received signal (one is from the direct link and the other is from the indirect link) are combined using the MRC technique. The combined signal at the MRC detector can be written as

$$y = a_1 y_{\mathrm{S,D}} + a_2 y_{\mathrm{R}_i,\mathrm{D}}, \tag{2.26}$$

where the factors a_1 and a_2 are determined such that the SNR of the MRC output is maximized, they can be specified as

$$a_1 = \sqrt{P_{\mathrm{S}}} h^*_{\mathrm{S,D}} / \mathcal{N}_0, a_2 = \sqrt{P_{\mathrm{R}}} h^*_{\mathrm{R}_i,\mathrm{D}} / \mathcal{N}_0. \tag{2.27}$$

Assume that the transmitted symbol x has average power 1, then the received instantaneous SNR can be expressed as

$$\gamma_{\mathrm{D}} = \gamma_{\mathrm{SD}} + \max_{i \in \Omega} (\gamma_{\mathrm{R}_i\mathrm{D}}) \tag{2.28}$$

where $\gamma_{\mathrm{SD}} = P_{\mathrm{S}} |h_{\mathrm{S,D}}|^2 / \mathcal{N}_0$ is the instantaneous SNR between S and D, and $\gamma_{\mathrm{R}_i\mathrm{D}} = P_{\mathrm{R}} |h_{\mathrm{R}_i,\mathrm{D}}|^2 / \mathcal{N}_0$ is the instantaneous SNR between the selected relay R_i and the destination D.

2.4.2 Symbol error rate analysis

SER formulation

The SER formulations for an uncoded system with M-PSK or M-QAM modulation are given by [89]:

$$\psi_{\mathrm{PSK}}(\gamma) = \frac{1}{\pi} \int_0^{(M-1)\pi/M} \exp(-\frac{g_{\mathrm{PSK}}\gamma}{\sin^2\theta}) \mathrm{d}\theta, \tag{2.29}$$

$$\psi_{\mathrm{QAM}}(\gamma) = 4K\mathrm{Q}(\sqrt{2g_{\mathrm{QAM}}\gamma}) - 4K^2\mathrm{Q}^2(\sqrt{2g_{\mathrm{QAM}}\gamma}), \tag{2.30}$$

in which the γ is SNR, $g_{\mathrm{PSK}} = \sin^2(\pi/M)$, $K = 1 - (1/\sqrt{M})$, $g_{\mathrm{QAM}} = 3/2(M-1)$, and $\mathrm{Q}(u) = (1/\sqrt{2\pi}) \int_u^\infty \exp(-t^2/2)\mathrm{d}t$ is the Gaussian Q-function. In this paper we prefer an alternate definite integral form for the Gaussian Q-function, which was implied in the work of Pawula et.al. [78] as follows:

$$\mathrm{Q}(u) = \frac{1}{\pi} \int_0^{\pi/2} \exp(-\frac{u^2}{2\sin^2\theta}) \mathrm{d}\theta, \tag{2.31}$$

$$\mathrm{Q}^2(u) = \frac{1}{\pi} \int_0^{\pi/4} \exp(-\frac{u^2}{2\sin^2\theta}) \mathrm{d}\theta. \tag{2.32}$$

This form of the Gaussian Q-function simplifies the analysis and evaluation of the average SER by allowing to average the channel coefficients inside the integral with a final integration, e.g. as shown in (2.37).

Therefore, if M-PSK modulation is used in the S-DF cooperative system, with the instantaneous SNR γ_{D} in (2.28), the instantaneous SER of the system with channel coefficients $h_{\mathrm{S,D}}$ and $h_{\mathrm{R}_i,\mathrm{D}}$ can be written as

$$P_{\mathrm{PSK}}^{h_{\mathrm{S,D}},h_{\mathrm{R}_i,\mathrm{D}}} = \psi_{\mathrm{PSK}}(\gamma_{\mathrm{D}}) = \frac{1}{\pi} \int_0^{(M-1)\pi/M} \exp(-\frac{g_{\mathrm{PSK}}\gamma_{\mathrm{D}}}{\sin^2\theta}) \mathrm{d}\theta. \tag{2.33}$$

If M-QAM signals are used in this system, the instantaneous SER of the system can also be expressed as

$$\begin{aligned} P_{\mathrm{QAM}}^{h_{\mathrm{S,D}},h_{\mathrm{R}_i,\mathrm{D}}} &= \psi_{\mathrm{QAM}}(\gamma_{\mathrm{D}}) \\ &= 4K\frac{1}{\pi} \int_0^{\pi/2} \exp(-\frac{g_{\mathrm{QAM}}\gamma_{\mathrm{D}}}{\sin^2\theta}) \mathrm{d}\theta - 4K^2\frac{1}{\pi} \int_0^{\pi/4} \exp(-\frac{g_{\mathrm{QAM}}\gamma_{\mathrm{D}}}{\sin^2\theta}) \mathrm{d}\theta. \end{aligned} \tag{2.34}$$

To compute the average SER , we must statistically average the conditional SER over the joint PDF of the received instantaneous SNR γ_{D}, as follows

$$P_e = \mathbb{E}_{\gamma_{\mathrm{D}}} \left\{ \psi_{\mathrm{PSK/QAM}}(\gamma_{\mathrm{D}}) \right\}, \tag{2.35}$$

where $\mathbb{E}\{\}$ denotes the expectation operator.

In the following, we derive the PDF expressions for the received instantaneous SNR. The relay network in Figure 2.6 can be visualized as a system that has $N+1$ paths (one direct path and N indirect paths) between the source and destination. Let Path 0 represents the direct link ($\mathrm{S} \rightarrow \mathrm{D}$) and Path i represents the relay link ($\mathrm{S} \rightarrow \mathrm{R}_i \rightarrow \mathrm{D}$) where $i = 1, .., N$. We assume a random variable y_i denote the square of the gain on the i^{th} indirect link($\mathrm{S} \rightarrow \mathrm{R}_i \rightarrow \mathrm{D}$). Since the relay is assumed to forward the source information only if it is able to decode correctly, we can write the PDF of y_i as [18]

$$f_{y_i}(x) = A_i \delta(x) + (1 - A_i) \frac{1}{\bar{\gamma}_{\mathrm{R}_i\mathrm{D}}} \exp(-\frac{x}{\bar{\gamma}_{\mathrm{R}_i\mathrm{D}}}), \tag{2.36}$$

where $\delta(x)$ is the delta function, $\bar{\gamma}_{\mathrm{R}_i\mathrm{D}} = \mathbb{E}\left\{ h^2_{\mathrm{R}_i,\mathrm{D}} P_{\mathrm{R}} / \mathcal{N}_0 \right\} = \delta^2_{\mathrm{R}_i,\mathrm{D}} P_{\mathrm{R}} / \mathcal{N}_0$ and A_i represents the probability that the i-th relay node will not be in the decoding set. Let us take M-PSK as an example, from previous subsection we could conclude that

$$\begin{aligned} A_i &= \mathbb{E}_{\gamma_{\mathrm{SR}_i}} \left\{ \psi_{\mathrm{PSK}}(\gamma_{\mathrm{SR}_i}) \right\} \\ &= \frac{1}{\pi} \int_0^{(M-1)\pi/M} \mathbb{E}_{\gamma_{\mathrm{SR}_i}} \left\{ \exp(-\frac{g_{\mathrm{PSK}} \gamma_{\mathrm{SR}_i}}{\sin^2\theta}) \right\} \mathrm{d}\theta, \end{aligned} \tag{2.37}$$

where $\gamma_{\mathrm{SR}_i} = P_{\mathrm{S}} \left| h_{\mathrm{S,R}_i} \right|^2 / N_0$. As $h_{\mathrm{S,R}_i}$ exhibits a Rayleigh distribution, the PDF of $\left| h_{\mathrm{S,R}_i} \right|^2$ is $f_{\left| h_{\mathrm{S,R}_i} \right|^2}(z) = \frac{1}{\delta^2_{\mathrm{S,R}_i}} \exp(-\frac{z}{\delta^2_{\mathrm{S,R}_i}})$. Then equation (2.37) can be rewritten as

$$\begin{aligned} A_i &= \frac{1}{\pi} \int_0^{(M-1)\pi/M} \left\{ \int_0^{\infty} \exp(-\frac{g_{\mathrm{PSK}} P_{\mathrm{S}} z}{N_0 \sin^2\theta}) f_{\left| h_{\mathrm{S,R}_i} \right|}(z) \mathrm{d}z \right\} \mathrm{d}\theta \\ &= \frac{1}{\pi} \int_0^{(M-1)\pi/M} \frac{1}{1 + \frac{g_{\mathrm{PSK}} P_{\mathrm{S}} \delta^2_{\mathrm{S,R}_i}}{N_0 \sin^2\theta}} \mathrm{d}\theta. \end{aligned} \tag{2.38}$$

In order to simplify the analysis of the destination instantaneous SNR, we introduce a new random variable Z given by the summation of two random variables as $Z = \gamma_{\mathrm{SD}} + \chi$, where $\chi = \max_{i=1,\ldots,N}(\gamma_{\mathrm{R}_i\mathrm{D}})$. Since the two random variables γ_{SD} and χ are independent, the PDF of their sum (Z) is the convolution of the PDFs of γ_{SD} and χ [77]. The PDF of γ_{SD} can be easily shown as an exponential distribution function $f_{\gamma_{\mathrm{SD}}}(x) = \frac{1}{\bar{\gamma}_{\mathrm{SD}}} \exp(-\frac{x}{\bar{\gamma}_{\mathrm{SD}}})$,

while the PDF of χ can be found as follows. The CDF of χ can be written as

$$\begin{aligned} F_\chi(x) &= \Pr(\max_{i\in N} y_i \le x) \\ &= \Pr(y_1 \le x, ..., y_N \le x) \\ &= \prod_{i=1}^{N} \Pr(y_i \le x) = \prod_{i=1}^{N} F_{y_i}(x) \end{aligned} \tag{2.39}$$

where $F_{y_i}(x)$ is the CDF of y_i, which can be easily derived from (2.36). By using the CDF of y_i, the PDF of χ can be found by taking the derivative of (2.39) with respect to x and after some manipulations. Ikki and Ahmed [45] give the closed-form expression of $f_\chi(x)$ as

$$\begin{aligned} f_\chi(x) \;=\; & \left(\prod_{i=1}^{N} A_i\right)\delta(x) + \sum_{k=1}^{N}(-1)^{k+1}\sum_{\lambda_1=1}^{N-k+1}\sum_{\lambda_2=\lambda_1+1}^{N-k+2}\cdots \\ & \sum_{\lambda_k=\lambda_{k-1}+1}^{N}\prod_{i=1}^{k}(1-A_{\lambda_i})\exp\left(-\frac{x}{\bar{\gamma}_{\mathrm{R}_{\lambda_i}\mathrm{D}}}\right)\times\sum_{i=1}^{k}\frac{1}{\bar{\gamma}_{\mathrm{R}_{\lambda_i}\mathrm{D}}}. \end{aligned} \tag{2.40}$$

By using the PDFs of γ_{SD} and χ and doing the convolution, the PDF of γ_{D} can be written as

$$\begin{aligned} f_{\gamma_{\mathrm{D}}}(x) \;=\; & \frac{\left(\prod_{i=1}^{N} A_i\right)}{\bar{\gamma}_{\mathrm{SD}}}\exp\left(-\frac{x}{\bar{\gamma}_{\mathrm{SD}}}\right) \\ & + \sum_{k=1}^{N}(-1)^{k+1}\sum_{\lambda_1=1}^{N-k+1}\sum_{\lambda_2=\lambda_1+1}^{N-k+2}\cdots\sum_{\lambda_k=\lambda_{k-1}+1}^{N}\frac{\prod_{i=1}^{k}(1-A_{\lambda_i})}{\bar{\gamma}_{\mathrm{SD}}-\frac{1}{\sum_{i=1}^{k}\frac{1}{\bar{\gamma}_{\mathrm{R}_{\lambda_i}\mathrm{D}}}}} \\ & \times\left[\exp\left(-\frac{x}{\bar{\gamma}_{\mathrm{SD}}}\right)-\prod_{i=1}^{k}\exp\left(-\frac{x}{\bar{\gamma}_{\mathrm{R}_{\lambda_i}\mathrm{D}}}\right)\right], \end{aligned} \tag{2.41}$$

where $\bar{\gamma}_{\mathrm{SD}} = \delta^2_{\mathrm{S,D}}P_{\mathrm{S}}/\mathcal{N}_0$ and $\bar{\gamma}_{\mathrm{R}_{\lambda_i}\mathrm{D}} = \delta^2_{\mathrm{R}_{\lambda_i},\mathrm{D}}P_{\mathrm{R}}/\mathcal{N}_0$. Although (2.41) has multiple summations and multiplications, all these operations are finite and easy to handle numerically. In a special case, where all the relay links are identical($\bar{\gamma}_{\mathrm{R}_i\mathrm{D}} = \bar{\gamma}$ and $A_i = A$), the PDF of γ_{D} can be simplified to

$$\begin{aligned} f_{\gamma_{\mathrm{D}}}(x) \;=\; & \frac{A^N}{\bar{\gamma}_{\mathrm{SD}}}\exp\left(-\frac{x}{\bar{\gamma}_{\mathrm{SD}}}\right)+\sum_{k=1}^{N}(-1)^{k+1}\binom{N}{k}\frac{(1-A)^k}{\bar{\gamma}_{\mathrm{SD}}-\bar{\gamma}/k} \\ & \times\left[\exp\left(-\frac{x}{\bar{\gamma}_{\mathrm{SD}}}\right)-\exp\left(-\frac{xk}{\bar{\gamma}}\right)\right]. \end{aligned} \tag{2.42}$$

Average symbol error rate

As we mentioned before, the average symbol error rate can be found by averaging the instantaneous SER (2.33),(2.34) over the Rayleigh fading channels $h_{\mathrm{S,D}}$, $h_{\mathrm{S,R}_i}$ and $h_{\mathrm{R}_i,\mathrm{D}}$

with variances $\delta^2_{\mathrm{S,D}}$, $\delta^2_{\mathrm{S,R}_i}$ and $\delta^2_{\mathrm{R}_i,\mathrm{D}}$, respectively. After computing the PDF of the instantaneous SNR, we are able to obtain the average SER of S-AF system by substituting (2.41) into (2.35). If M-PSK modulation is used, the average SER can be written as

$$\begin{aligned}
P_{e,M\text{-PSK}} &= \mathbb{E}_{\gamma_D}\left\{\psi_{\mathrm{PSK}}(\gamma_{\mathrm{D}})\right\} \\
&= \frac{1}{\pi}\int_0^{(M-1)\pi/M}\left\{\int_0^{\infty}\exp(-\frac{g_{\mathrm{PSK}}x}{\sin^2\theta})f_{\gamma_{\mathrm{D}}}(x)\mathrm{d}x\right\}\mathrm{d}\theta \\
&= \frac{1}{\pi}\int_0^{(M-1)\pi/M}\prod_{i=1}^{N}A_i\frac{1}{1+\frac{g_{\mathrm{PSK}}\bar{\gamma}_{\mathrm{SD}}}{\sin^2\theta}} \\
&\quad+\sum_{k=1}^{N}(-1)^{k+1}\sum_{\lambda_1=1}^{N-k+1}\sum_{\lambda_2=\lambda_1+1}^{N-k+2}\cdots\sum_{\lambda_k=\lambda_{k-1}+1}^{N} \\
&\quad\left(\frac{\prod_{i=1}^{k}(1-A_{\lambda_i})}{\bar{\gamma}_{\mathrm{SD}}-\frac{1}{\sum_{i=1}^{k}\frac{1}{\bar{\gamma}_{\mathrm{R}_{\lambda_i}\mathrm{D}}}}}\cdot\frac{1}{\frac{g_{\mathrm{PSK}}}{\sin^2\theta}+\frac{1}{\bar{\gamma}_{\mathrm{SD}}}}\right. \\
&\quad\left.-\frac{\prod_{i=1}^{k}(1-A_{\lambda_i})}{\bar{\gamma}_{\mathrm{SD}}-\frac{1}{\sum_{i=1}^{k}\frac{1}{\bar{\gamma}_{\mathrm{R}_{\lambda_i}\mathrm{D}}}}}\cdot\frac{1}{\frac{g_{\mathrm{PSK}}}{\sin^2\theta}+\sum_{i=1}^{k}\frac{1}{\bar{\gamma}_{\mathrm{R}_{\lambda_i}\mathrm{D}}}}\right)\mathrm{d}\theta, \qquad (2.43)
\end{aligned}$$

where $\bar{\gamma}_{\mathrm{SD}} = \delta^2_{\mathrm{S,D}}P_{\mathrm{S}}/\mathcal{N}_0$ and $\bar{\gamma}_{\mathrm{R}_{\lambda_i}\mathrm{D}} = \delta^2_{\mathrm{R}_{\lambda_i},\mathrm{D}}P_{\mathrm{R}}/\mathcal{N}_0$.

If M-QAM modulation is used, the average SER can be written as

$$\begin{aligned}
P_{e,M\text{-QAM}} &= \mathbb{E}_{\gamma_{\mathrm{D}}}\left\{\psi_{\mathrm{QAM}}(\gamma_{\mathrm{D}})\right\} \\
&= \frac{4K}{\pi}\int_0^{\pi/2}\left\{\int_0^{\infty}\exp(-\frac{g_{\mathrm{QAM}}x}{\sin^2\theta})f_{\gamma_{\mathrm{D}}}(x)\mathrm{d}x\right\}\mathrm{d}\theta \\
&\quad-\frac{4K^2}{\pi}\int_0^{\pi/4}\left\{\int_0^{\infty}\exp(-\frac{g_{\mathrm{QAM}}x}{\sin^2\theta})f_{\gamma_{\mathrm{D}}}(x)\mathrm{d}x\right\}\mathrm{d}\theta, \qquad (2.44)
\end{aligned}$$

where

$$\begin{aligned}
\int_0^{\infty}\exp(-\frac{g_{\mathrm{QAM}}x}{\sin^2\theta})f_{\gamma_{\mathrm{D}}}(x)\mathrm{d}x &= \prod_{i=1}^{N}A_i\frac{1}{1+\frac{g_{\mathrm{QAM}}\bar{\gamma}_{\mathrm{SD}}}{\sin^2\theta}}+\sum_{k=1}^{N}(-1)^{k+1}\sum_{\lambda_1=1}^{N-k+1}\sum_{\lambda_2=\lambda_1+1}^{N-k+2}\cdots\sum_{\lambda_k=\lambda_{k-1}+1}^{N} \\
&\quad\left(\frac{\prod_{i=1}^{k}(1-A_{\lambda_i})}{\bar{\gamma}_{\mathrm{SD}}-\frac{1}{\sum_{i=1}^{k}\frac{1}{\bar{\gamma}_{\mathrm{R}_{\lambda_i}\mathrm{D}}}}}\cdot\frac{1}{\frac{g_{\mathrm{QAM}}}{\sin^2\theta}+\frac{1}{\bar{\gamma}_{\mathrm{SD}}}}\right. \\
&\quad\left.-\frac{\prod_{i=1}^{k}(1-A_{\lambda_i})}{\bar{\gamma}_{\mathrm{SD}}-\frac{1}{\sum_{i=1}^{k}\frac{1}{\bar{\gamma}_{\mathrm{R}_{\lambda_i}\mathrm{D}}}}}\cdot\frac{1}{\frac{g_{\mathrm{QAM}}}{\sin^2\theta}+\sum_{i=1}^{k}\frac{1}{\bar{\gamma}_{\mathrm{R}_{\lambda_i}\mathrm{D}}}}\right). \qquad (2.45)
\end{aligned}$$

2.4.3 Bandwidth efficiency

In a conventional multiple relay cooperation scenario, each relay receives the information from the source and re-transmits the information to the destination if necessary. This protocol achieves full diversity order, however, it requires $N+1$ (N is the number of cooperated relays) phases and the bandwidth efficiency is only $n_{\mathrm{BE}}^{\mathrm{conv}} = 1/(N+1)$ symbols per channel use (SPCU). In the relay selection scenario, the objective is to increase the bandwidth efficiency, while achieving full diversity order.

We derive the achievable bandwidth efficiency of S-DF cooperation system as follows. From the previous section, the probability of the relay i not belonging to the decoding set is A_i, as defined by equation (2.38). If none of relays is in the decoding set, then the source does not cooperate with any of the relays. Therefore, the probability of direct transmission Pr_{D} can be written as:

$$\mathrm{Pr}_{\mathrm{D}} = \prod_{i\in\Omega} A_i. \tag{2.46}$$

By substituting (2.38) into (2.46), in the PSK case, this probability can be expressed as

$$\mathrm{Pr}_{\mathrm{D}} = \prod_{i\in\Omega} \frac{1}{\pi} \int_0^{(M-1)\pi/M} \frac{1}{1+\frac{g_{\mathrm{PSK}} P_{\mathrm{S}} \delta^2_{\mathrm{S,R}_i}}{N_0 \sin^2\theta}} \mathrm{d}\theta. \tag{2.47}$$

Therefore, the probability of the relay cooperation case Pr_{C} is

$$\mathrm{Pr}_{\mathrm{C}} = 1 - \mathrm{Pr}_{\mathrm{D}}. \tag{2.48}$$

The bandwidth efficiency of the direct transmission is 1 SPCU, whereas the bandwidth efficiency of the relay cooperation is 1/2 SPCU since it requires 2 phases for one transmission. Then the average bandwidth efficiency of the S-DF can be written as

$$n_{\mathrm{BE}} = \mathrm{Pr}_{\mathrm{D}} + \frac{1}{2}\mathrm{Pr}_{\mathrm{C}}. \tag{2.49}$$

Figure 2.7 depicts the bandwidth efficiency of the S-DF cooperation system and the conventional cooperative scenario for different numbers of relays and unity source-relay channel variances. In S-DF system, it is obvious that the bandwidth efficiency decreases down to 0.5 as relay number N increases, because the probability of the direct transmission decreases down to 0 as N approaches to ∞. Furthermore, we plot the bandwidth efficiency of the conventional cooperative scenario, $n_{\mathrm{BE}}^{\mathrm{conv}} = 1/(N+1)$ (SPCU), to show the significant advantage of the S-DF cooperative system over the conventional cooperative scenario.

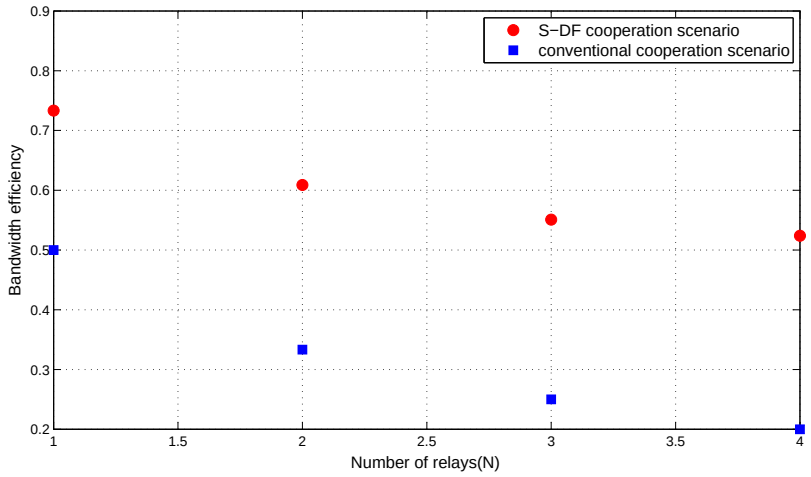

Figure 2.7: Bandwidth efficiency of the S-DF cooperation system.

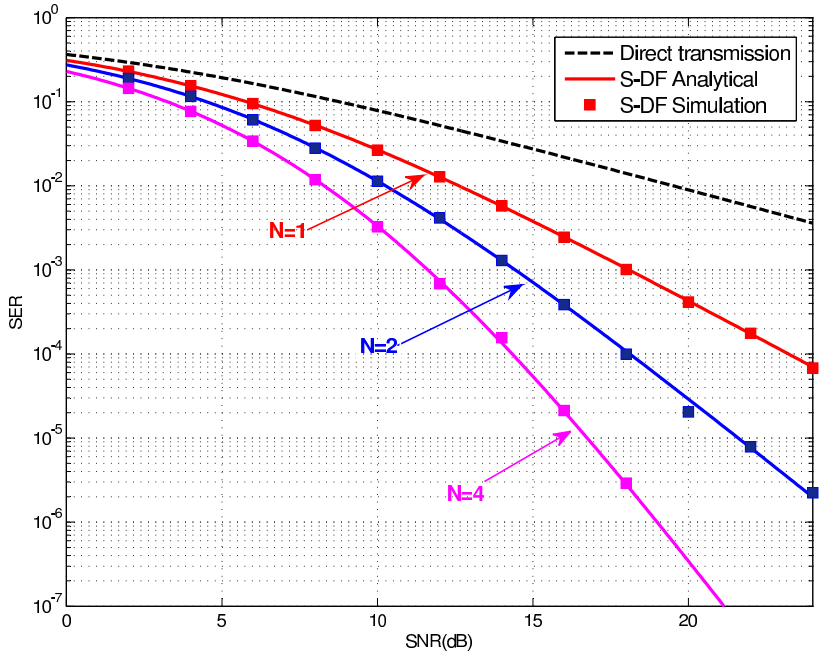

Figure 2.8: SER performance of S-DF cooperative scheme with QPSK modulation and different number of relay nodes. It is assumed that $\delta^2_{\mathrm{S,D}} = \delta^2_{\mathrm{S,R}_i} = \delta^2_{\mathrm{R}_i,\mathrm{D}} = 1$ and $P_{\mathrm{S}} = P, P_{\mathrm{R}} = P/2$.

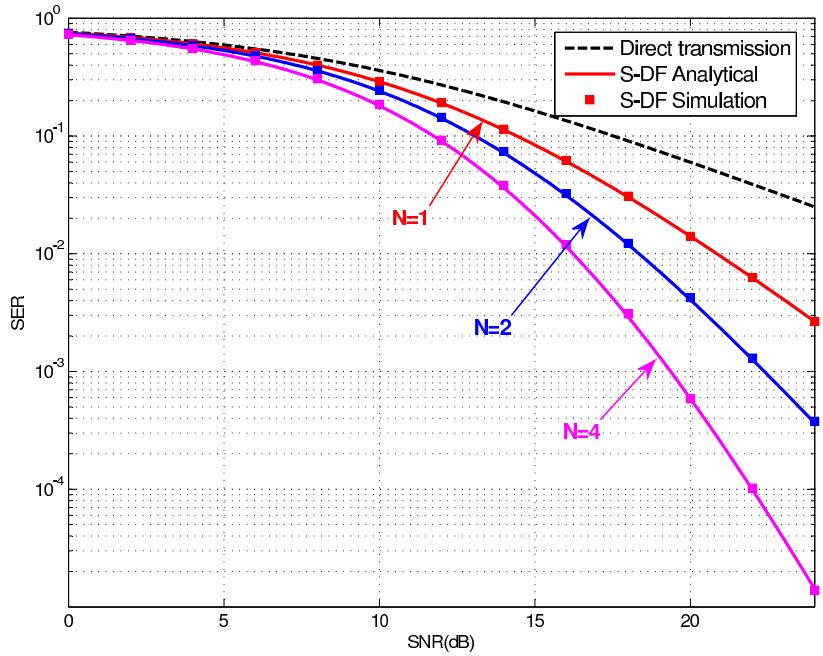

Figure 2.9: SER performance for S-DF cooperative scheme with 16QAM modulation and different number of relay nodes. It is assumed that $\delta^2_{\mathrm{S,D}} = \delta^2_{\mathrm{S,R}_i} = \delta^2_{\mathrm{R}_i,\mathrm{D}} = 1$ and $P_{\mathrm{S}} = P, P_{\mathrm{R}} = P/2$.

2.4.4 SER performance

In this section, we provide the results obtained from the mathematical expressions presented in the previous Section. We plot the performance curves in terms of SER versus the SNR of the transmitted signal. We also show the results from computer simulations for the selective relay system shown in Figure 2.6 and compare the results with those found from the previous analytical model.

Figure 2.8 and Fig 2.9 show the SER of a multi-node S-DF cooperative communication system with different values of the number of relay nodes considering QPSK and 16QAM signalling, respectively. We plot the simulated SER curves, which verified the correctness of the analytical SER results obtained in (2.43) and (2.44). The direct-transmission SER curve is plotted as well to show the effect of employing the relays in a cooperative way. We can see that as the number of relay node N increases, the corresponding improvement also increases. From Figure 2.8 and Figure 2.9, we can also notice that the number of cooperating relays has a strong impact on the performance enhancement since the achieved diversity order of the analyzed system is equal to $N + 1$.

2.4.5 Conclusion

This section presents the performance analysis for the decode-and-forward cooperative diversity network with relay selection over Rayleigh fading channels. The exact novel closed-form expressions for the total SNR at the destination and symbol error rate performance are obtained. Computer simulation results verified the accuracy and the correctness of the proposed analysis. Numerical results are provided to show the significant advantages of the relay selection in a cooperative communication system. Furthermore, it can be seen that cooperative diversity networks with relay selection have better SER performance and bandwidth efficiency compared with that of the regular relay networks.

2.5 Joint beamforming design and relay selection

In previous section, the relay selection scheme is explored in the SISO case. Next, we focus on a scenario of a half-duplex MIMO relay network with cooperation of multiple relay nodes.

2.5.1 State of the art and motivation

The beamforming vector design for a MIMO relay system is discussed recently in several literature. The half-duplex MIMO AF relay channel has been considered in [96], the beamforming vector for relay node is designed to maximize the capacity between the source and the destination in the absence of a direct link between the source and the destination. The author developed the optimal linear transceiver for a single relay station system by assuming that the channel state information (CSI) of the source-relay link and the relay-destination link is available at the relay station. In [41], the author designed a joint receive and transmit beamforming for a wireless network consisting of a transmitter, a receiver, and a relay node. Results show that joint processing outperforms the separate optimization of receive and transmit beamforming significantly.

Most of beamforming schemes assume that full CSI knowledge is available at the transmitter side. This assumption is unfortunately infeasible in practice, especially in current frequency division duplex (FDD) systems. A more efficient method is to share a predefined codebook between the source and the destination. In this case, the destination can send back the label of the preferred beamforming vector. This technology is generally referred to the limited feedback technology [53],[110]. The author in [53] employs a Grassmannian codebook to reduce the feedback overhead by limited feedback. For Rayleigh fading channels, the optimal beamforming vector has been shown to be uniformly dis-

tributed on the unit sphere. Based on this observation, the Grassmannian codebook [69] is proved to be an appropriate choice to quantize the beamforming vectors.

In existing literature, the beamforming design and the relay selection is usually considered as two separate processes. In our work, we jointly optimize the beamforming vectors and the relay selection matrix under a limited feedback situation. And we also address the direct link in the system model to provide cooperative diversity gain.

2.5.2 System model

Consider a wireless system where a source node with M_{S} antennas transmits the information to a destination with M_{D} antennas with the help of N relay nodes, which are all equipped with M_{R} antennas. A cooperative communication strategy with two phases is considered, i.e. transmissions are orthogonal either through time or frequency division.

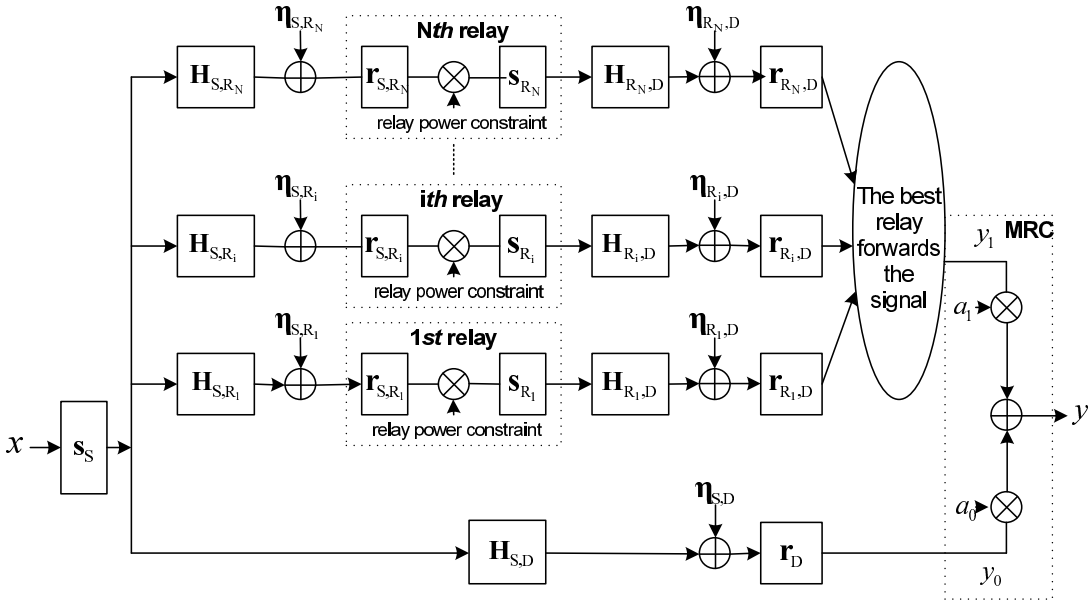

Figure 2.10: Channel model of a half-duplex multiple MIMO AF relay system.

As shown in Figure 2.10, in Phase 1, the source employs the source beamforming vector $\mathbf{s}_{\mathrm{S}}$ to map the input symbol to its antennas and broadcasts its information to the destination and relays. The received signals $\mathbf{y}_{\mathrm{S,D}}$ and $\mathbf{y}_{\mathrm{S,R}_i}$ at the destination and relays can be written as, respectively,

$$\mathbf{y}_{\mathrm{S,D}} = \sqrt{P_{\mathrm{S}}}\mathbf{H}_{\mathrm{S,D}}\mathbf{s}_{\mathrm{S}}x + \boldsymbol{\eta}_{\mathrm{S,D}}, \tag{2.50}$$

$$\mathbf{y}_{\mathrm{S,R}_i} = \sqrt{P_{\mathrm{S}}}\mathbf{H}_{\mathrm{S,R}_i}\mathbf{s}_{\mathrm{S}}x + \boldsymbol{\eta}_{\mathrm{S,R}_i}, \tag{2.51}$$

in which P_{S} is the transmitted power at the source, and x is the transmitted information symbol, here we have assumed $E\{|x|^2\} = 1$ to fulfill the source power constraint. $\boldsymbol{\eta}_{\mathrm{S,D}} \in$

$\mathbb{C}^{M_{\mathrm{R}}\times 1}$ and $\boldsymbol{\eta}_{\mathrm{S,R}_i} \in \mathbb{C}^{M_{\mathrm{D}}\times 1}$ are additive noise vectors, which are modeled as zero-mean, complex Gaussian random variables with variance $\mathcal{N}_0$. The matrices $\mathbf{H}_{\mathrm{S,D}} \in \mathbb{C}^{M_{\mathrm{D}}\times M_{\mathrm{S}}}$ and $\mathbf{H}_{\mathrm{S,R}_i} \in \mathbb{C}^{M_{\mathrm{R}}\times M_{\mathrm{S}}}$ model the flat Rayleigh fading channels of the source-destination and source-ith relay, respectively.

Relays use combining vectors $\mathbf{r}_{\mathrm{S,R}_i}$ to recover input symbol. In Phase 2, the appropriate relay which offers the largest received SNR at the destination will be activated and multiplies the recovered symbol by the relay beamforming vector $\mathbf{s}_{\mathrm{R}_i}$. The relay forwards the transmit signal to the destination with the power P_{R}. The relay transmitted signal is:

$$\mathbf{x}_{\mathrm{relay}} = \mathbf{s}_{\mathrm{R}_i}\sigma\mathbf{r}_{\mathrm{S,R}_i}^H(\sqrt{P_{\mathrm{S}}}\mathbf{H}_{\mathrm{S,R}_i}\mathbf{s}_{\mathrm{S}}x + \boldsymbol{\eta}_{\mathrm{S,R}_i}) \tag{2.52}$$

where σ is the relay amplifier factor to fulfill the relay power constraint. The power constraint limits the power of the relay transmit signal what can be expressed as: $\mathbb{E}\{||\mathbf{x}_{\mathrm{relay}}||^2\} = P_{\mathrm{S}}||\mathbf{s}_{\mathrm{R}_i}\sigma\mathbf{r}_{\mathrm{S,R}_i}^H\mathbf{H}_{\mathrm{S,R}_i}\mathbf{s}_{\mathrm{S}}||^2 + ||\mathbf{s}_{\mathrm{R}_i}\sigma\mathbf{r}_{\mathrm{S,R}_i}^H||^2 = 1$. Therefore, $\sigma = (P_{\mathrm{S}}||\mathbf{H}_{\mathrm{S,R}_i}\mathbf{s}_{\mathrm{S}}||^2 + 1)^{-\frac{1}{2}}$.

The destination uses combining vectors $\mathbf{r}_{\mathrm{D}}$ and $\mathbf{r}_{\mathrm{R}_i,\mathrm{D}}$ to recover two versions of the input symbol which are separated in two phases:

$$y_0 = \sqrt{P_{\mathrm{S}}}\mathbf{r}_{\mathrm{D}}^H\mathbf{H}_{\mathrm{S,D}}\mathbf{s}_{\mathrm{S}}x + \mathbf{r}_{\mathrm{D}}^H\boldsymbol{\eta}_{\mathrm{S,D}} \tag{2.53}$$

$$\begin{aligned} y_1 = {} & \sqrt{P_{\mathrm{R}}P_{\mathrm{S}}}\mathbf{r}_{\mathrm{R}_i,\mathrm{D}}^H\mathbf{H}_{\mathrm{R}_i,\mathrm{D}}\mathbf{s}_{\mathrm{R}_i}\sigma\mathbf{r}_{\mathrm{S,R}_i}^H\mathbf{H}_{\mathrm{S,R}_i}\mathbf{s}_{\mathrm{S}}x \\ & + \mathbf{r}_{\mathrm{R}_i,\mathrm{D}}^H(\sqrt{P_{\mathrm{R}}}\mathbf{H}_{\mathrm{R}_i,\mathrm{D}}\mathbf{s}_{\mathrm{R}_i}\sigma\mathbf{r}_{\mathrm{S,R}_i}^H\boldsymbol{\eta}_{\mathrm{S,R}_i} + \boldsymbol{\eta}_{\mathrm{R}_i,\mathrm{D}}), \end{aligned} \tag{2.54}$$

where $\boldsymbol{\eta}_{\mathrm{R}_i,\mathrm{D}} \in \mathbb{C}^{M_{\mathrm{D}}\times M_{\mathrm{R}}}$ is the destination additive noise vector distributed according to $\mathcal{CN}(0,\mathcal{N}_0)$. The matrices $\mathbf{H}_{\mathrm{R}_i,\mathrm{D}} \in \mathbb{C}^{M_{\mathrm{D}}\times M_{\mathrm{R}}}$ model the flat Rayleigh fading channel of the ith relay-destination link. $\mathbf{r}_{\mathrm{D}}$ and $\mathbf{r}_{\mathrm{R}_i,\mathrm{D}}$ are combining vectors to recover input symbol at the destination.

Therefore, the received SNRs for the source-destination, source-relay, and relay-destination link can be expressed as:

$$\begin{aligned} \gamma_0 &= P_{\mathrm{S}}|\mathbf{r}_{\mathrm{D}}^H\mathbf{H}_{\mathrm{S,D}}\mathbf{s}_{\mathrm{S}}|^2 \\ \gamma_{1,\mathrm{R}_i} &= P_{\mathrm{S}}|\mathbf{r}_{\mathrm{S,R}_i}^H\mathbf{H}_{\mathrm{S,R}_i}\mathbf{s}_{\mathrm{S}}|^2 \\ \gamma_{2,\mathrm{R}_i} &= P_{\mathrm{R}}|\mathbf{r}_{\mathrm{R}_i,\mathrm{D}}^H\mathbf{H}_{\mathrm{R}_i,\mathrm{D}}\mathbf{s}_{\mathrm{R}_i}|^2. \end{aligned} \tag{2.55}$$

Next, the destination combines the signals of the direct link and the selected indirect link by using the MRC technique. The combined signal at the MRC detector can be written as

$$y = a_0y_0 + a_1y_1, \tag{2.56}$$

where the factors a_0 and a_1 are determined such that the SNR of the MRC output is maximized. They can be specified as

$$\begin{aligned} a_0 &= (\sqrt{P_{\mathrm{S}}}\mathbf{r}_{\mathrm{D}}^H\mathbf{H}_{\mathrm{S,D}}\mathbf{s}_{\mathrm{S}})^H/||\mathbf{r}_{\mathrm{D}}||^2, \\ a_1 &= (\sqrt{P_{\mathrm{R}}P_{\mathrm{S}}}\mathbf{r}_{\mathrm{R}_i,\mathrm{D}}^H\mathbf{H}_{\mathrm{R}_i,\mathrm{D}}\mathbf{s}_{\mathrm{R}_i}\sigma\mathbf{r}_{\mathrm{S,R}_i}^H\mathbf{H}_{\mathrm{S,R}_i}\mathbf{s}_{\mathrm{S}})^H/ \\ &\quad (||\mathbf{r}_{\mathrm{R}_i,\mathrm{D}}^H(\sqrt{P_{\mathrm{R}}}\mathbf{H}_{\mathrm{R}_i,\mathrm{D}}\mathbf{s}_{\mathrm{R}_i}\sigma\mathbf{r}_{\mathrm{S,R}_i}^H||^2 + ||\mathbf{r}_{\mathrm{S,R}_i}^H||^2). \end{aligned} \tag{2.57}$$

If we assume the appropriate relay is selected, the received total SNR can be expressed as:

$$\begin{aligned} \gamma_{\mathrm{D}} &= \gamma_0 + \gamma_{\mathrm{R}_i} \\ &= \gamma_0 + \frac{\gamma_{1,\mathrm{R}_i}\gamma_{2,\mathrm{R}_i}}{\gamma_{1,\mathrm{R}_i} + \gamma_{2,\mathrm{R}_i} + 1} \\ &= \frac{P_{\mathrm{S}}P_{\mathrm{R}}|\mathbf{r}_{\mathrm{R}_i,\mathrm{D}}^H\mathbf{H}_{\mathrm{R}_i,\mathrm{D}}\mathbf{s}_{\mathrm{R}_i}\sigma\mathbf{r}_{\mathrm{S,R}_i}^H\mathbf{H}_{\mathrm{S,R}_i}\mathbf{s}_{\mathrm{S}}|^2}{||\mathbf{r}_{\mathrm{R}_i,\mathrm{D}}^H\sqrt{P_{\mathrm{R}}}\mathbf{H}_{\mathrm{R}_i,\mathrm{D}}\mathbf{s}_{\mathrm{R}_i}\sigma\mathbf{r}_{\mathrm{S,R}_i}^H||^2 + 1} + P_{\mathrm{S}}||\mathbf{r}_{\mathrm{D}}^H\mathbf{H}_{\mathrm{S,D}}\mathbf{s}_{\mathrm{S}}||^2, \end{aligned} \tag{2.58}$$

where we have assumed $\mathbb{E}\{|x|^2\} = 1$ and $||\mathbf{r}_{\mathrm{D}}|| = ||\mathbf{r}_{\mathrm{S,R}_i}|| = ||\mathbf{r}_{\mathrm{R}_i,\mathrm{D}}|| = 1$ without loss of generality.

2.5.3 Optimal beamforming design and relay selection approach with full CSI assumption

Previous related work on beamforming design has been done in [43] which aims at optimizing the system rate by using an iterative approach in the scenario of a single MIMO AF relay network without cooperation with the direct link. Here, we intend to find the optimal source beamforming vector $\mathbf{s}_{\mathrm{S}}^*$, the appropriate relay index i and the relay beamforming vector $\mathbf{s}_{\mathrm{R}_i}^*$ which maximize the total received SNR subject to the relay power constraints. This optimization problem can be expressed as:

$$\begin{aligned} \max_{\mathbf{s}_{\mathrm{S}},\mathbf{s}_{\mathrm{R}_i},i} & \frac{P_{\mathrm{S}}P_{\mathrm{R}}|\mathbf{r}_{\mathrm{R}_i,\mathrm{D}}^H\mathbf{H}_{\mathrm{R}_i,\mathrm{D}}\mathbf{s}_{\mathrm{R}_i}\sigma\mathbf{r}_{\mathrm{S,R}_i}^H\mathbf{H}_{\mathrm{S,R}_i}\mathbf{s}_{\mathrm{S}}|^2}{||\mathbf{r}_{\mathrm{R}_i,\mathrm{D}}^H\sqrt{P_{\mathrm{R}}}\mathbf{H}_{\mathrm{R}_i,\mathrm{D}}\mathbf{s}_{\mathrm{R}_i}\sigma\mathbf{r}_{\mathrm{S,R}_i}^H||^2+1} + P_{\mathrm{S}}||\mathbf{r}_{\mathrm{D}}^H\mathbf{H}_{\mathrm{S,D}}\mathbf{s}_{\mathrm{S}}||^2, \\ & \text{s.t.} \quad \sigma = (P_{\mathrm{S}}||\mathbf{H}_{\mathrm{S,R}_i}\mathbf{s}_{\mathrm{S}}||^2 + 1)^{-\frac{1}{2}} = 1. \end{aligned} \tag{2.59}$$

To solve this optimization problem we first consider the single relay scenario in Figure 2.11 as a sub-problem.

For each relay, the total SNR is maximized if γ_0 and γ_{R_i} are maximized, which are shown in (2.58). The only common parameter in maximizing these two parts is the source beamforming vector $\mathbf{s}_{\mathrm{S}}$. By fixing $\mathbf{s}_{\mathrm{S}}$ the optimal values of the other parameters can be

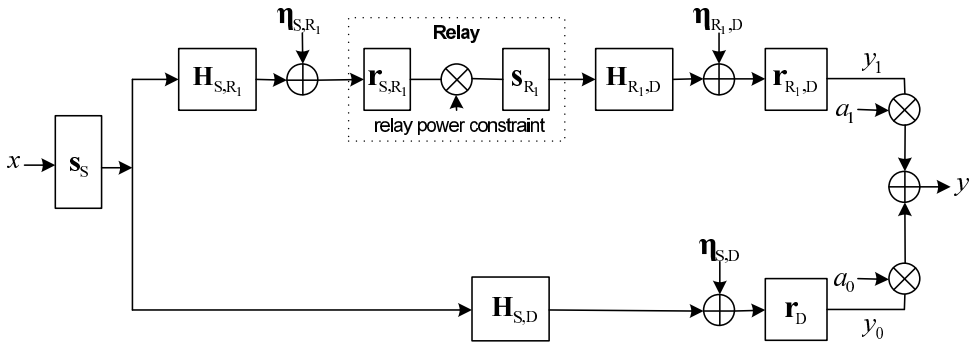

Figure 2.11: Half-duplex single MIMO AF relay channel model with the direct link.

easily obtained as shown in [53]. After other parameters are determined, the optimal $\mathbf{s}_{\mathrm{S}}^{*}$ for a specific relay can be expressed as:

$$\mathbf{s}_{\mathrm{S}}^{*} = \arg \max_{||\mathbf{s}_{\mathrm{S}}||=1} \frac{P_{\mathrm{S}}||\mathbf{H}_{\mathrm{S},\mathrm{R}_i}\mathbf{s}_{\mathrm{S}}||^2 P_{\mathrm{R}}||\mathbf{H}_{\mathrm{R}_i,\mathrm{D}}\mathbf{s}_{\mathrm{R}_i}^{*}||^2}{1 + P_{\mathrm{S}}||\mathbf{H}_{\mathrm{S},\mathrm{R}_i}\mathbf{s}_{s}||^2 + P_{\mathrm{R}}||\mathbf{H}_{\mathrm{R}_i,\mathrm{D}}\mathbf{s}_{R_i}^{*}||^2} + P_{\mathrm{S}}||\mathbf{H}_{\mathrm{S},\mathrm{D}}\mathbf{s}_{\mathrm{S}}||^2, \tag{2.60}$$

where the optimal relay beamforming vector is $\mathbf{s}_{\mathrm{R}_i}^{*} = \arg\max_{||\mathbf{s}_{\mathrm{R}_i}||=1} P_{\mathrm{R}}||\mathbf{H}_{\mathrm{R}_i,\mathrm{D}}\mathbf{s}_{\mathrm{R}_i}||^2$.

After the source and relay beamforming vectors are determined, the appropriate relay which offers the maximum result of the objective function (2.59) will be selected.

It has to be noted that the objective function in (2.59) may have multiple local maximal points. This problem does not have analytic solution. Hence, we use an iterative approach to perform this optimization. Therefore, we are more interested in a suboptimal scheme which has a more simple structure and can provide some insight on the design of a limited feedback beamforming scheme.

2.5.4 Proposed scheme with limited feedback

After having identified the optimal scheme, we continue to consider the limited feedback scheme for the beamforming design and relay selection in the current system. In this section, we assume that channel state information is only available at the receiver side, i.e. the relay node knows $\mathbf{H}_{\mathrm{S},\mathrm{R}_i}$ and the destination node knows $\mathbf{H}_{\mathrm{S},\mathrm{D}}$ and $\mathbf{H}_{\mathrm{R}_i,\mathrm{D}}$. Respect to the limited feedback, we assume that the source beamforming vector $\mathbf{s}_{\mathrm{S}}$ is chosen from a codebook $\mathbf{C}_0$ shared between the source and destination. The relay beamforming vector $\mathbf{s}_{\mathrm{R}_i}$ is chosen from a codebook $\mathbf{C}_2$ shared between the relay and the destination.

To solve the optimization problem in (2.59), the knowledge of $\mathbf{H}_{\mathrm{S},\mathrm{R}_i}$ and $\mathbf{H}_{\mathrm{S},\mathrm{D}}$ should be available at one node (the relay or the destination). That means the destination and relays should exchange their information about $\mathbf{H}_{\mathrm{S},\mathrm{R}_i}$ and $\mathbf{H}_{\mathrm{S},\mathrm{D}}$. In [53], the author proposed a scheme of quantizing the channel $\mathbf{H}_{\mathrm{S},\mathrm{D}}$ and feedback this information to the

relay node. This scheme requires extreme accuracy for channel quantization and generates additional feedback delay. Therefore, we propose a limited forwarding strategy, in which relays quantize the source-relay channel $\mathbf{H}_{\mathrm{S,R}_i}$ by using a proper codebook and forward this information to the destination. It has to be noted that, $||\mathbf{H}_{\mathrm{S,R}_i}\mathbf{s}||^2 = \sum_{i=1}^{M} d_i^2 |\mathbf{v}_i^H \mathbf{s}|^2$, where $M = \mathrm{rank}(\mathbf{H}_{\mathrm{S,R}_i})$, $\mathbf{v}_i$ and d_i^2 are right singular vectors and singular values of $\mathbf{H}_{\mathrm{S,R}_i}$, respectively. With this theorem, the destination only needs to be aware of singular values and right singular vectors of the source-relay channels. Since our focus in this work is on the vector quantization feedback scheme, the channel information can be exchanged by using the existing well-designed vector codebook instead of other matrix codebooks.

The singular value is real scalar and can be efficiently quantized with a conventional scalar quantizer. For quantizing the singular vectors, the relay and the destination share a codebook $\mathbf{C}_1$. Each singular vector $\mathbf{v}_i$ is quantized to a vector $\tilde{\mathbf{v}}_i \in \mathbf{C}_1$ with minimal chordal distance [39]:

$$\tilde{\mathbf{v}}_i = \arg \min_{\mathbf{w} \in \mathbf{C}_1} \sqrt{1 - |\mathbf{w}^H \mathbf{v}_i|^2}, \tag{2.61}$$

where the chordal distance of two unit vectors is the sine of the angle between the two vectors.

It is known that these right singular vectors are uniformly distributed on the unit sphere for a Rayleigh fading channel matrix. [69] has shown that the criterion of maximizing the minimum Grassmannian subspace distance between any pair of codewords is quasi-optimal in this situation. [43] discussed the source and relay beamforming codebook design criteria. It showed that the conventional Grassmannian subspace packing method is able to guarantee the overall performance in dual hop pre-coding systems. However, it is still an open problem whether the developed codebook design can be directly employed in our system.

By substituting all the quantized vectors into (2.58), the destination obtains the received SNR of all individual relay links combined with the direct link:

$$\gamma_{\mathrm{D}_i} = \gamma_0 + \frac{\gamma_{1,\mathrm{R}_i} \gamma_{2,\mathrm{R}_i}}{\gamma_{1,\mathrm{R}_i} + \gamma_{2,\mathrm{R}_i} + 1}, \tag{2.62}$$

where γ_{1,R_i}, γ_{2,R_i} and γ_0 are given in (2.55).

The destination node compares all γ_{D_i} values and the relay creating the largest received SNR is selected as the appropriate relay node. In the following, we outline the steps to determine beamforming vectors and the preferred relay with the limited feedback schemes:

- Each relay quantizes the right singular vectors and singular values of the source-relay channels using a codebook $\mathbf{C}_1$, which is shared between the relay and the

destination. Labels of these quantized vectors and quantized values are sent to the destination.

- The destination computes all received SNR objective functions (2.62). The optimal relay and optimal beamforming vector with the maximum γ_{D_i} are selected.

- The destination feedbacks the label of the relay beamforming vector to the selected relay, which will be used in the second transmit phase. Moreover, it sends the label of the source beamforming vector and selected relay to the source. The source uses this vector as its beamforming vector in the first transmit phase.

2.5.5 Simulation results

To evaluate the SER performance of the optimal and the proposed beamforming design as well as relay selection schemes in a multiple MIMO AF relay network, the simulation configurations are shown as follows. The antenna configuration is focused on $(M_{\mathrm{S}}, M_{\mathrm{R}}, M_{\mathrm{D}}) = (2, 2, 1)$. The input symbols belong to a QPSK constellation with unit power. We assume a quasi-static flat fading channel model, in which the channel matrices are modeled as i.i.d Rayleigh fading channels according to $\mathcal{CN}(0, \mathcal{N}_0)$. The transmitted power at all the relay stations is set to $10 \log P_{\mathrm{R}} = 8$dB. The Grassmannian codebook provided in [68] is employed with different codebook sizes (see Appendix A).

In Figure 2.12, we compare several schemes in a single relay scenario, which is shown in Figure 2.11, including the optimal beamforming scheme with full CSI, the quantizing scheme from [53], the random vector quantization and our proposed scheme. The SER values are recorded for different values of the transmitted power P_{S} at the source node. From these SER curves, we find that our scheme outperforms other quantization schemes and only shows slight performance loss compared to the optimal beamforming scheme in the single relay scenario. For the optimal beamforming scheme, we use the brute-force method to find the locally optimal source beamforming by using (2.60).

Our proposed scheme consists of three codebooks $\mathbf{C}_0$, $\mathbf{C}_1$ and $\mathbf{C}_2$ with size N_0, N_1 and N_2 bits, respectively. Following the three steps for our proposed scheme, one can easily conclude that it needs in total $N*R*(b+N_1)+N_0+N_2$ feedback bits, where R is the rank of source-relay channel, b is the number of bits that a scalar quantizer uses and N is the number of relays. Whereas the scheme proposed in [53] requires $(R+1)*b+N_0^R+N_1+N_2$ feedback bits. Table 2.1 compares these values for the case of $N = N_0 = N_1 = N_2 = 3, \text{or } 4$. When we consider the case of a 4 relays scenario and $b = 3$, the proposed algorithm has about 35% less feedback bits compared with the existing work in [53]. From these

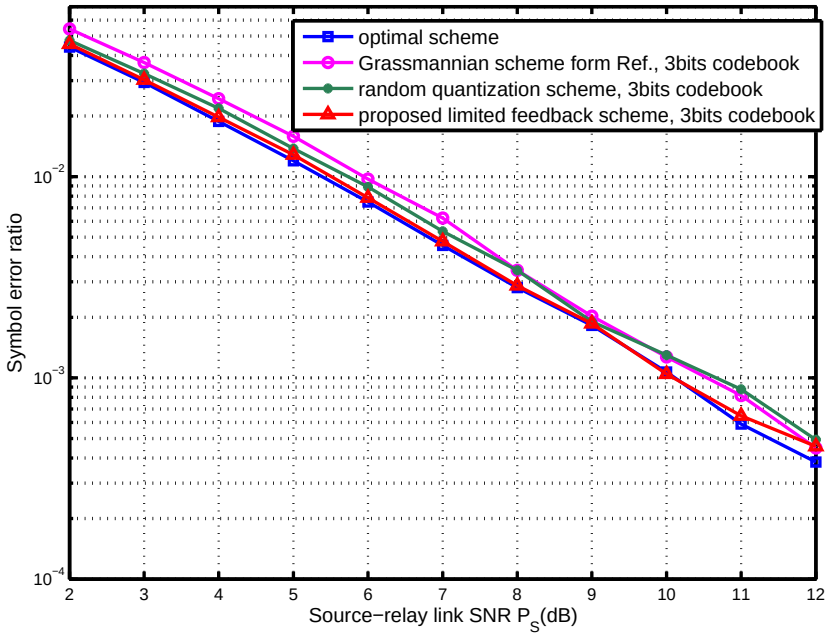

Figure 2.12: SER performance of different schemes in single MIMO relay scenario with direct link.

results, we can also conclude that our proposed algorithm shows more advantage over the existing approach in literature when the number of cooperated relays increases.

Table 2.1: Comparison of feedback bits for different quantization schemes

Scheme	Number of feedback bits	
	Codebook size=3 bits	Codebook size=4 bits
Quantized scheme from [53]	$(3b+12)*N$	$(4b+15)*N$
Proposed scheme	$(2b+6)*N+6$	$(3b+9)*N+6$

Figure 2.13 compares the SER performance of a multiple MIMO AF relay system with different values of the number of relay nodes. Our proposed scheme shows only slight performance degradation compared with the optimal full CSI case. The simulation results verify that as the number of relay nodes N increases the performance of this cooperative system also increases due to the so-called "selection diversity" effect. We can also notice that the number of cooperating relays has a strong impact on performance enhancement since the achieved diversity order of the analyzed system is equal to $N+1$.

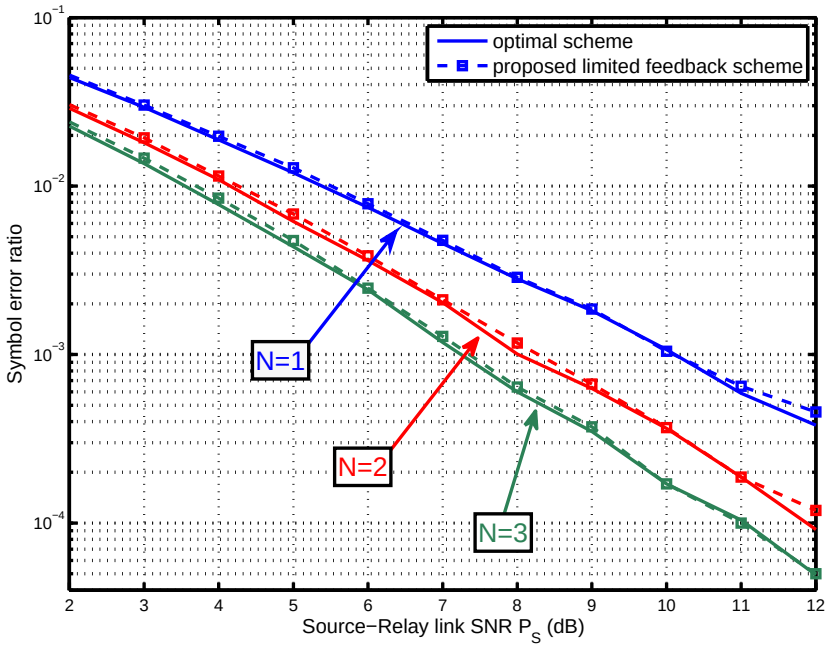

Figure 2.13: SER performance of the optimal and the proposed schemes with different numbers of relay nodes.

2.5.6 Conclusion

In this section, relay selection and beamforming vector design schemes for a half-duplex multiple MIMO AF relay network has been discussed. We firstly assumed the channel state information is available at all nodes to investigate the optimal source and relay beamforming vector design and the relay selection. Based on this structure, a new limited feedback joint relay selection and beamforming vector design scheme, which employs a new channel quantization strategy and centralized selection, was proposed. The proposed scheme, which chooses the best relay and optimizes the beamforming vectors maximizing the received SNR, can significantly reduce the required number of feedback bits and maintain a suitable performance compared to the optimal non-practical solution. Simulation results show that our scheme approaches the performance of the scheme with full CSI assumption and outperforms conventional schemes, while having lower computational complexity and lower feedback delay. The cooperative diversity gain is also verified by the simulation result.

2.6 Summary

This chapter starts with a brief overview of cooperative communications. The relay protocol differs according to relay signal processing capabilities. Three of main relaying protocols are the amplify-and-forward, decode-and-forward, and compress-and-forward relaying.

Then we have discussed the performance comparisons of basic cooperation protocols through calculating outage capacity and characterizing diversity gains in a single relay scenario. In a multiple relay scenario, the research of relay selection always attracts attention since the performance of relay transmissions is strongly affected by the collaborative strategy.

We have derived an exact closed-form expression for the symbol error probability of the selective DF relaying strategy over Rayleigh fading channels. Simulation results verify the accuracy and the correctness of the proposed analysis. Numerical results show the significant advantages of the relay selection in a cooperative communication system and can be considered as a performance lower bound for the future research.

Furthermore, an effective joint beamforming vector design and relay selection scheme for a MIMO relay system has been proposed. Most of existing literature assumes that the channel state information is available at all nodes. We have employed a new channel quantization strategy to jointly design beamforming vectors and perform relay selection with limited feedback. Simulation results show that proposed scheme outperforms other quantization schemes and only shows slight performance loss compared to the theoretical optimal beamforming design. With respect to the number of feedback bits, our algorithm shows great advantage compared to the scheme proposed in [53].

Chapter 3

Relay enhanced LTE-A cellular network

3.1 Evolution of LTE

The Long Term Evolution (LTE) technology was standardized as part of the 3GPP Release 8, which was finalized in December 2008. The LTE standard is an evolution of the UMTS (3G) with many improved features. The LTE utilizes orthogonal frequency domain multiple (OFDM) and MIMO technologies to improve the spectral efficiency and transmission rate. It can provide downlink peak rate of 300 Mbit/s, uplink peak rates up to 75 Mbit/s and a radio access network delay of less than 5 ms. LTE supports scalable carrier bandwidths, from 1.4 MHz to 20 MHz, to increase the spectrum flexibility. The LTE specification improves the support for fast-moving mobiles (up to 350 km/h) and multi-cast broadcast streams. Both frequency division duplex (FDD) and time-division duplex (TDD) communication systems are included in the LTE standard. Moreover, the LTE utilizes orthogonal frequency domain multiple access (OFDMA) for downlink transmission and single-carrier frequency domain multiple access (SC-FDMA) for uplink to conserve power.

The 3GPP Release 9 as an minor enhancement of Release 8 brought some additional features and smaller optimizations:

- deployment of Home eNodeB (HeNB) (LTE femtocells),
- location services to pinpoint the location of a mobile device (LTE positioning),
- self organizing network (SON) features,
- evolved multimedia broadcast and multicast service (eMBMS) for LTE,
- public warning system (PWS) .

LTE-Advanced, which is an enhanced evolution of LTE, is motivated by meeting the performance requirements set by the international telecommunication union (ITU) for 4G cellular networks to be deployed globally [109]. LTE-Advanced refers to 3GPP Release 10 which is a major release compared to 3GPP Release 9. In recent years, the technology

of LTE-Advanced develops very fast because of the aim of achieving high-speed, high-capacity and high-coverage communications. There are some important new techniques brought out: carrier aggregation (CA), relay nodes, enhanced MIMO, enhanced inter-cell interference coordination (eICIC), and coordinated multipoint processing (CoMP) as shown in Figure 3.1. During Release 10 time frame, all of them except CoMP were standardized. Notable features of LTE-A included:

- Increased peak data rate: DL 3 Gbit/s, UL 1.5 Gbit/s,
- Higher spectral efficiency: from a maximum of 16 bit/s/Hz in R8 to 30 bit/s/Hz in R10,
- Allowing the combination of up to five separate carriers to enable bandwidths up to 100 MHz,
- Higher order MIMO antenna configurations up to 8x8 downlink and 4x4 uplink,
- Increased number of simultaneously active subscribers,
- Improved performance at cell edges, e.g. for DL 2x2 MIMO at least 2.40 bit/s/Hz/cell.

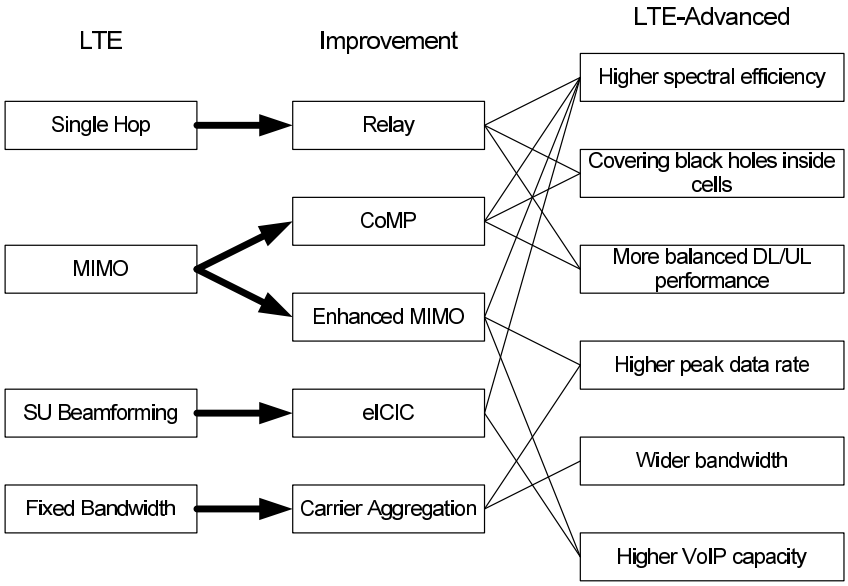

Figure 3.1: The key features from LTE to LTE-Advanced.

3GPP Release 11, which was finalized in 2013, was built on the platform of Release 10 with a number of refinements to existing capabilities, e.g., enhancements to carrier aggregation, MIMO, relay nodes and eICIC, introduction of new frequency bands, and

coordinated multipoint transmission and reception to enable simultaneous communication with multiple cells.

The next evolutionary step of LTE (Release 12) started at a 3GPP RAN workshop in June 2012. The expected freeze date for Release 12 is September 2014. New requirements of Release 12 are energy saving, cost efficiency, support for diverse application and traffic types, and backhaul enhancements [13]. Some of new features for Release 12 included:

- enhanced small cells for LTE,
- inter-site carrier aggregation, to mix and match the capabilities and backhaul of adjacent cells,
- enhanced multi-antenna transmission: massive MIMO,
- inter-operation between LTE and WiFi or HSPDA,
- new and enhanced services.

3.2 Relay in LTE-Advanced

Relaying is one of the features being proposed for the 4G LTE-Advanced system. In the LTE system, the use of technologies such as MIMO and OFDM can significantly improve the spectral efficiency and the network capacity for the whole network, but do not fully mitigate the problems experienced at the cell edge. As the cell edge performance is becoming more critical, it is necessary to look at solutions that will enhance the performance at the cell edge with a comparatively low cost. One solution that is being investigated and proposed is that of the use of LTE relays.

3.2.1 Classifications of current relaying concepts

In different application scenarios, it may require different types of relay node. Categorization of relay can be done according to many aspects, e.g., the duplex format, the transmission scheme, and so on. Figure 3.2 summarizes technical criteria of different fundamental relaying approaches.

Half and full duplex relay

With the respect to duplex format, the relay nodes can be classified into the half-duplex and full-duplex relay. In the half-duplex relay, the transmission and reception cannot happen simultaneously, i.e. the transmissions must be time multiplexed or frequency multiplexed. In the full-duplex relay, the relay is able to transmit and receive at the same time, if there is good isolation between the transmit and receive antennas.

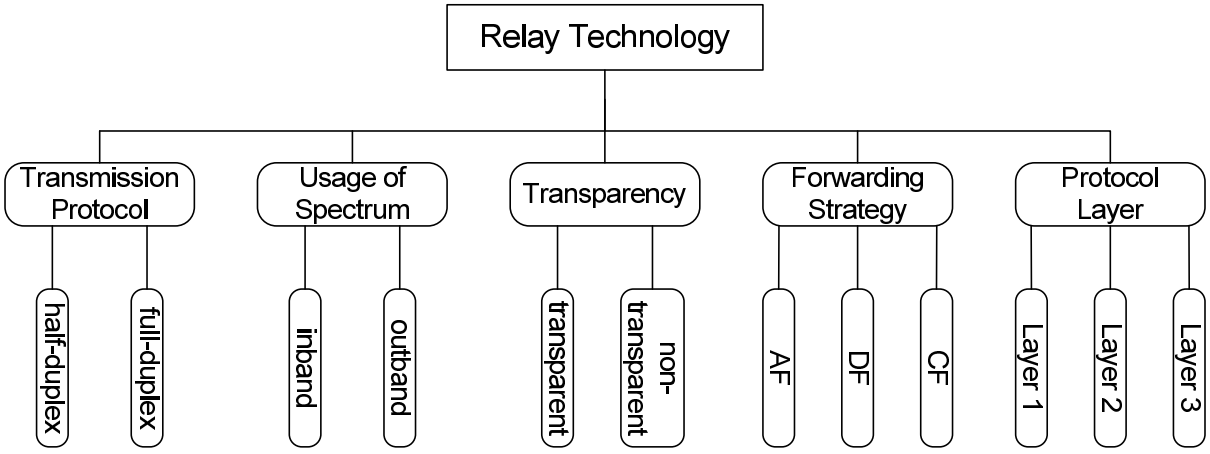

Figure 3.2: A taxonomy of current relaying technologies.

Inband and outband relay

With the respect to the relay node's usage of spectrum, its operation can be classified into inband and outband. In inband case, the eNB-relay link shares the same carrier frequency with relay-user equipment (UE) links. Whereas, in outband case, the eNB-relay link does not operate in the same carrier frequency as relay-UE links. During inband relaying, the relay node might cause interference to its own receiver because the relay transmitter could be transmitting on the same frequency band as its own relay UEs. This implies backhaul link transmission and access link reception, or backhaul link reception and access link transmission cannot happen simultaneously. Therefore, half-duplex mode should be deployed for inband relaying, unless a sufficient isolation of the outgoing and incoming signals is provided, such as by means of well-isolated antenna structures. In contrast, outband relay operation is straightforward, since it only requires adequate frequency planning.

Transparent and non-transparent relay

With the respect to the knowledge at the UE, relays can be classified into transparent and non-transparent. In the transparent case, the UE is not aware of whether or not it communicates with the network via the relay. In non-transparent case, the UE is aware of whether or not it is communicating with the network via the relay.

Different forwarding strategies relay

As we mentioned in Chapter 2, a relay can be classified with regarding to forwarding strategies. An AF relay, which is normally referred to as repeater, simply scales the signal and transmits an amplified version of it to the destination. DF relay is more sophisticated, since it first decodes and then regenerates the transmitted signal. Due to

this ability, the DF relay can utilize link adaptation and interference control. However, this behavior causes additional complexity and protocol overhead. In CF relay, the relay sends a compressed version of the source transmission to the destination.

Relay protocol layers

According to the protocol layers in which the main functionality is performed, the relays can be classified as Layer 1, Layer 2 and Layer 3 relay [48]. As their names imply, they work at different Layers of the protocol stack. The Layer 1 relay is also called as repeater, which works at the physical layer (PHY) , is mainly used for coverage extension with advantages of low-cost implementation and short processing delays. Specifications on repeater performance are already defined in LTE Rel. 8. The Layer 2 relay works up to the medium access control (MAC) and radio link control (RLC) layers. With demodulation and decoding processing, the Layer 2 relay overcomes the drawback in Layer 1 relays caused by amplification of interference and noise. A better throughput effect can therefore be expected compared with Layer 1 relay. The Layer 3 relay, which has fractional functions of the base station (BS), can improve throughput by eliminating inter-cell interference and noise. In 3GPP, it has been standardized specifications for the layer 3 relay technology in LTE Rel. 10.

3.2.2 Relay types in 3GPP

As defined in 3GPP specification, there are two basic types of relay node (RN) that are being proposed [9]: Type 1 relay and Type 2 relay, which are nontransparent and transparent, respectively.

- Type-1 relays: The basic Type 1 LTE relay provides half duplex with inband transmission. The relay nodes, which appear in the same way as a regular eNB, control cells with their own identity including the transmission of their own synchronization channels and reference symbols.
- Type-2 relays: From the perspective of the UE, UEs are not able to distinguish a relay from the main eNB within the cell, i.e., a relay node just expands the cell spanned by the donor eNB (DeNB) .

The relay classification and corresponding features in LTE-A are summarized in Table 3.1.

Type-1 relays

The baseline for Type-1 relays has been deeply discussed in the LTE-A specification Release 10, i.e., including all relevant parts that have been standardized. From the

Table 3.1: Summary of relay classification & features

Relay type	Duplex format	Knowledge in the UE	Usage of spectrum	Cell ID
Type 1	Half-duplex	Non-transparent	Inband	Yes
Type 1.a	Full-duplex	Non-transparent	Outband	Yes
Type 1.b	Full-duplex	Non-transparent	Inband	Yes
Type 2	Full-duplex	Transparent	Inband	No

DeNB point of view, the Type-1 relay initially acts as a UE when it attaches to the network. After receiving information with signaling messages from the eNB, the RN identifies itself as a relay. The wireless backhaul link (eNB-RN) is specified in form of a new introduced air interface Un between DeNB and RN in LTE-A. From the UE point of view, a Type-1 relay behaves similarly to an eNB. The wireless access link (relay-UE) is therefore compliant to the standard air interface Uu in 3GPP, which ensures backward compatibility to LTE Release 8 UEs. However, it has significant differences from a macro cell eNB. First of all, a Type-1 relay has much lower transmit power and antenna gains, and the number of antennas might be very limited due to the size of relay sites. Also, since the channel capacity of wireless backhaul is generally inferior to wire backhaul, the performance of relay link will be limited by the wireless backhaul.

As mentioned before, the RN communicates with the eNB via the backhaul link and with the UE via the access link. To avoid self-interference, these two transmissions should be separated either in time, frequency, or antenna configuration. Hence, 3GPP further distinguishes three different sub-types within Type-1 relays [9]:

- Type 1 relay: This relay is an inband relay in which the backhaul link and access link share the same carrier frequency. Isolation is done in the time domain, implying that some of the sub-frames are reserved for the backhaul link and cannot be used for the access link to the relay-attached UEs.

- Type 1a relay: This relay is an outband relay in which separate carrier frequencies are used for the backhaul and access link. Isolation is already achieved in the frequency domain.

- Type 1b relay: This relay is also an inband relay; however, isolation is not done in the time domain, but via adequate antenna configuration.

In 3GPP Release 10, only the first two classes are envisioned.

Type-2 relays

As already mentioned above, Type-2 relay nodes are transparent, which means that the UE is not aware of the presence of an RN in the transmission path. More specifically, a Type-2 RN is characterized by the following features in 3GPP [9] (although the detailed scheme and functionality of Type-2 relay have not been defined so far in LTE-A specification):

- Type-2 relays do not have a separate physical cell ID, synchronization, or broadcast channels.
- Type-2 relays are transparent to Release 8 LTE UEs; a Rel-8 UE should not be aware of the presence of a Type-2 RN.
- Type-2 relays can transmit their own physical downlink shared channel (PDSCH) to achieve an increase in overall cell capacity.
- Type-2 relays at least do not transmit cell-specific reference signal (CRS) and physical downlink shared channel (PDCCH).

With these features, the main objective of a Type 2 relay is to increase the system capacity. It is mainly used to increase data throughput for local UEs. Type 2 relays can eliminate propagating the interference and noise to the next hop, so they can reinforce signal quality and achieve much better link performance. Since a UE is also unable to provide a channel quality indicator (CQI) feedback for relay signals in a Type 2 relay, effective link adaptation is not possible. Moreover, as UE is unaware of the existence of the relay, it is unable to provide a measurement report to aid the eNB in selection of the best relay node.

3.2.3 LTE-A relay scenarios

The relay technology attracts more research interests after it is announced to be considered as part of the LTE Advanced standard. In [30], several potential relay scenarios, which are of current interest to major operators, are presented as shown in Figure 3.3. Although not all of them were included in the 3GPP Release 11 specification, the discussion still makes sense to identify future relay technologies.

- Rural area

  In a rural area, the environment varies slowly and features low user density. Additional relay node deployment can provide an efficient solution to reduce the macro eNBs deployment cost in this case. As line of sight (LOS) situations are mostly

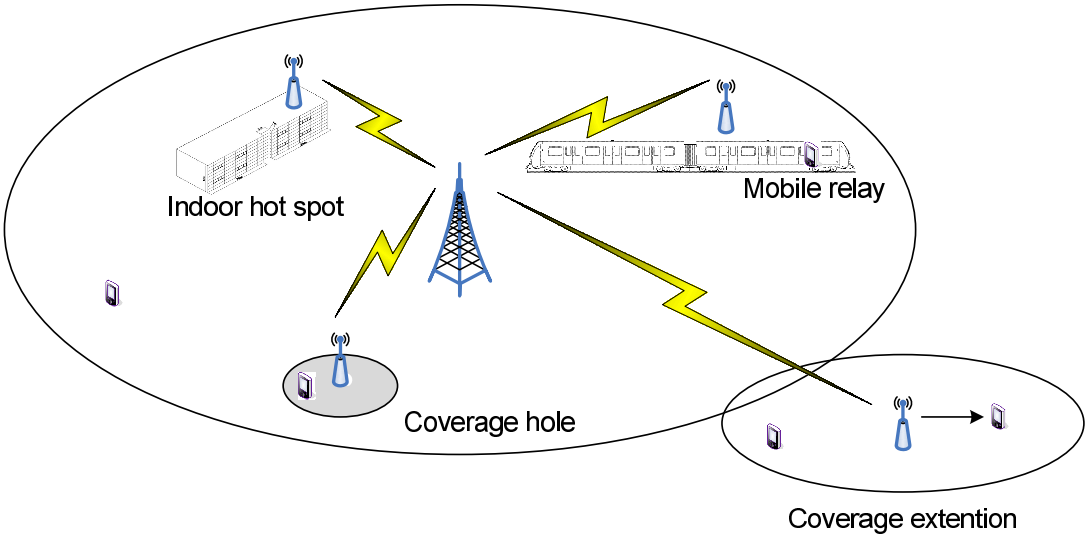

Figure 3.3: Potential LTE-A relay scenarios.

dominating to non-line-of-sight (NLOS) in rural, the density of RN can be very low and the coverage radius is expected to be several kilometers. Furthermore, considering the long distance between the RN and eNB, the signal-to-interference-plus-noise ratio (SINR) at the relay node is usually low, which prompts the need for decode and forward relay to improve the SNR at the UEs side.

- Urban scenario

  In the urban scenario, the user density is quite high, so that the whole network may become congested. By deploying relay nodes inside a macro eNB, the network could obtain a higher capacity while providing coverage enhancement. However, due to the densely deployed macro eNBs and RNs, interference scenarios become very complex and difficult to predict. Hence, good interference cancellation and relay selection schemes are desired in such a scenario.

- Coverage hole

  In this case, the aim is to achieve coverage extension for users in coverage holes, e.g., significant building blocking creates an isolated area where signals from nearby eNBs can barely reach. Fixed relay nodes with site planning are proposed for this scenario to remove a coverage hole in the original service area without harm to the total cell throughput.

- Indoor hot spot

  In this scenario, the relay is supposed to enhance the received signal power of

indoor users, similarly to a home eNB (femto cell or pico cell). The benefit of the relay is its flexibility since it uses a wireless backhaul with less position limitation. This scenario is different from the urban hot spot in the sense that most users are indoors and stationary. The main challenge in this scenario is to combat with superior shadowing and indoor penetration loss. The backhaul link may suffer building penetration loss if the relay backhaul antenna is inside the building. To ensure that the RN can offer better performance compared to the macro and UE connection, the RN's antenna of the backhaul link can be placed in a location that would result in good backhaul connection. Test results in [81] show that a relay can be a good candidate to provide outdoor to indoor coverage due to its flexibility to be deployed.

- Mobile relay

  This scenario refers to a mobile relay station intended to facilitate higher throughput and lower handover outage for on-board users, who are in a highly mobile public transport (train or bus). The aim of this scenario is to mitigate the frequent handover problem which is caused by high speed mobility of a group of UEs. In this scenario, the RNs are installed on the top of the moving vehicles. Consequently, the access links between RN and UEs are relatively stationary. However, the capacity of the backhaul link is likely to be the bottleneck for this scenario. Recently, relays for high speed trains have gained significant interest. Building high speed railways have become national key projects in some countries. To provide high speed communications for on-board passengers is also part of those national-key projects. Fast communications are crucial as passengers on high speed trains are more likely to be data-hungry professionals and would access the internet and emails when on-board.

- Emergency or temporary network deployment

  Because of the natural self-backhaul functionality, the relay technology can be used to provide temporary wireless communication services in the case of after a disaster or during special events such as sport games, outdoor concerts, public gatherings, etc. Self-organizing network mechanisms should support the network roll-out and operation.

3.3 Dynamic system level simulator for relay-enhanced LTE-A network

System-level simulations (SLS) typically are aimed at the performance evaluation at layer 1 and 2. Hence, both link-level and higher-layer effects are typically abstracted and/or

taken from detailed offline simulations of the respective resolution.

At the system level, a geographical deployment of the user equipment, base stations, relay nodes, are simulated. The path gain between each entity is evaluated by taking into consideration the relative position of the two entities, their antenna patterns, a path loss and shadowing model. Frequency selective channels can be generated by these parameters. From the set of channel gains and transmit powers, SINR for each receiver is computed. Furthermore, with considering the scheduling and retransmission strategy, the user throughput can be directly derived by look-up tables generated from independent simulators. Of course, the higher the realism of a simulator, the larger its complexity.

In our work, we develop a dynamic system level simulator for a relay-enhanced LTE-A system based on the existing work of M. Simsek [90]. Our SLS is based on resource element basis, i.e. per sub-carrier (in frequency) and per OFDM symbol (in time).

3.3.1 Deployment model

First aspects in the characterization of a wireless system are the environments for which it is designed and the usage conditions. These include, e.g., the cellular environment/coverage area (macro cells, micro cells or local hotspots), antenna configuration, channel models, user density/distribution and intended mobility (full mobility at different speed or stationary access) and traffic models. These aspects are typically summarized in the so-called deployment scenario. While the deployment scenario serves as a comparison criterion in itself, it also has implications on the typical radio conditions and influences the expected performance. Separate system performance comparisons should be made for each deployment scenario.

Macro environment

Cellular networks are divided into cells, each cell being served by one or more transceivers composing a base station. Base stations with three transceivers serving three sectors per site are placed on a hexagonal grid with wrap around to avoid border effects. The number of sites can be vary, and the typical values are 1, 7 and 19. Typical inter-site distances (ISD) of macro cells are 500 m (ITU urban macro cell / 3GPP case 1) and 1732 m (ITU high speed rural macro cell / 3GPP case 3). The macro UEs are distributed uniformly in the entire cellular environment. And to get statistically representative results the typical minimum number of UEs for a macro cell scenario is 30 UEs for each sector [9], i.e., 570 UEs for layout with 19 cells / 57 sectors and 210 UEs for layout with 7 cells / 21 sectors. Deployment scenarios considered for LTE are essentially urban and suburban. The system will be optimized for low velocities (i.e. below 30 km/h) but shall provide

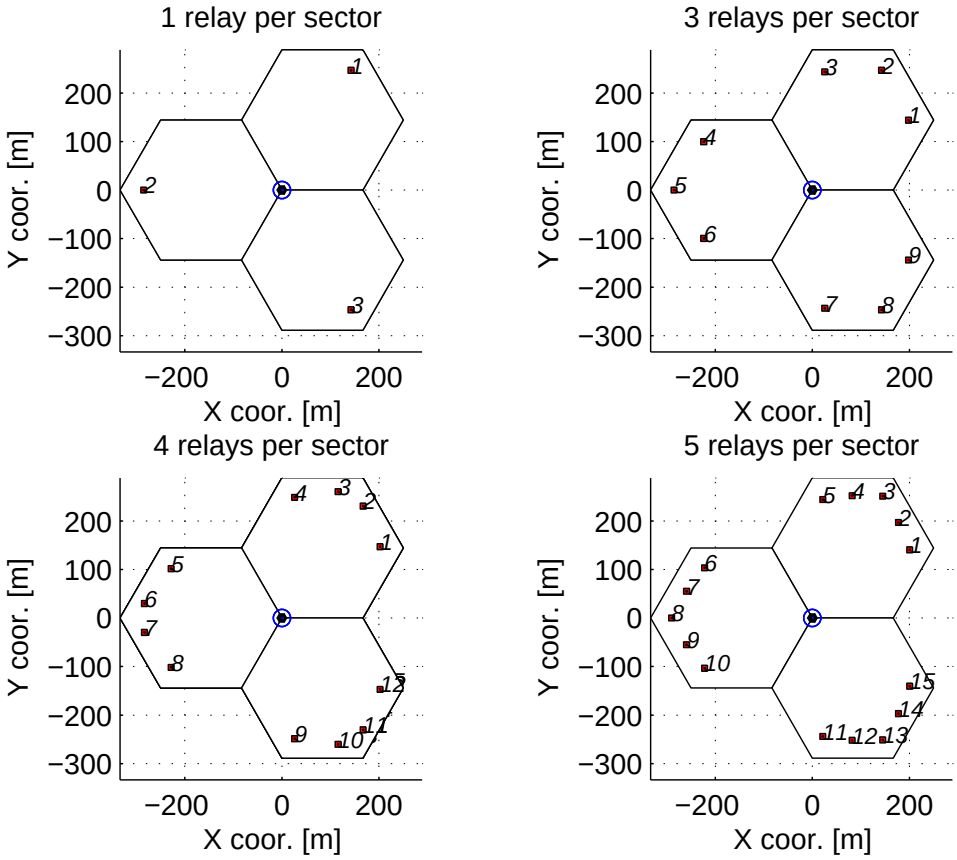

Figure 3.4: Relay node deployments.

satisfactory performance up to 120 km/h. It can be noted that UE speeds of 3 km/h, 30 km/h and 120 km/h are preferred.

Relay environment

Numbers of supporting relays per sector are considered as 1, 3, 4, 5. Relay stations are positioned on a circle with the circle center position merged with the hexagonal sector center [9]. Figure 3.4 and Table 3.2 give the relay positions depending on the number of relays per sector.

3.3.2 Simulation flow

Figure 3.5 shows the general simulation flow. Our simulator continuously simulates the temporal development of cells by calculating densely spaced snapshots k, which can be considered as transmit time interval (TTI). Within each snapshot, the position of the macro mobile stations may change and the traffic situation is updated. Next, the channels between all links are newly calculated and the scheduling process could be performed for

Table 3.2: Relay node positions

Number of Relays per sector	Distance from eNB to Relay	Visibility angle from eNB to Relay in relation to eNB antenna direction in horizontal plane
1	0.57∗ISD	0
3	[0.5 0.57 0.5]∗ISD	[−24 0 +24] degree
4	[0.5 0.57 0.57 0.5]∗ISD	[−24 −6 +6 +24] degree
5	[0.5 0.54 0.58 0.54 0.5]∗ISD	[−26 −12 0 +12 +26] degree

each snapshot. UMTS-LTE allows different timing granularity [1]. In this simulation, we assume the time interval to be TTI = 1 ms.

3.3.3 Initialization

As we design a real dynamic simulator, in the function of the initialization procedure all the parameters that remain constant during the whole simulation can be set:

- number of macro sites (1 or 7 or 19 or 57),
- simulation scenario (3GPP case 1 or 3GPP case 3),
- number of UEs per macro cell ,
- velocity of UEs,
- number of UE transmit and receive antennas,
- number of BS transmit and receive antennas,
- number of relay stations per cell,
- number of RN transmit and receive antennas,
- bandwidth,
- carrier frequency,
- scheduling algorithm.
- relay scenario

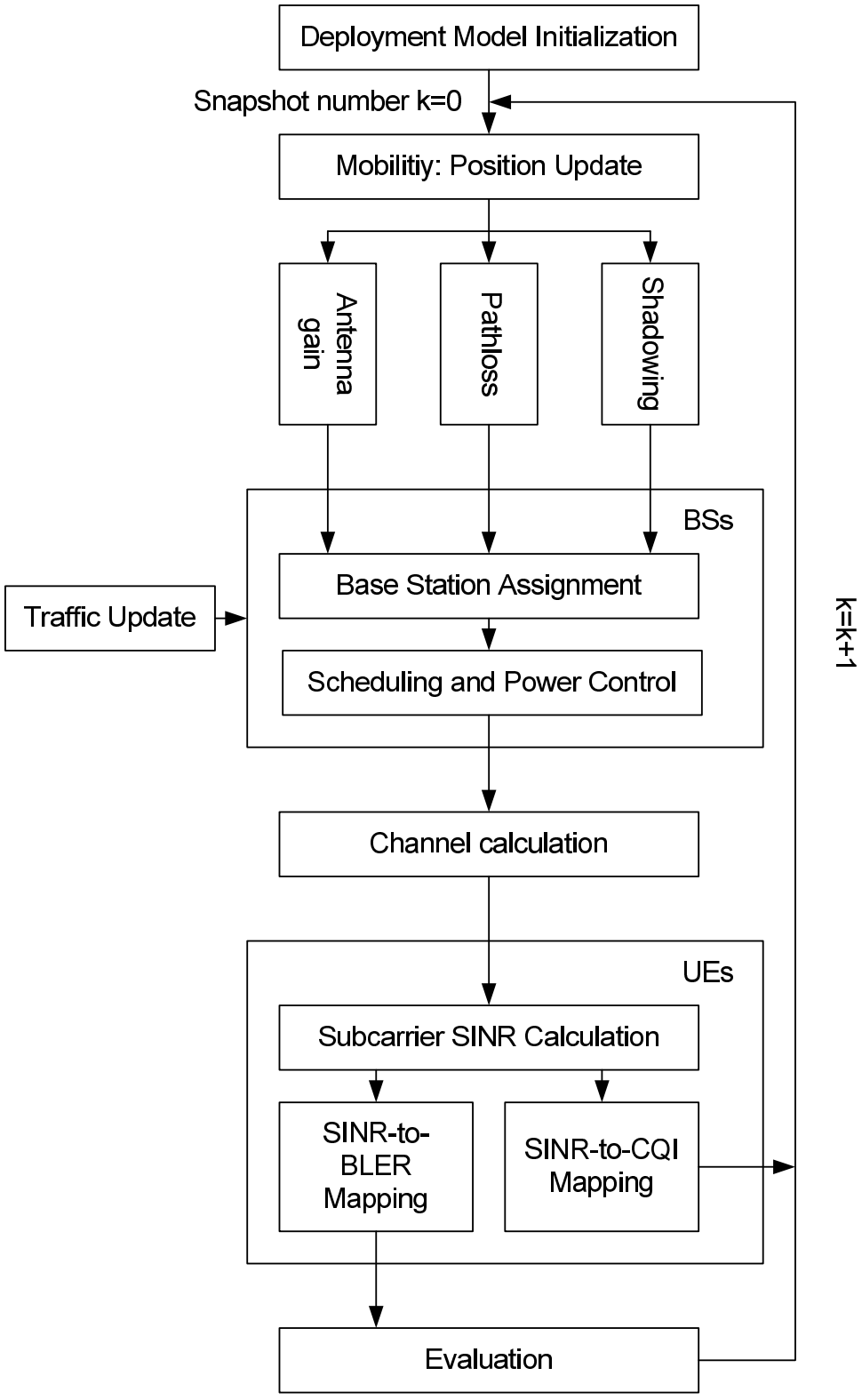

Figure 3.5: Simulation flow.

3.3.4 Mobility model

The locations $l_i(t)$, direction of movement $d_i(t)$ of macro MSs and their velocities $v_i(t)$ are updated every snapshot according to:

$$\begin{aligned} l_i(kT+T) &= l_i(kT) \cdot v_i(T) \cdot T, \\ d_i(kT+T) &= d_i(kT) + A \cdot \Delta d_i(kT). \end{aligned} \tag{3.1}$$

The direction of movement $d_i(t)$ of each macro MS at the $(k+1)$-th snapshot is obtained by updating its direction at the k-th snapshot by multiplying a uniformly distributed random variable Δd_i (with $f_{\Delta d_i}(\Delta d_i) = \frac{1}{\Delta d}\text{rect}(\frac{\Delta d_i}{\Delta d})$) with another random variable A generated from a discrete probability density function $f_A(A) = p_{\text{dc}}\delta(A-1)+(1-p_{\text{dc}})\delta(A)$. Thus the maximum change in direction, also called maximum swing angle is limited to $\Delta d_{\max}$. The probability of direction change p_{dc} is used to make a decision whether or not a particular macro MS changes its direction. Obviously, the random variable A can take values of either zero or one. If the mobile station (MS) does not change its direction ($A = 0$), the direction calculated at the previous snapshot remains unchanged [38].

3.3.5 Traffic model

In our dynamic simulator, traffic models can be grouped in the service types 'best effort packet transmission' and 'real time transmission'. The best effort packet service type includes FTP and HTTP, while real time services include video streaming, VoIP and interactive gaming. The detailed statistical traffic model and associated parameters are defined in [73]. However, in most cases, "Full buffer traffic" at the end node will be considered for our system level simulations that do not include a delay aspect in the analysis. We consider that the traffic generators are only located at the DeNB for downlink and the UE for the uplink direction. Therefore, the traffic arrival pattern for relay nodes depends on the situation on the feeder link, i.e. the backhaul link for the downlink and the RN access link for the uplink.

3.3.6 Scheduling

As a baseline we implemented two known scheduling algorithms namely, 'Round-Robin' and 'Proportional Fair'. In further developed versions of our simulator, these scheduling algorithms will be compared with more complex newly designed scheduling algorithms.

3.3.7 Channel model

In general, there are two ways of modeling a channel: deterministic and stochastic [71]. Deterministic channel models are site-specific, as they depend on specific transmitter

location, receiver location, and environment. They are thus most suitable for network planning and deployment. However, it is not possible or desirable to model the propagation channel in a specific way in many cases. Especially for system testing and evaluation, stochastic channel modeling is more suitable. In a typical system level simulation, the geometry of a wireless deployment is first defined (e.g., typically a cellular topology is assumed), based on which the long-term fading behaviors and large scale parameters are derived. After that, the short-term time-variant spatial fading channels are generated. The 3GPP spatial channel model (SCM) [2], which is also mandated in 3GPP36.814 [9], has been widely used in system simulation. It models the physical propagation environment using paths and sub-paths with randomly specified angles, delays, phases, and powers.

The general modeling approach is based on the geometry of a network layout. The large-scale parameters such as path loss and shadowing factor are generated according to the geometric positions of the BS and MS. Then the statistical channel behavior is defined by some distribution functions of delay and angle and also by the power delay and angular profiles. Typically, an exponential power delay profile and Laplacian power angular profile are assumed with the function completely defined once the RMS delay spread and angular spread (both angle of departure (AoD) and angle of arrival (AoA)) are specified. The generic channel model is applicable for all scenarios, e.g. indoor, urban and rural.

Antenna pattern

- eNB-UE link

  A 3-D antenna pattern with 15 degree electrical downtilt for 500 m ISD case and 6 degree for 1732 m ISD case will be used as described in [9] and summarized in Appendix B. The heights of the DeNB and UE antenna are 32 m and 1.5 m, respectively. The minimum distance between UE and DeNB is 35 m.

- eNB-RN link(backhaul link)

  A 2-D directional atenna pattern with an RN antenna height of 5 m, as listed in [9] and Appendix B, will be used for the backhaul link.

- RN-UE link(relay access link)

  A 2-D omni-directional antenna pattern with 5 dBi gain is considered. The height of the relay nodes is 5 m. The minimum distance between UE and RN is 10 m. In case of multi-hop relay deployments, the intermediate RN-RN link will be treated in

the same way as a relay access link, but assuming the same height of the transmitter and receiver antenna.

Path loss

- eNB-UE link

  The path loss on this link consists of both LOS and NLOS components, which alternate based on a certain probability as summarized in Table 3.3. It has to be mentioned that the random change between LOS and NLOS conditions is statistically independent between the serving and all interfering links.

Table 3.3: Path loss models for eNB-UE link [9]

Parameter	Setting for 3GPP case 1	Setting for 3GPP case 3
LOS link model	$L_{\text{LOS}}(R) = 103.4 + 24.2\log_{10}(R)$	
NLOS link model	$L_{\text{NLOS}}(R) = 131.1 + 42.8\log_{10}(R)$	
LOS probability	$\text{Prob}(R)=\min(\frac{0.018}{R}, 1)*$ $(1-\exp(-\frac{R}{0.063}))+\exp(-\frac{R}{0.063})$	$\text{Prob}(R)=\exp(-\frac{R-0.01}{0.2})$

(the eNB-UE distance R is given in km.)

- eNB-RN link

  [74] has submitted a contribution on the impact of relay site planning on the eNB-RN link. The impact of the site planning can be reflected in a bonus on the eNB-RN path loss model and shadow standard deviation. The path loss on the backhaul link also consists of the LOS and NLOS component as shown in Table 3.4. With site planning, the NLOS component gets an extra reduction by the site-planning gain and a higher LOS probability as shown in Table 3.5. The site-planning gain only applies to the links from the serving DeNB.

- RN-UE and RN-RN link

  The path loss on the RN-RN link (used for inter-relay interference) is based on the RN-UE access link, which also consists of a LOS and a NLOS component as listed in Table 3.6. For path loss on the RN-RN link, the difference from the basic RN-UE link is the lack of a penetration loss.

Table 3.4: Path loss models for eNB-RN link [9]

Parameter	Setting for 3GPP case 1	Setting for 3GPP case 3
LOS link model	$L_{\text{LOS}}(R) = 100.7 + 23.5\log_{10}(R)$	
NLOS link model	$L_{\text{NLOS}}(R) = 125.2 + 36.3\log_{10}(R)$	
LOS probability	$\text{Prob}(R)=\min(\frac{0.018}{R}, 1)*$ $(1-\exp(-\frac{R}{0.072}))+\exp(-\frac{R}{0.072})$	$\text{Prob}(R)=\exp(-\frac{R-0.01}{0.23})$

(the eNB-RN distance R is given in km.)

Table 3.5: Corrections of site planning [9]

Parameter	Setting for 3GPP case 1	Setting for 3GPP case 3
LOS probability	$\text{Prob}(R) = 1-(1-\text{Prob}(R))^N$ where $N=3$, for donor macro (from each of its sectors) to relay, otherwise, for non-donor cell and non optimized deployment $N=1$	
Site-planning gain	$L_{\text{NLOS}}(R) = L_{\text{NLOS}}(R) - 5\text{dB}$	$L_{\text{NLOS}}(R) = L_{\text{NLOS}}(R) - 11\text{dB}$

Table 3.6: Path loss models for RN-UE and RN-RN link [9]

Parameter	Setting for 3GPP case 1	Setting for 3GPP case 3
LOS link model	$L_{\text{LOS}}(R) = 103.8 + 20.9\log_{10}(R)$	
NLOS link model	$L_{\text{NLOS}}(R) = 145.4 + 37.5\log_{10}(R)$	
LOS probability	$\text{Prob}(R)=0.5-\min(0.5, 5\exp(-$ $\frac{0.156}{R}))+\min(0.5, 5\exp(-\frac{R}{0.03}))$	$\text{Prob}(R)=0.5-\min(0.5, 3\exp(-$ $\frac{0.3}{R}))+\min(0.5, 3\exp(-\frac{R}{0.095}))$

(the RN-UE and RN-RN distance R is given in km.)

Shadowing

The shadow fading is caused by obstacles between the transmission source and the destination. And the shadow fading has been well modeled as a log-normal random variable in the literature [63]. It may be sufficient to generate a one-dimensional random function of time to simulate small scale fading, as the fading waveform changes significantly. However, since shadowing effects occur over a relatively large area, a 2-dimensional Gaussian process model is proposed to capture the spatial correlation of shadowing processes [31]. The corresponding parameters are specified in Table 3.7.

Table 3.7: Shadowing parameters [9]

Parameter	eNB-UE link	eNB-RN link	RN-UE link
Standard Deviation	8dB	6dB	10dB
Correlation distance	50m	50m	13m
Correlation Factor	0.5 between sites & 1.0 between sectors		

Multipath model

The multipath propagation conditions consist of the power delay profile and the Doppler effect. A delay profile in the form of a 'tapped delay-line', characterized by a number of taps at fixed positions on a sampling grid. Conventional six-tap models [47] were developed for 5 MHz bandwidth channels, but they are not sufficient to describe a system which has 10 MHz bandwidth. As the bandwidth increases, the delay profiles, which are proposed in [3], are selected to be representative of low, medium and high delay spread environments (See Appendix C). The resulting model parameters are defined in Table 3.8 and the tapped delay line models are defined in [3].

Table 3.8: Delay profiles for E-UTRA channel models [3]

Model	Number of channel taps	Delay spread (r.m.s.)	Maximum excess tap delay (span)
Extended Pedestrian A (EPA)	7	45 ns	410 ns
Extended Vehicular A model (EVA)	9	357 ns	2510 ns
Extended Typical Urban model (ETU)	9	991 ns	5000 ns

3.3.8 SINR calculation

All PHY abstraction metrics are computed based on the function of post-processing SINR values across the coded block at the input to the decoder. With generated channel gains, it is possible to evaluate the post-processing SINR, which is dependent on the implemented transmission mode to receive and demodulate the symbols. Here, we summarize the function of post-processing SINR of the desired user i with the transmit power $P_{i,n}$ on the n-th subcarrier as:

- Transmission mode 1: Single-input Single-output (SISO)

$$\gamma_{i,n} = \frac{P_{i,n}(|h_{i,k(i),n}|^2)}{(\sum_{l=1,\ l\neq i}^{N} P_{l,n}|h_{i,k(l),n}^H|^2) + \sigma_n^2} \tag{3.2}$$

  where
  N: the number of total links (desired link and interfering links)
  $h_{i,k(i),n}$: channel gain of the n-th subcarrier between the i-th user and k-th BS
  k: BS index
  σ_n^2: variance of the white Gaussian noise on the n-th subcarrier

- Transmission mode 2: Transmit diversity

- Transmission mode 3: Open-loop spatial multiplexing (SM)
  LTE uses open-loop SM, where independent data streams are transmitted from different antennas. A minimum mean square error (MMSE) receiver will be assumed as the baseline receiver in the system level simulation methodology.

- Transmission mode 4: Closed-loop spatial multiplexing
  In closed-loop spatial multiplexing, precoding is applied at the base station before transmission. Pre-coders are carried out corresponding to TS 36.211, 6.3.4 [5].

- Transmission mode 5: Multi-user multiple-input multiple-output (MU-MIMO)
  This case corresponds to transmission mode 4, i.e. the single layer transmission of the closed-loop spatial multiplexing.

- Transmission mode 6: Closed-loop rank 1 precoding
  This mode amounts to beamforming and it can be regarded as a special case of transmission mode 4 (single layer transmission).

- Transmission mode 7: If the number of the physical broadcast channel antenna ports is one, Single-antenna port, port 0; otherwise transmit diversity (see transmission mode 1 and 2).

3.3.9 Link level quality estimation

For system level simulations, instantaneous link performance can be predicted by the physical layer abstraction methodology, which has been discussed in existing literature [33]. Since the OFDM systems may experience frequency selective fading, the coded block may be transmitted over several sub-carriers with different channel gain. The post-processing SINR values of the pre-decoded streams are thus non-uniform. As the link level performance curves (SINR-PER or SINR-Throughput) are generated assuming the frequency flat channel case, an effective SINR (γ_{eff}) is required to accurately map the system level SINR onto the link level curves to determine system level performance. Such method is termed effective SINR mapping (ESM). The ESM PHY abstraction is thus defined as compressing multiple received SINR values to a single effective SINR value, which can then be further mapped to desired system level performance metrics.

Several ESM approaches to predict the instantaneous link performance have been proposed as the link adaptation techniques in the literature. These approaches include:

- Instantaneous SNR [88],
- Raw or uncoded bit error rate mapping (RawBER) [80],
- Exponential effective SNR mapping (EESM) [34],
- Mutual information effective SINR mapping (MIESM) [25].

Each of these PHY abstractions uses a different function to map the set of SINR values from sub-carriers into a single scalar value. Out of all above algorithms, EESM will be considered in our simulator due to its stable performance under most of channel conditions [98]. The EESM method computes an effective SINR by taking the individual sub-carrier SINRs as input and using an exponential combining function:

$$\gamma_{\text{eff}} = -\beta \log \left(\frac{1}{N_{ss} N_{sd}} \sum_{j=1}^{N_{ss}} \sum_{k=1}^{N_{sd}} \exp \left(\frac{-\gamma_j [k]}{\beta} \right) \right), \tag{3.3}$$

where N_{ss} indicates the number of spatial streams, N_{sd} indicates the number of sub-carriers and the parameter β is used to fit the model to the system performance.

In Figure 3.6, the link level to system level interface used in our simulator is depicted. Several input parameters e.g., channel frequency response, powers, MIMO modes and CQI values, are given for the system level to the link level. In the link level abstraction function the post-processing SINR on each sub-carrier is calculated in order to determine the effective SINR. The output of the link level abstraction is block error rate (BLER) and throughput.

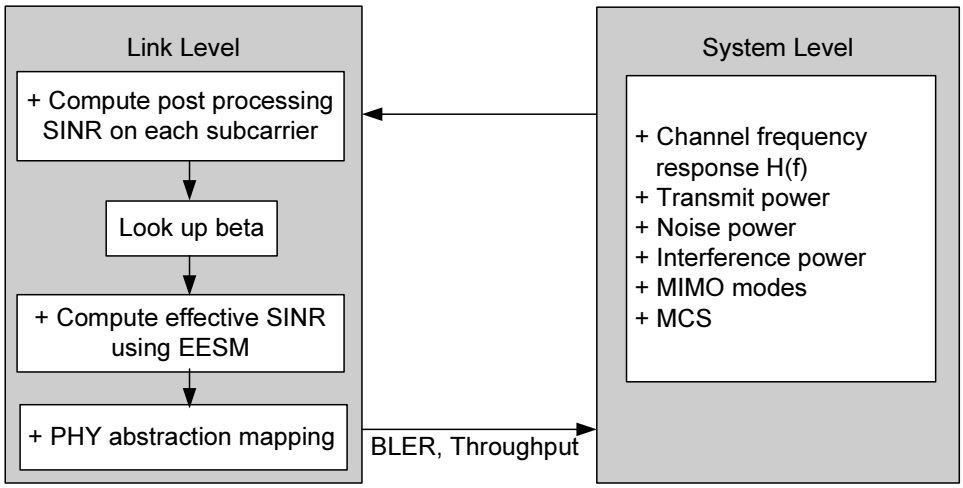

Figure 3.6: Link level to system level interface [90].

In cellular systems, it is state-of-the-art to use hybrid automatic repeat request (HARQ) protocols accompanied by retransmissions to achieve a high system capacity. As introduced in [54] a synchronous HARQ scheme will be employed for slowly varying channels. The use of HARQ is also an undisputed assumption to LTE. HARQ techniques are also used to improve the throughput performance of the link adaptation techniques by compensating link adaptation errors caused by inaccurate channel estimation and the channel quality feedback delay [26][29]. With our simulator, a trace of each resource block over the whole simulation time and the variation of their delay times are available.

3.4 Evaluating fixed relays in an LTE-A cellular network

In the following sections, we mainly evaluate the relay-aided LTE-A cellular network through system level simulations. The evaluated system is assumed to use fixed location, decode-and-forward, LTE-A type 1 relays. For application of relays to cellular networks, the LTE release 10 has given preference to the decode-and-forward protocol over the amplify-and-forward relaying protocol. We concentrate on decode-and-forward relays in the rest of this thesis. The LTE type 1 relay is an in-band relay in which the backhaul link and the access link work on the same carrier frequency of 2 GHz. Users served directly by the macro base station are called macro UEs and the other UEs associated with relay stations are called relay UEs. To avoid the self-collision problem, some of the sub-frames are reserved for the backhaul link and cannot be used for the access link at the relay node. In our work, we consider two different resource allocation schemes for an in-band

relay. One of the schemes uses dynamic sub-frame assignment in time domain, whereas the other one considers static allocation.

For in-band relay, the backhaul link and the access link work on the same carrier frequency of 2 GHz, which leads to the half-duplex mode at the relay node. Hence, we consider two resource allocation schemes for in-band relay and compare the performance of both algorithms. One of the schemes is dynamic in time division, but the other is static.

3.4.1 Resource allocation for an in-band relay

- Static time division resource allocation

  In this work, the frequency reuse factor is assumed to be 1 for the whole system and the relay stations are assumed to work in the in-band mode, in which the downlink relay backhaul and access link transmissions are time division multiplexed. In one subframe, it can exist either eNB-UE/ eNB-RN or eNB-UE/ RN-UE, but it is not allowed to allocate resources on the same subframe to both eNB-RN and RN-UE links. The static time division resource allocation scheme is the straightforward solution for such a problem as shown in Figure 3.7. In the 1st time slot, the eNB transmits information to its own macro UEs or RNs and all RNs work in receiving mode. In the 2nd time slot, RNs forward the received signal to relay UEs and the eNB transmits the information only to macro UEs. The communication in the 2nd time slot will suffer additional inter-cell interference since all base stations and relay nodes transmit simultaneously.

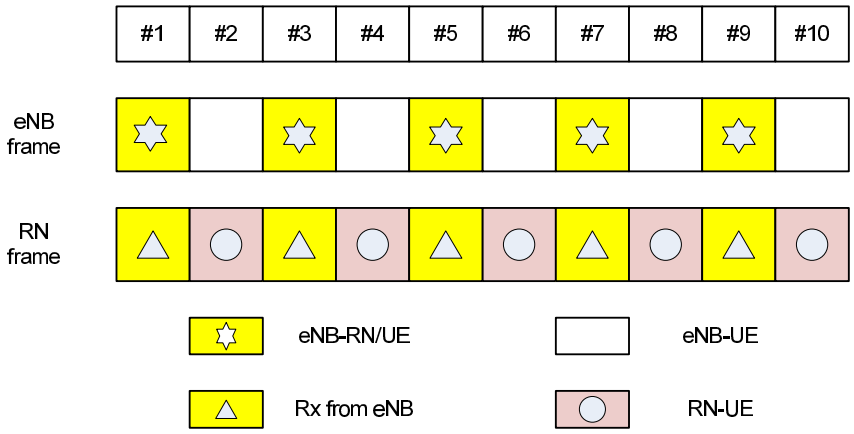

Figure 3.7: Static time division resource allocation for in-band relay.

In this case, the traffic pattern at relay nodes is depended on the arrival traffic from eNB-RN link. In the 1st time slot, only partial resource blocks are allocated to

relay node, which limits the resource allocation at the relay node in the 2nd time slot.

- Dynamic time division resource allocation

  The 3GPP has defined the multicast broadcast single frequency network (MBSFN) subframe which is used for backhaul reception at the relay node as shown in Figure 3.8 [6]. This special type of subframe gives the opportunity for RN to switch to the

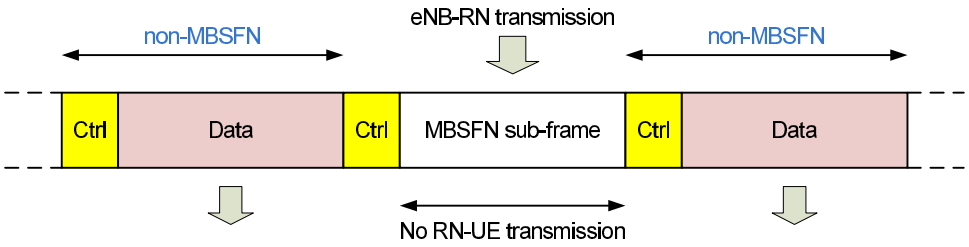

Figure 3.8: The MBSFN sub-frame structure.

reception mode where the RN can receive data from the eNB. During that time, the UEs assigned to the RNs are not served with data. At the end of an MBSFN subframe, the RN again switches back to sending mode. A LTE-A radio frame has an overall length of 10 ms and comprises 10 subframes. Moreover, the maximum configurable number of MBSFN subframes is 6 out of 10, which limits the time division multiplexing rate between the access and the backhaul to $R = k/10$, with $k = 0, 1, ..., 6$. In the LTE FDD downlink frame structure, some subframes are configured for system relevant information such as the physical broadcast channel or primary/secondary synchronization signal. It is worth to mention that both macro UEs and RNs can be scheduled on such a subframe.

This resource allocation scheme is based on dynamic time division multiplexing. The number of MBSFN subframes, which is suggested by the upper layer, is related to the resource demand from the relay UEs. All relays' buffer status will be checked before using an MBSFN subframe for backhaul transmission. If they are full, the relay is allowed to use this sub-frame for the access as shown in Figure 3.9.

3.4.2 Simulation environment

We consider a cellular network with 7 hexagonal cell sites and 3 sectors per site as shown in Figure 3.10. For relay deployment, 1, 3 or 5 type 1 relay nodes are placed near the cell edge as defined in previous section. Besides, both indoor and outdoor users are considered, in which 30 UEs are uniformly distributed in each sector. Such cell selection is done by

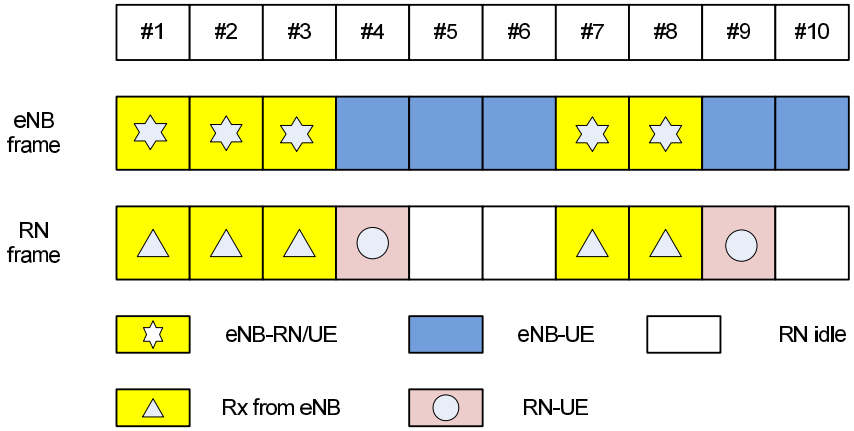

Figure 3.9: Dynamic time division resource allocation for in-band relay.

reference signal received power (RSRP) criteria: $\text{RSRP}_{\text{eNB}} > \text{RSRP}_{\text{RN}} + \Delta_{\text{RSRP}}$, in which Δ_{RSRP} is a tuning parameter to balance the load between RN and eNB. Users suffer from interference from all other cells.

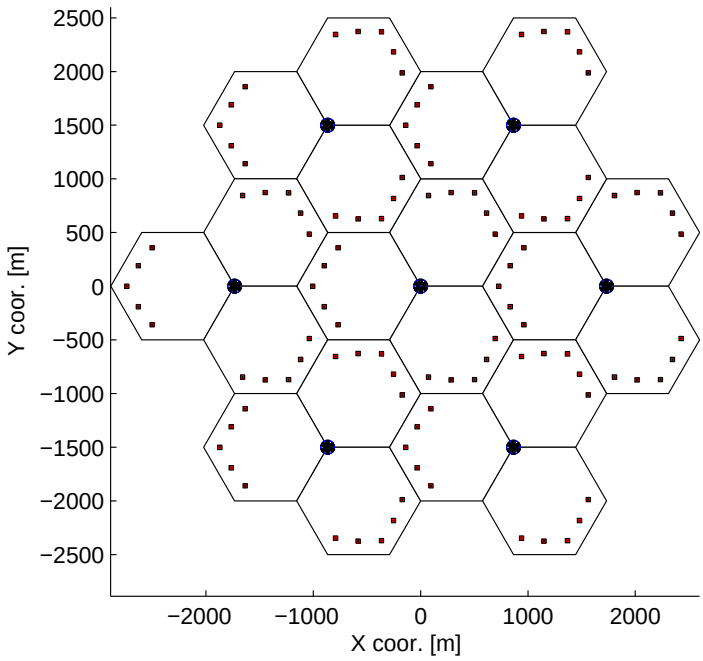

Figure 3.10: Network Layout, 7 macro sites, 3sectors/site, 5 relays/sector.

Most of common simulation parameters are described in previous sections, e.g. the network deployment and channel configurations. Remaining parameters, which are summarized in Table 3.9, follow the latest parameter settings agreed in 3GPP 36.814.

Table 3.9: System level simulation parameters

Parameter	Value
TTI	1 ms
Transmission bandwidth	10 MHz, DL
Carrier frequency	2 GHz
Type of relay	LTE Type 1 & DF relaying
Antenna configuration in DL	MIMO 2x2
Modulation and coding scheme (MCS)	CQI1-CQI16
Number of used sub-carriers per OFDMA symbol	600
Number of RBs per sub-frame	50
FFT size	1024
Scheduling scheme	round robin
Traffic mode	full buffer

3.4.3 Simulation results

In this section, the evaluation of a fixed LTE-A type 1 relay scenario by system level simulation is described. Urban and suburban scenarios with ISDs of 500 m and 1732 m (3GPP case 1 and case 3 [9]) are considered. System level simulations are focused on average user spectral efficiency and the 5%-ile user spectral efficiency as the cell edge user performance, which indicates the coverage extension capabilities. The eNB-only deployment is considered as a reference to identify the performance gains.

Urban scenario

Table 3.10 lists the performance gain in average UE spectral efficiency for different number of relay nodes deployment compared with macro eNB-only deployment in the urban

Table 3.10: Spectral efficiency performance of LTE-A with relay in 3GPP case 1 scenario

Relay scenario	Average UE spectral efficiency	5%-ile UE spectral efficiency
without relay	2.31	0.19
1 relay	2.60	0.37
3 relays	2.90	0.47
5 relays	2.78	0.44

(All values are measured in bit/s/Hz.)

case. It can be observed that the relay deployment shows its advantage compared to the traditional macro eNB-only deployment in an urban scenario. With three relay nodes deployed in each sector, the average user spectral efficiency increases up to 25% and the cell edge user performance increases 147% compared to the system without a relay node. However, the performance will decrease with more than five relay nodes deployed in each sector, since additional relay stations cause strong interference to other cells (other relay cells and all macro cells). In the urban case, inter-cell interference is becoming critical with too many small cells in the original communication service area. Simulation results show that the average user spectral efficiency with 5 relays deployment has around 4% degradation compared to that with 3 relays deployment. In addition, the simulation results are also depicted for all approaches as spectral efficiency cumulative distribution functions (CDF) as shown in Figure 3.11. The CDF results illustrate the same trends.

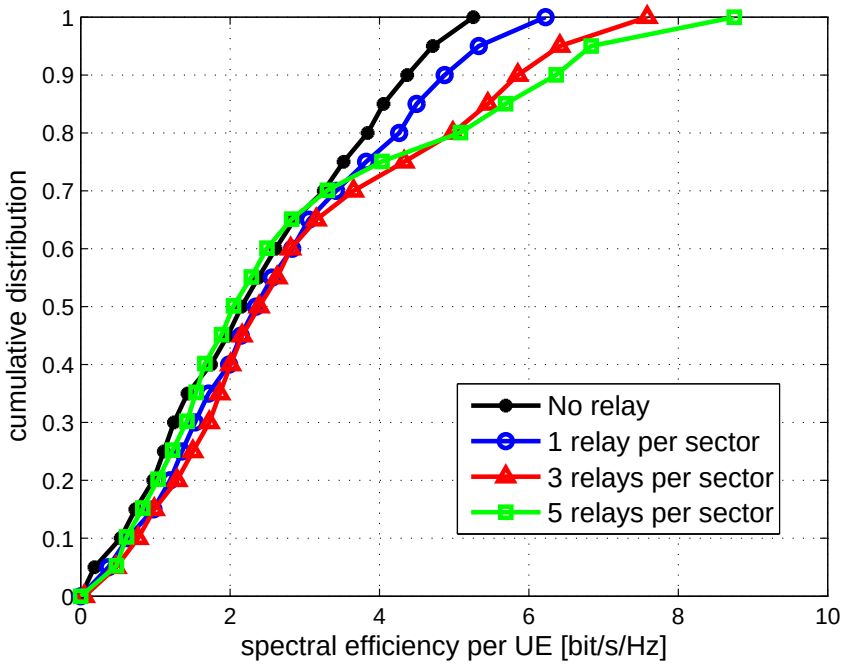

Figure 3.11: Performance comparison for different number of RNs deployment in 3GPP case 1 scenario.

Suburban scenario

Table 3.11 lists the performances of different relay scenarios in the case of a suburban scenario (3GPP case 3). Since the communication area in a suburban scenario is relative large compared with the urban scenario, the average user spectral efficiency is lower than that in the urban case. However, from the simulation results, it can be observed that

Table 3.11: Spectral efficiency performance of LTE-A with relay in 3GPP case 3 scenario

Relay scenario	Average UE spectral efficiency	5%-ile UE spectral efficiency
without relay	2.00	0.14
1 relay	2.24	0.34
3 relays	2.45	0.45
5 relays	2.55	0.47

(All values are measured in bit/s/Hz.)

the relay deployment also shows its advantage over the macro eNB-only deployment in this case. With more relay nodes deployed in each sector, both average UE spectral efficiency and 5%-ile UE spectral efficiency increase. As the communication service range is very large in suburban case, additional relay nodes deployment can provide an efficient solution to enhance the network density. With 5 relay nodes deployed in each sector, the average user spectral efficiency increases by 28% and the cell edge user performance increases up to 236% compared to the system without relay node. Spectral efficiency CDF results illustrate the same trends as shown in Figure 3.12.

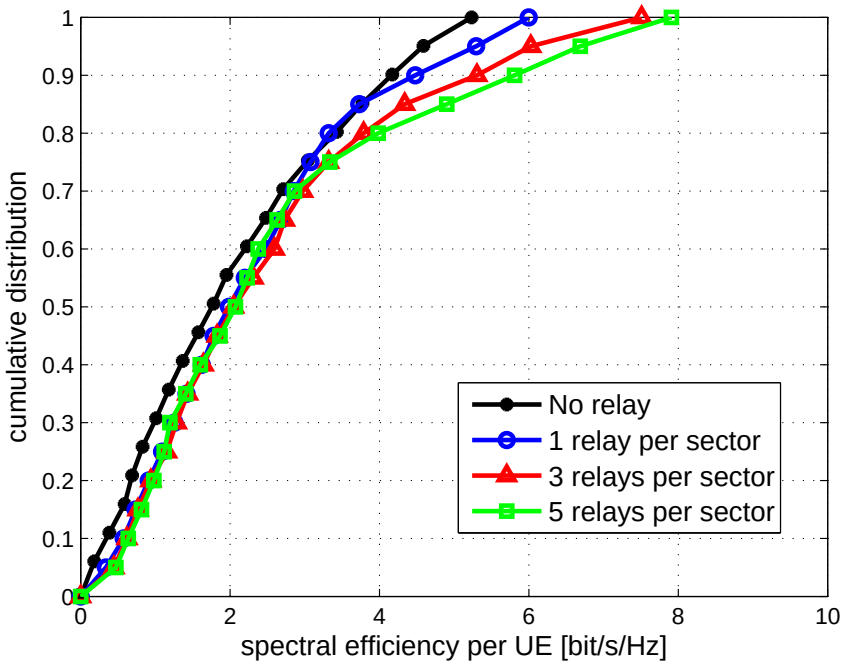

Figure 3.12: Performance comparison for different number of RNs deployment in 3GPP case 3 scenario.

Table 3.12: Spectral efficiency performance of dynamic resource allocation scheme in 3GPP case 3 scenario

Relay Scenario	Average UE spectral efficiency	5%-ile UE spectral efficiency
1 relay	3.07	0.59
3 relays	3.28	0.92
5 relays	3.24	1.02

(All values are measured in bit/s/Hz.)

Performance with two resource allocation schemes

As mentioned before, there are two resource allocation schemes for fixed relay scenario considering in our work. Figure 3.13 shows the performance comparison between these two schemes. Comparing results in Table 3.11 and Table 3.12, dynamic resource allocation scheme shows more than 25% average spectral efficiency gain and 100% cell edge user spectral efficiency gain compared with the static scheme because of the buffer ability at the relay node.

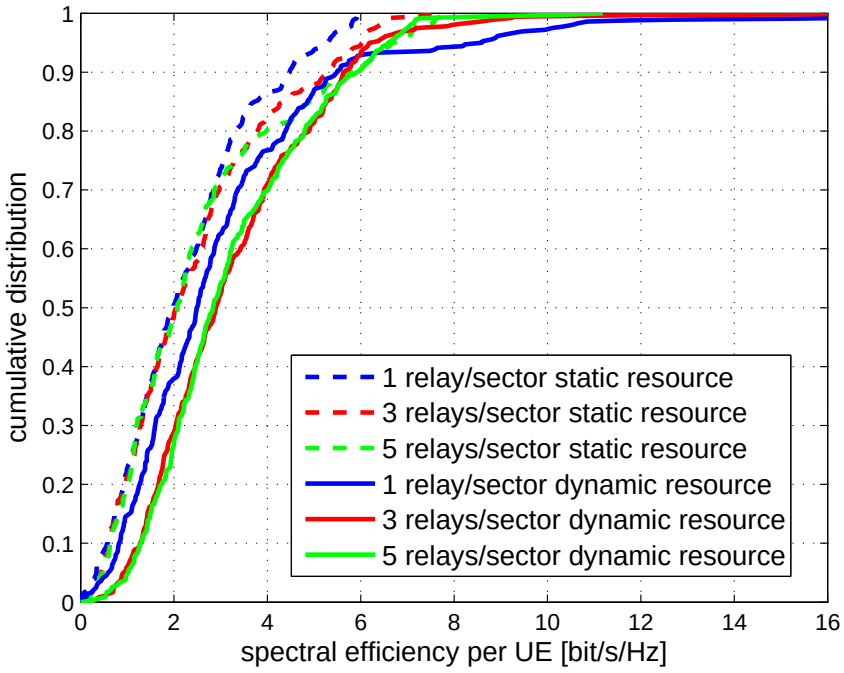

Figure 3.13: Performance comparison for different resource allocation schemes in 3GPP case 3.

3.5 Summary

In this chapter, baseline assumptions for relay-enhanced LTE-A systems have been introduced in detail. Relaying is one of the features being proposed for the 4G LTE-Advanced system, since several potential relay scenarios, such as rural area, urban scenario, coverage hole, indoor hot spot, mobile relay scenarios, are of current interest to major operators. As defined in 3GPP specifications, there are two basic types of relays that are being proposed [9]: Type 1 relay and Type 2 relay, which are nontransparent and transparent, respectively. In 3GPP Release 10, only the type 1 and the type 1.a relay are envisioned.

We have developed a dynamic system level simulator for a relay-enhanced LTE-A network. With the system level simulator, it is possible to evaluate the downlink communication performance of an LTE-A cellular network with relay nodes deployment. Simulation results show that the relay deployment, which is a part of a heterogeneous network, can reduce the high interference at cell edges and improve the performance. However, as the deployment density of relay cells increases, additional interference caused by relays will limit the whole network performance. Therefore, the number of relay nodes in each sector should be determined carefully. From our simulation results, suitable numbers of relay nodes for urban case and suburban case are three and five, respectively. In the next chapter, some new approaches will be investigated to reduce the impact of inter-cell interference for relay-enhanced cellular networks, which will help to increase the whole network capacity.

Chapter 4

Proposals for interference management with relays

4.1 Introduction

The relay technology is considered as one of the key features in LTE-A because of its ability of extending communication coverage, reducing overall transmission costs, and enhancing the whole network capacity. In chapter 3.4, we have shown the performance of relay deployment in interference limited cellular systems. A relay-aided cellular system is shown in Figure 4.1. In addition to the desired signal from the home base station, each relay or user receives interference from other-cell base stations or relays. The performance of such multi-cell wireless networks is limited by other-cell interference (OCI), since multiple transmissions take place simultaneously in the same frequency band. In relay-enhanced cellular networks, the main challenge is hence to combat OCI problem due to co-channel transmission in other cells.

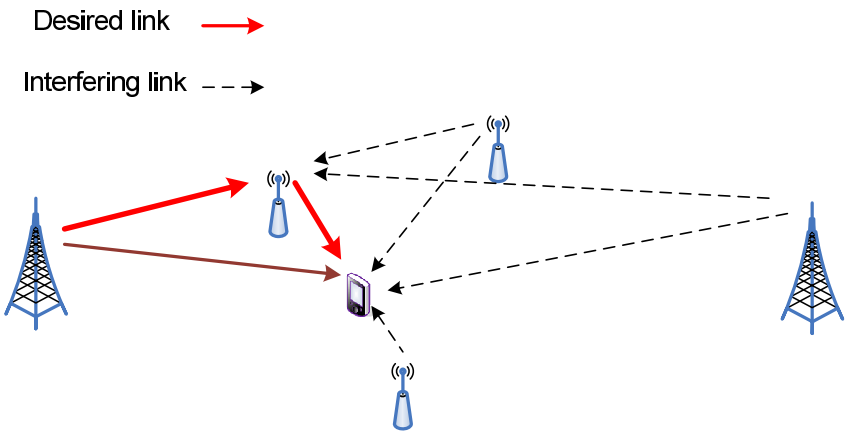

Figure 4.1: An interference limited relay-enhanced cellular system.

There have been a variety of different approaches to reduce the impact of interference, which include power control technology, static frequency reuse, resource allocation optimization, beamforming design, and the deployment of shared relays. In [87], authors design an enabling power control approach to alleviate co-channel interference in cooperative relay networks. Frequency reuse is another approach which was proposed to

improve cell edge performance and reduce effects of interference [106]. However, the technology of frequency reuse does not allocate bandwidth and resources efficiently and still suffers from significant interferences in large networks with more relays. An adaptive aggregate method of resource allocation, which is aimed at maximizing throughput with interference mitigation capability, has been proposed for OFDMA based downlink relay-enhanced wireless systems, with the application to LTE-Advanced cellular networks [64]. In case of RN with multiple antennas, interference cancellation is good for downlink cell-edge users. This is because the spatial domain can be utilized in addition to the time and frequency domain for interference management. In [110], a robust beamforming was proposed based on the zero forcing (ZF) and MMSE technology for MIMO relay broadcast systems. Another approach is to consider shared relays, which are shared among multiple base stations. Sharing a multi-antenna relay among several sectors is a simple and cost-effective way to achieve much of the gains of local interference mitigation in cellular networks [76]. In our work, we will focus on beamforming design for cooperative communication and the deployment of shared relays.

4.2 Adaptive beamforming design with limited feedback

In this section, we focus on a half-duplex downlink cellular system with relay cooperation. We consider the beamforming design problem with a limited amount of feedback for channel state information (CSI), which is only available at the receiver side.

4.2.1 Introduction and motivation

In beamforming, the transmitted signal is multiplied by complex weights that adjust the magnitude and phase of the signal on each antenna. The output from the array of antennas can be formed as a transmit or receive beam for the desired direction and minimizes the output in other directions. Beamforming technology is a decent solution to reduce interference levels and improve the system capacity in an interference limited system. Two typical beamforming strategies are maximum ratio transmission (MRT) and zero-forcing. MRT beamforming serves its own user with eigen-beamforming and does not cancel interference in other cells [67]. On the other hand the ZF beamforming algorithm allows a transmitter to send data to desired users together with nulling out the directions to undesired users [91]. If the transmitter knows the channel status information perfectly by a feedback channel, ZF beamforming can achieve close to optimal capacity especially when the number of users is sufficient. Furthermore, the minimum mean-square error beamforming was introduced in [79].

For a relay system, the joint beamforming design for a non-regenerative MIMO relay system was proposed in [40] by neglecting the direct link. However, the above beamforming schemes all require full channel state information at the BSs which is not realistic especially in frequency division duplex (FDD) systems. An intuitive method is to exchange quantized CSI with a limited number of feedback bits. This technology is generally referred to limited feedback technology [53],[110]. The authors in [53] employ a Grassmannian codebook to reduce the feedback overhead by limited feedback. In [110], a robust beamforming was proposed based on the ZF and MMSE technology for MIMO relay broadcast systems.

In previous studies, most researchers consider the beamforming design for cooperative relay networks as a single-cell problem. However, the performance of the user, which is served by the relay station, is limited by interference from macro base stations and other relay stations. As mentioned before, this interference is considered as other-cell interference [16]. Coordinated transmission techniques are proposed to suppress OCI. In these techniques, the CSI should be distributed among the serving base station and the interfering BS for cooperative processing. This cooperation creates signaling overhead in the uplink channel and the relay backhaul channel and therefore the shared information must be kept as low as possible. This is another motivation why we consider limited feedback technology.

In this work, we start from a two-cell scenario, in which a multiple-input single-output (MISO) cooperative relay network with a relay station deployed in a macro cell is considered. We assume that only one active user is served by the macro BS and another user is served by the relay station (RS). Random vector quantization (RVQ) [17] is used to facilitate the analysis in this work, where the quantized vectors are chosen independently from an isotropic distribution on a unit hypersphere. Cooperative beamforming requires the user to feedback CSI of both the desired link and interfering links. Conventional approaches consider equal distribution of the feedback bits of the desired and interfering link. How to partition the bits for quantizing CSI of the desired link and the interfering links is an ongoing research topic. We use some preliminary results from [111] and propose a bit partitioning scheme for cooperative beamforming design to maximize the channel capacity. In addition, we develop an adaptive beamforming strategy, which adaptively chooses ZF or eigen-beamforming to maximize the sum-rate of the whole system.

4.2.2 System model

Consider a MISO downlink cooperative relay system with a macro base station (1st BS) and a relay station (2nd BS), which are both equipped with N_t transmit antennas as

shown in Figure 4.2. A UE served by the macro base station is named macro UE (1st UE) and the UE associated with the relay station is relay UE (2nd UE), each mobile UE is equipped with a single antenna. The desired channels are shown as solid lines and the interference from other cells is shown as dashed arrows in Figure 4.2. A relay backhaul channel exists to exchange CSI and signaling for cooperative beamforming.

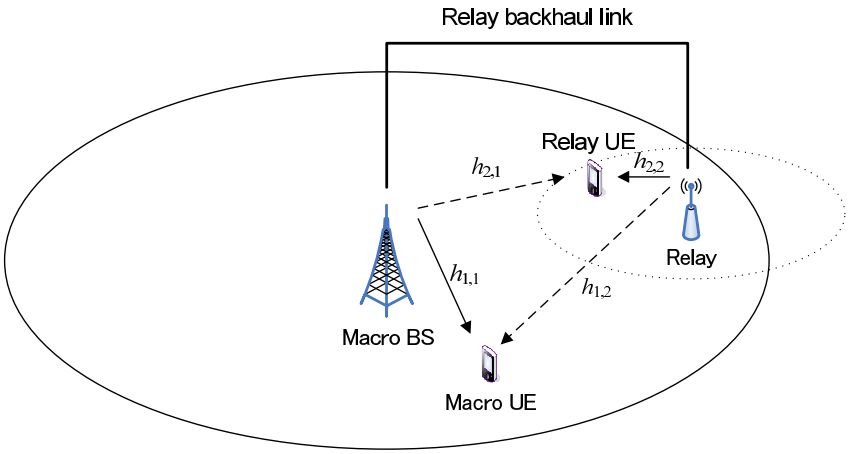

Figure 4.2: Channel model of a half-duplex downlink MISO AF relay cooperative system.

Problem formulation

The received signals of macro UE and relay UE are given as:

$$y_1 = \sqrt{P_m}\mathbf{h}_{1,1}\mathbf{f}_1 x_1 + \sqrt{P_r}\mathbf{h}_{1,2}\mathbf{f}_2 x_2 + n_1, \tag{4.1}$$

$$y_2 = \sqrt{P_r}\mathbf{h}_{2,2}\mathbf{f}_2 x_2 + \sqrt{P_m}\mathbf{h}_{2,1}\mathbf{f}_1 x_1 + n_2, \tag{4.2}$$

where P_m and P_r are the transmit power at the macro base station and the relay station, respectively. x_i ($i \in \{1,2\}$) is the transmitted information symbol for the i-th UE, here we have assumed $\mathbb{E}\{|x_i|^2\} = 1$ to fulfill the source power constraint. n_1 and n_2 are additive noise, which are modeled as zero-mean, complex Gaussian random variables with variance $\mathcal{N}_0$. The vectors $\mathbf{h}_{i,j} \in \mathbb{C}^{1\times N_t}$ model the flat Rayleigh fading channels from j-th base station to the i-th UE. $\mathbf{f}_i \in \mathbb{C}^{N_t\times 1}$ is the beamforming vector at the i-th base station. The received signal-to-interference-plus-noise ratio of two UEs can be written as:

$$\begin{aligned}\gamma_1 &= \frac{P_m \left|\mathbf{h}_{1,1}\mathbf{f}_1\right|^2}{\mathcal{N}_0 + P_r \left|\mathbf{h}_{1,2}\mathbf{f}_2\right|^2},\\ \gamma_2 &= \frac{P_r \left|\mathbf{h}_{2,2}\mathbf{f}_2\right|^2}{\mathcal{N}_0 + P_m \left|\mathbf{h}_{2,1}\mathbf{f}_1\right|^2}.\end{aligned} \tag{4.3}$$

The average normalized achievable rate of UEs are:

$$R_1 = \mathbb{E}\{\log_2(1+\gamma_1)\} \quad R_2 = \mathbb{E}\{\log_2(1+\gamma_2)\}. \tag{4.4}$$

The objective of our design is to jointly select beamforming vectors to maximize the sum-rate, i.e. to solve the following problem:

$$\left\{\tilde{\mathbf{f}}_1, \tilde{\mathbf{f}}_2\right\} = \arg\max_{\mathbf{f}_1,\mathbf{f}_2} (R_1 + R_2). \tag{4.5}$$

Transmit Beamforming Strategies

Here we consider two typical beamforming strategies:

- Eigen-beamforming

  Without considering the interference to other users the beamforming vector is designed according to the direction of the desired channel to maximize the received power of the desired signal [102]. The beamforming vector of the BS_i is given by $\mathbf{f}_{i,E} = \mathbf{h}_{i,i}^H / \left\|\mathbf{h}_{i,i}^H\right\|$. As introduced in [111], the desired signal term in (4.3) is distributed as $\left|\mathbf{h}_{i,i}\mathbf{f}_{i,E}\right|^2 \sim \chi^2_{2N_t}$ for Rayleigh fading channels, where χ^2_n denotes the chi-square random variable with n degrees of freedom.

- ZF beamforming

  ZF beamforming nulls out the interference caused to the users in other cells. Meanwhile, it tries to maximize the desired signal power. A BS with N_t transmit antennas can perfectly cancel the interference to $N_t - 1$ users with single receive antenna in other cells. Taking the macro base station as an example, the beamforming vector f_1 needs to fulfill the orthogonality condition: $\mathbf{h}_{2,1}\mathbf{f}_1 = 0$. Therefore, $\mathbf{f}_1$ can be chosen in the direction of the projection of $\mathbf{h}_{1,1}$ on the null space of $\mathbf{h}_{2,1}$, i.e.:

  $$\mathbf{f}_{1,Z} = (\mathbf{I} - \mathbf{P})\,\mathbf{h}_{1,1}^H, \tag{4.6}$$

  where $\mathbf{P} = \mathbf{H}^H \left(\mathbf{H}\mathbf{H}^H\right)^{-1} \mathbf{H}$ and $\mathbf{I}$ is the identity matrix [111]. When a BS creates interference to more than one user in other cells, $\mathbf{H}$ is selected as the concatenation of all the interfering channels, in our scenario $\mathbf{H} = \mathbf{h}_{2,1}$. From [50], we have the distribution of the signal term in (4.3) as $\left|\mathbf{h}_{i,i}\mathbf{f}_{i,Z}\right|^2 \sim \chi^2_{2(N_t-(K-1))}$, where K is the number of all channels.

Limited feedback design

In realistic scenarios, there will always be inaccuracy in the available CSI. Here, we assume that each user obtains perfect channel knowledge by channel estimation and the feedback channel is error-free and without delay. With limited feedback, only the channel direction information (CDI) , i.e., $\tilde{\mathbf{h}} = \mathbf{h} / \|\mathbf{h}\|$ is fed back using a quantization codebook which is shared at both the transmitter and receiver. All the channels $\mathbf{h}_{i,j}$ use separate codebooks of unit norm vectors of size $L = 2^B$, where B is the number of feedback bits. We denote

the codebooks as $C_{i,j} = \{\mathbf{c}_1, \mathbf{c}_2, \ldots, \mathbf{c}_L\}$. Each user quantize its channel direction to the closest codeword with minimal chordal distance:

$$\tilde{\mathbf{h}} = \arg \min_{\mathbf{c}_i \in C_{i,j}} \sqrt{1 - |\mathbf{c}_i^H \mathbf{h}_{i,j}|^2}. \tag{4.7}$$

Then the users send the index of this codeword in the codebook to the BS as the feedback information. The BS uses the corresponding codeword as the estimated CSI ($\tilde{\mathbf{h}}_{i,j}$) to design the beamforming vector. It has to be mentioned that, different beamforming schemes require different CSI. For example, ZF beamforming needs both CSI from the desired channel and the interfering channels while the eigen-beamforming only requires the CSI of the desired link. The usage of the estimated CSI leads to a performance degradation in the sum-rate due to quantization errors. In the next section we will discuss the effect of this error analytically and propose a bit splitting scheme for ZF beamforming, which adaptively allocates the feedback bits for quantizing the desired link and the interfering link.

4.2.3 Feedback bit partitioning scheme

The objective of the ZF beamforming is nulling out the interference to the undesired users if the BS holds full channel knowledge. In case of a limited feedback channel, the interference term in the denominator of (4.3) can not be totally eliminated, i.e., limited feedback causes residual interference. We assume uncorrelated Rayleigh channels and hence each component of $\mathbf{h}_{i,j}$ is independent and identically distributed (i.i.d.) according to $\mathcal{CN}(0,1)$. Since eigen-beamforming is not a cooperative beamforming, bit partitioning is not required. Therefore, in this sub-section we consider that the macro base station and the relay station both perform ZF beamforming.

As introduced in [111], the limited feedback has differing impact on the received signal term and the interference term in (4.3). The desired signal term of user i in (4.3) is distributed as $|\mathbf{h}_{i,i}\mathbf{f}_i|^2 \sim \xi_{i,i} Z$, where Z is a chi-squared random variable fulfills $Z \sim \chi^2_{2(N_\mathrm{t}-1)}$ and $\xi_{i,i}$ is the degradation factor of the desired signal power due to quantization. If $B_{i,i}$ bits are used for quantizing $\mathbf{h}_{i,i}$, $\xi_{i,i}$ can be calculated as [17]:

$$\xi_{i,i} = 1 - 2^{B_{i,i}} \cdot \beta\left(2^{B_{i,i}}, \frac{N_\mathrm{t}}{N_\mathrm{t}-1}\right), \tag{4.8}$$

where $\beta(\cdot)$ denotes the Beta function. The interference term of user i can be distributed as $|\mathbf{h}_{i,j}\mathbf{f}_j|^2 \sim \kappa_{i,j} Y$, where $Y \sim \chi^2_2$ and $\kappa_{i,j} = 2^{-\frac{B_{i,j}}{N_\mathrm{t}-1}}$ is the residual interference term factor. With these two parts, we can re-write the received SINR of user i as:

$$\gamma_i = \frac{\xi_{i,i} P_i Z}{\mathcal{N}_0 + \kappa_{i,j} P_j Y}, \tag{4.9}$$

where P_i is the transmit power at the served base station and P_j is the transmit power at the interfering base station. Therefore, the average rate of user i can be written as

$$R_i(P_i, P_j, B_{i,i}, B_{i,j}) = \mathbb{E}\left\{\log_2\left(1 + \frac{\xi_{i,i} P_i Z}{\mathcal{N}_0 + \kappa_{i,j} P_j Y}\right)\right\}, \tag{4.10}$$

where $B_{i,i}$ and $B_{i,j}$ are feedback bits used to quantize the desired channel and the interfering channel, respectively.

In this paper we assume that each user has a fixed number of feedback bits B, which can be used to quantize the desired and interfering channels. To obtain the maximized sum-rate, we attempt to maximize the rate of each user (4.10) separately. This leads to our optimization problem for each user:

$$\begin{aligned} \max \quad & R_i(P_i, P_j, B_{i,i}, B_{i,j}) \\ \text{subject to} \quad & B_{i,i} + B_{i,j} = B. \end{aligned} \tag{4.11}$$

In the high SINR regime the rate of user i can be approximated as

$$\begin{aligned} R_i(P_i, P_j, B_{i,i}, B_{i,j}) \;&\approx\; \mathbb{E}\left\{\log_2\left(\frac{\xi_{i,i} P_i Z}{N_0 + \kappa_{i,j} P_j Y}\right)\right\} \\ &=\; \log_2(\xi_{i,i}) + \log_2(P_i) + \mathbb{E}\{\log_2(Z)\} \\ &\quad -\mathbb{E}\{\log_2(N_0 + \kappa_{i,j} P_j Y)\}. \end{aligned} \tag{4.12}$$

Using the concave property of the logarithmic function and Jensen's inequality, (4.12) can be further written as

$$\begin{aligned} R_i(P_i, P_j, B_{i,i}, B_{i,j}) \;&\geq\; \log_2(\xi_{i,i}) + \log_2(P_i) + \mathbb{E}\{\log_2(Z)\} - \log_2(N_0 + \kappa_{i,j} P_j \mathbb{E}\{Y\}) \\ &=\; \log_2(\xi_{i,i}) + \log_2(P_i) + \frac{1}{\ln 2}\psi(N_\mathrm{t} - 1) - \log_2(N_0 + \kappa_{i,j} P_j), \end{aligned} \tag{4.13}$$

where $\psi(\cdot)$ is Euler's psi function [72]. Since the derivative of the Beta function in (4.8) is very complicated, for later calculations we use a lower bound of the degradation factor [49]

$$\xi_{i,i} \geq 1 - 2^{-\frac{B_{i,i}}{N_\mathrm{t}-1}}.$$

Hence the rate of user i is lower bounded by

$$\begin{aligned} R_i(P_i, P_j, B_{i,i}, B_{i,j}) \;&\geq\; \log_2(1 - 2^{-\frac{B_{i,i}}{N_\mathrm{t}-1}}) + \log_2(P_i) + \frac{1}{\ln 2}\psi(N_\mathrm{t} - 1) - \log_2(N_0 + \kappa_{i,j} P_j) \\ &\triangleq\; R_i^{\mathrm{LB}}. \end{aligned} \tag{4.14}$$

To find the maximum of R_i^{LB} with the constraint in (4.11) we construct the Lagrange function with the help of the Lagrange multiplier λ. We obtain the suboptimal solution

of (4.11) by the method of Lagrange multipliers:

$$\begin{aligned} B_{i,i} &= (N_\mathrm{t}-1)\log_2\left(\frac{\sqrt{\rho_j C}+\sqrt{\rho_j C+1}}{\sqrt{\rho_j C}}\right), \\ B_{i,j} &= (N_\mathrm{t}-1)\log_2\left(\frac{\rho_j\sqrt{\rho_j C+1}-\sqrt{\rho_j C}}{\sqrt{\rho_j C}}\right), \end{aligned} \tag{4.15}$$

where $\rho_j = \frac{P_j}{N_0}$ is the received interference-to-noise ratio (INR) of user i and $C = 2^{-\frac{B}{N_\mathrm{t}-1}}$. Since in total there are B bits available, $B_{i,i}$ and $B_{i,j}$ must be determined by B and rounded versions of (4.15). In case that the calculated $B_{i,i}$ is not an integer, we need to consider $\lceil B_{i,i} \rceil$ and $\lfloor B_{i,i} \rfloor$ and choose the one which maximizes (4.13) as the final solution $\hat{B}_{i,i}$. The number of interfering feedback bits $\hat{B}_{i,j}$ can be easily calculated by $\hat{B}_{i,j} = B - \hat{B}_{i,i}$.

We can observe that the results in (4.15) depend on the number of transmit antennas N_t, the total number of available feedback bits B and the received INR $\rho_{i,j}$. From Figure 4.3, we can observe that, $B_{i,j}$ increases up to B when INR becomes larger, meaning that more bits should be spent on the interfering link for feedback. When INR is lower than -21 dB, noise totally dominates and all of the feedback bits should be used for the desired channel to maximize the desired power.

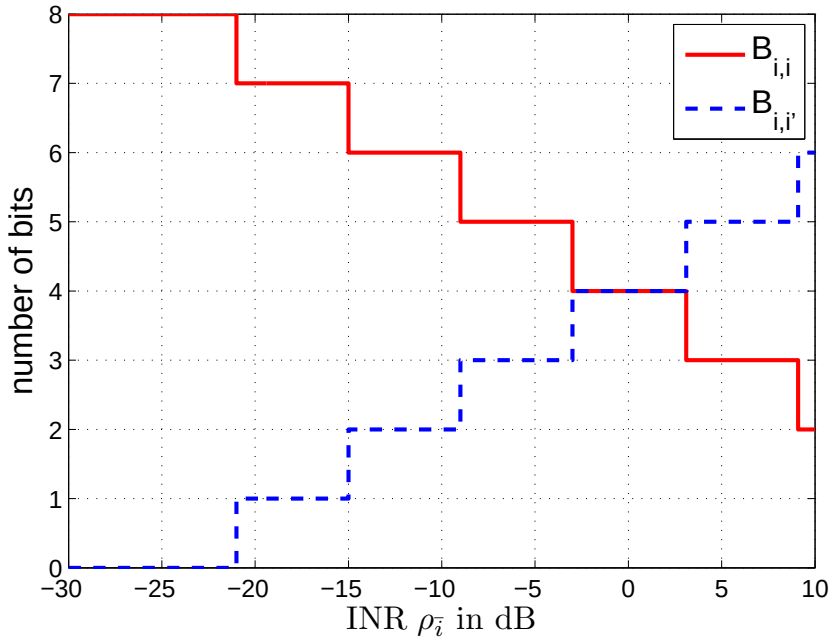

Figure 4.3: Bit partitioning for SNR=10 dB and B=8.

4.2.4 Adaptive beamforming strategy

In the previous section, we assumed that in the cooperative relay scenario both macro BS and RS always adopt ZF beamforming. Actually, ZF beamforming may not be the optimal choice especially when the user incurs weak OCI. In this case noise power dominates and a more proper transmission strategy is eigen-beamforming to increase the received signal power for the desired user. In this section, we consider that each BS can use either ZF beamforming or eigen-beamforming. Hence, in our assumed system there are four possible beamforming strategies for macro BS beamformer S_{B} and RS beamformer S_{R}: $(S_{\mathrm{B}}, S_{\mathrm{R}}) \in \{(Z,Z),(E,E),(Z,E),(E,Z)\}$, where Z and E stand for ZF beamforming and eigen-beamforming, respectively. The problem is to choose the suitable beamforming strategy that maximizes the sum-rate of the system.

Similar to (4.12), we first give the average rate of user i if different strategies are used:

$$R_i(P_i,P_j,B_{i,i},B_{i,j}) \approx$$
$$\begin{cases} \mathbb{E}\left\{\log_2\left(\dfrac{\xi_{i,i}P_iZ}{N_0+\kappa_{i,j}P_jY}\right)\right\},\ Z\sim\chi^2_{2(N_{\mathrm{t}}-1)}, Y\sim\chi^2_2, & \text{if}(S_{\mathrm{B}},S_{\mathrm{R}})=(Z,Z);\\ \mathbb{E}\left\{\log_2\left(\dfrac{\xi_{i,i}P_iZ}{N_0+P_jY}\right)\right\},\ Z\sim\chi^2_{2N_{\mathrm{t}}}, Y\sim\chi^2_2, & \text{if}(S_{\mathrm{B}},S_{\mathrm{R}})=(E,E);\\ \mathbb{E}\left\{\log_2\left(\dfrac{\xi_{i,i}P_iZ}{N_0+P_jY}\right)\right\},\ Z\sim\chi^2_{2(N_{\mathrm{t}}-1)}, Y\sim\chi^2_2, & \text{if}(S_{\mathrm{B}},S_{\mathrm{R}})=(Z,E);\\ \mathbb{E}\left\{\log_2\left(\dfrac{\xi_{i,i}P_iZ}{N_0+\kappa_{i,j}P_jY}\right)\right\},\ Z\sim\chi^2_{2N_{\mathrm{t}}}, Y\sim\chi^2_2, & \text{if}(S_{\mathrm{B}},S_{\mathrm{R}})=(E,Z). \end{cases} \tag{4.16}$$

The corresponding lower bound of each term in (4.16) according to the derivation in the previous section is

$$\begin{cases} \log_2\left(\dfrac{\xi_{i,i}}{1+\kappa_{i,j}\rho_j}\right)+\dfrac{1}{\ln 2}\psi(N_{\mathrm{t}}-1)+\log_2(\rho_i)\\ \log_2\left(\dfrac{\xi_{i,i}}{1+\rho_j}\right)+\dfrac{1}{\ln 2}\psi(N_{\mathrm{t}})+\log_2(\rho_i)\\ \log_2\left(\dfrac{\xi_{i,i}}{1+\rho_j}\right)+\dfrac{1}{\ln 2}\psi(N_{\mathrm{t}}-1)+\log_2(\rho_i)\\ \log_2\left(\dfrac{\xi_{i,i}}{1+\kappa_{i,j}\rho_j}\right)+\dfrac{1}{\ln 2}\psi(N_{\mathrm{t}})+\log_2(\rho_i) \end{cases}, \tag{4.17}$$

where $\rho_i=\frac{P_i}{N_0}$ is the received SNR of user i. Therefore, the sum-rate of the system R_i+R_j is lower bounded by the summation of two formulas in (4.17) depending on the strategy used by two BSs. Our idea is to choose the strategy which maximizes the lower bound of the sum-rate in (4.17). We conclude that if one user suffers higher interference from the other cell, the interfering BS should perform ZF beamforming to cancel the strong

interference to this user. Otherwise eigen-beamforming is used. We can observe that each formula in (4.17) contains a term related with the received SNR $\rho_{i,i}$. As a result, $\rho_{i,i}$ does not play any role in the final decision of the strategy. Therefore, we only consider the first two terms in each formula in (4.17), which further depend on $B_{i,i}$, $B_{i,j}$, N_{t} and $\rho_{i,j}$.

4.2.5 Simulation results and analysis

Two cell scenario

In this section we consider the two cell system as shown in Figure 4.2. Throughout the simulations we set the number of transmit antennas of the BSs $N_t = 2$ and the transmission bandwidth to be 1 MHz. We assume that the received interference-to-signal ratio (ISR) is distance-dependent. For macro UE and relay UE, the ISRs can be expressed as:

$$\gamma_{\mathrm{ISR},1} = \frac{P_r}{P_m}\left(\frac{d_m}{d_r}\right)^{\alpha}, \gamma_{\mathrm{ISR},2} = \frac{P_m}{P_r}\left(\frac{d_r}{d_m}\right)^{\alpha}, \tag{4.18}$$

where d_m and d_r denote the distance from macro BS and RS to the UE, respectively. α is the pathloss exponent, which is set to $\alpha = 3$ [62]. We assume that each user has some fixed received SNR values and incurs different interference-to-signal ratio (ISR) levels depending on the user channels. In the LTE-A standard, as defined in 3GPP simulation case 1, the minimum distance between UE to relay station is 10 m, the minimum distance between UE to macro BS is 35 m and the inter-site distance is 500 m. Furthermore, the transmit power levels for macro and relay BSs are 46 dBm and 30 dBm, respectively. Substituting these parameters into (4.18), we find that the ISR for relay UE and macro UE vary in the range of (-35 dB, 0 dB) and (-50 dB, 0 dB), respectively. The total number of feedback bits is set to $B = 8$.

Figure 4.4 shows the sum-rate performance of the system versus the average received SNR by using the ZF beamforming strategy. The proposed bit partitioning algorithm in (4.15) is denoted as *proposed* and *equal* is for equal allocation of feedback bits. $perfect$ indicates that the BS can obtain the full CSI knowledge. Obviously the perfect case outperforms both algorithms, but is not realistic. In case that we have the same number of bits $B = 8$ or $B = 4$, the proposed algorithm always outperforms equal bit distribution especially when the SNR is large. This is because the INR becomes larger in the high SNR regime where the interference dominates the noise. As shown in Figure 4.3, in this case the ZF beamforming plays an important role and sophisticated design of the allocation of feedback bits gains much. Moreover, the simulation results verify that the limited feedback algorithm can achieve more sum-rate gain when there are more feedback bits available.

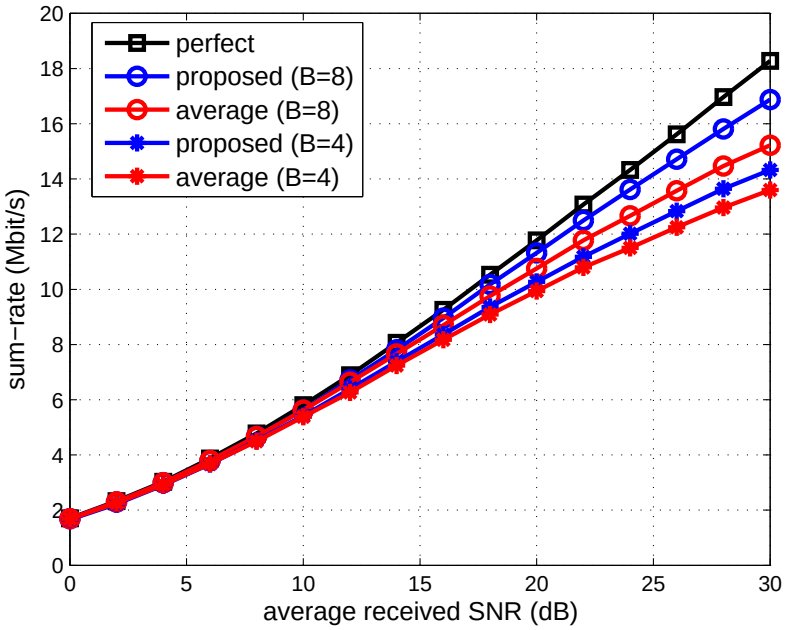

Figure 4.4: Sum-rate using ZF beamforming with different bit partitioning algorithms and numbers of available feedback bits.

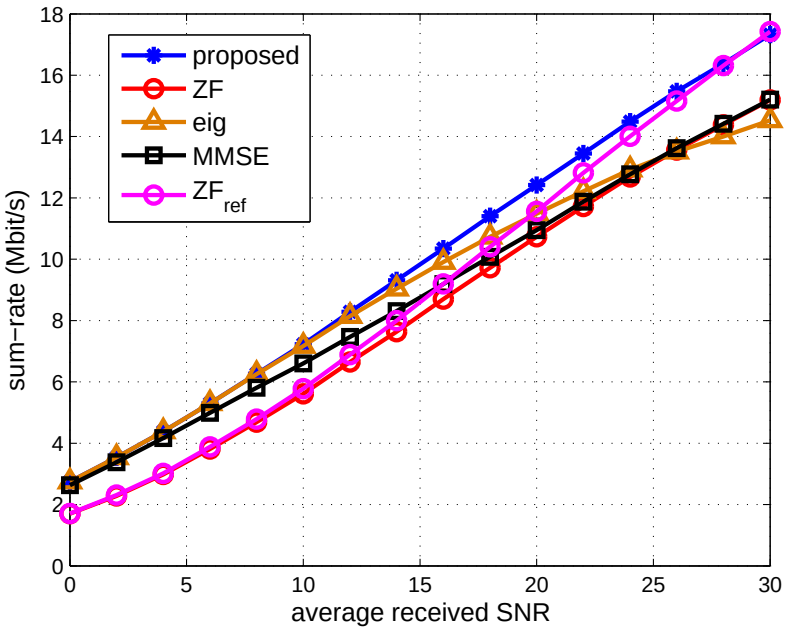

Figure 4.5: Performance comparison of different beamforming strategies for $B = 8$.

Next, we implement the proposed adaptive beamforming strategy. Figure 4.5 illustrates the performance comparison of using different beamforming schemes for $B = 8$. *eig* denotes the eigen-beamforming, which on average achieves a gain of 1 Mbit/s in the low SNR regime compared with ZF beamforming with equally allocated feedback bits. In the high SNR region eigen-beamforming shows poor performance due to the strong OCI. The MMSE approach [79] achieves around average 0.75 Mbit/s performance gain compared to ZF at low SNR and converges to ZF at high SNR. *proposed* indicates our proposed adaptive beamforming design with limited feedback. It outperforms all other strategies in the whole SNR region and performs similar to eigen-beamforming at low SNR. ZF_{ref} is the coordinated ZF beamforming in [61], which tries to eliminate the intra-cell interference and OCI without considering to enhance the desired power. Hence ZF_{ref} shows a degradation at low SNR and approaches to our proposed algorithm at high SNR.

Multi-cell scenario

The investigation of the simplified 2-cell (a macro cell and a relay cell) network provided insights about the strategy selection and motivated the adaptive coordination, but the result cannot be readily implemented in a general multi-cell network. Furthermore, we extend our adaptive strategy to general multi-cell networks and evaluate the performance by our dynamic system level simulator. We consider a cellular network with 7 hexagonal cell sites and 3 sectors per site. Type 1 and decode-and-forward relays are carried out. In each sector, three relay nodes are located near the cell edge and 30 UEs are uniformly distributed. Average user spectral efficiency and the 5%-ile user spectral efficiency, which are two major performance metrics, indicate the overall cell capacity and cell edge user performance, respectively.

Table 4.1 lists the performance comparison of using different beamforming schemes in the 3GPP case 3 relay-enhanced LTE-A suburban scenario. We first focus on the simulation result obtained from the ZF beamforming scheme, which shows only a slight performance gain compared with the case without beamforming. This is explained by the fact that there are too many interfering links existing in cellular networks especially with the deployment of relay nodes. ZF beamformer tries to cancel the impact from all interfering links, which will reduce the signal power from the desired link. We could therefore conclude that ZF beamforming can not offer decent performance in multi-cells scenario. With the eigen-beamforming strategy, the average and cell edge user spectral efficiency increase more than 35% and 75% compared with the case without beamforming. In our proposed beamforming scheme, we include the limited feedback strategy instead of full CSI assumption. We consider only 3 bits for each channel feedback. In Table

4.1, the system level simulations show that the average user spectral efficiency has 15% performance degradation compared with full CSI assumption. In addition, the simulation results are also depicted for all approaches as spectral efficiency CDF as shown in Figure 4.6. The CDF results illustrate the same trends.

Table 4.1: Spectral efficiency comparison of different beamforming strategies in 3GPP case 3

Beamforming strategy	Average UE efficiency	5%-ile UE efficiency
Equal-weighted beamforming	2.4	0.52
ZF beamforming with full CSI	2.54	0.56
Eigen-beamforming with full CSI	3.28	0.92
Adaptive BF with limited feedback	2.80	0.70

(All values are measured in bit/s/Hz.)

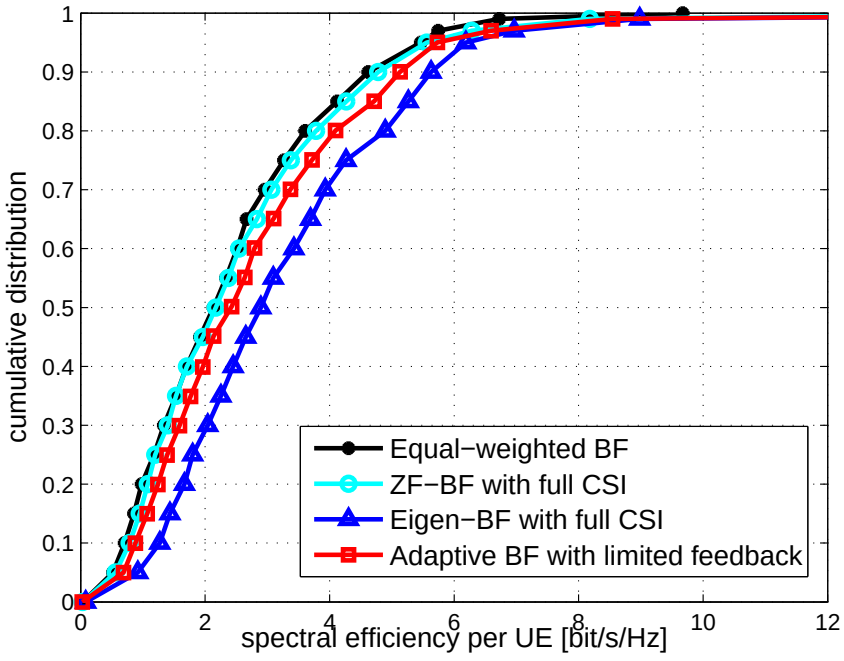

Figure 4.6: Performance comparison for different beamforming strategy.

4.2.6 Conclusion

Within this section, we analyzed the performance using ZF and eigen-beamforming with RVQ in a cooperative relay system. We calculated the sum-rate lower bound when ZF

or eigen-beamforming is implemented at the macro base station and relay station. With this lower bound, we proposed a bit partitioning algorithm which allocates the feedback bits for quantizing the serving and interfering channels. The simulation results show that a suitable bit partitioning can improve the system sum-rate especially in an OCI-dominated scenario. An adaptive beamforming strategy was also proposed and proved to outperform the conventional schemes in two cells system. The proposed strategy was extended into multi-cell LTE-A cellular network, and the performance comparison of different beamforming strategies was given.

4.3 Proposals of the shared relay deployment

In this section, we focus on a shared relay architecture in the cellular network instead of deploying multiple separated relays near cell edges. The advantage of shared relaying is the joint processing of signals at the relay to suppress the inter-cell interference (ICI) .

4.3.1 Introduction

The basic idea of a shared relay was firstly proposed in [66], where a relay station is deployed at the intersection of neighboring macro cells. Figure 4.7(a) illustrates a hexagonal layout cellular network with a shared relay station. Figure 4.7(b) shows the conventional relay deployment with separated relays located near the cell edge. A shared relay, which can be considered as a coordinated station of multiple separate relays, is used to serve the user equipments at the cell edge from different cell sectors. Hence, the ICI problem can be partially overcome by a cell deployment where multiple neighboring macro BSs share one RS.

There have been only a limited number of works in literature on the shared relay concept. In [95], it is shown that the shared relay is able to provide gain with respect to local base station coordination and to remove much of the dominant interference. Furthermore, a joint processing of cooperating BSs and the shared relay station in the relay transmission phase is proposed to increase the resource usage efficiency in [55]. The shared relay concept is further studied in [35], in which the simulation results show that a significant increase in throughput can be achieved by shared relays compared to the wireless cellular network without relays. The performance of a relay enhanced cellular system depends significantly on the resource allocation strategy [23]. To balance the competition between different links, the resource allocation is more important in the shared relay scenario. In [107], Yang et al. suggest a power and resource allocation scheme for the shared relay to efficiently manage ICI. However, they did not consider the transmission from the eNB to the shared relay link. In addition, the authors in [65] propose a fair scheduling and

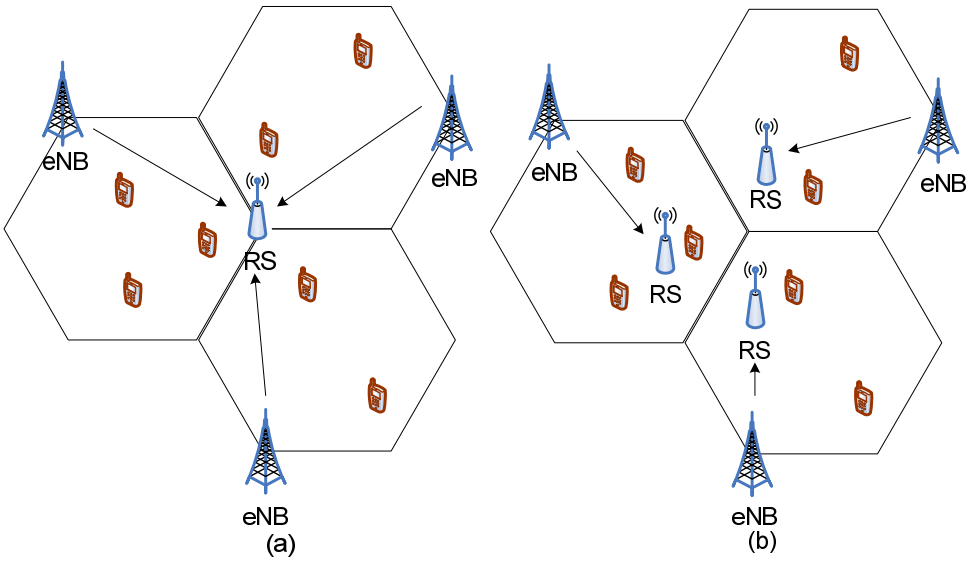

Figure 4.7: Cellular network with relay stations. (a) Shared relays for three adjacent sectors. (b) Separated relay near the edge of each sector.

resource allocation algorithm for users in adjacent cells to maximize the benefit of the shared relay but without taking into account the effect of resource demands from different links.

As introduced in Chapter 3, the 3GPP has defined the multicast broadcast single frequency network (MBSFN) subframe which is used for backhaul reception at the relay node in [6]. We propose an MBSFN subframe based resource allocation algorithm for shared relays and macro BSs to maximize the spectral efficiency of the whole system and cell edge users. We evaluate the system level view spectral efficiency in different resource demand situations to quantify the benefit by using shared relays.

We adopt the following assumptions and definitions during the research:

- A half-duplex decode-and-forward (DF) relay strategy is assumed since the shared relay has most of functions that an eNB has.
- Users can be served by macro BSs or RNs, the selection is based on the reference symbol received power (RSRP) [10].
- Perfect channel estimation is assumed in all links across different subchannels.
- MBSFN subframes are assumed to be synchronous.

4.3.2 Network layout

We consider a cellular network with 19 hexagonal cell sites and 3 sectors per site as shown in Figure 4.8. In the shared relay deployment, the relay stations are deployed at the intersection of three adjacent sectors. In the separated relay system, 1, 3 or 5 relay nodes are placed near the cell edge as defined in the LTE-A standard [9].

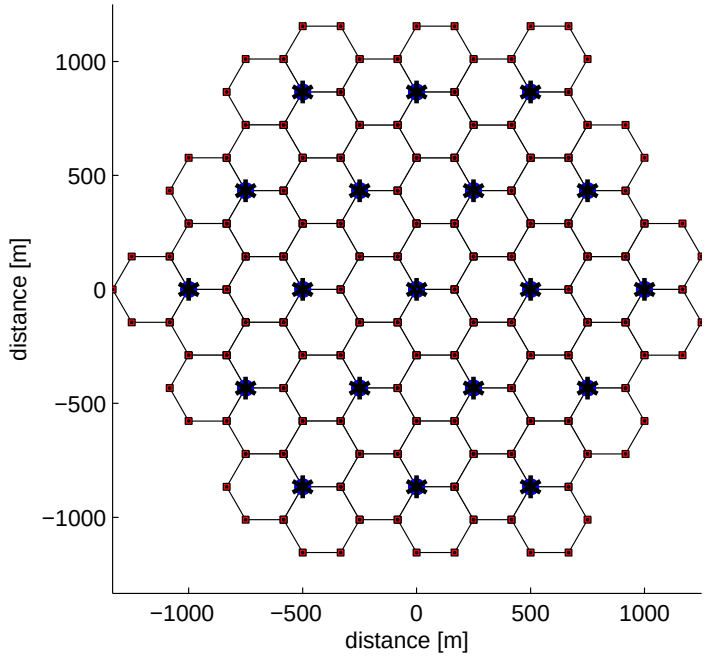

Figure 4.8: Network Layout, 19 macro sites, 3sectors/site, with shared relays.

4.3.3 Resource demand discussion

Different from conventional LTE systems, the resource allocation at the macro BS is to split resources between macro UEs and relay stations in a relay enhanced network. The resource demand of relay stations is related to that of relay UEs, since the functionality of the relay is to forward information from the BS to relay UEs. Most of previous studies consider the resource demand of relay stations is determined based on the ratio of the number of relay served UEs to the total number of UEs [36]. For example, considering 30 UEs are served by the macro BS and 10 UEs are attached to relay stations, the resource allocation at the macro BS is to split 75 % resources to macro UEs and 25 % resources to relay stations. However, this assumption is too optimistic in the realistic case, because it may happen that a few UEs require huge resources. In our work, we will evaluate the

spectral efficiency performance of the shared relay deployment under cases of different resource demand levels from relay users.

The number of MBSFN sub-frames, which is configured by the upper layer, is assumed to be associated with resource demands in different links in our work. If the communication data requirement of relay users (cell edge users) is huge, it means the macro BS should configure more MBSFN sub-frames to support the relay access link. Contrary, in the low resource demand case, the macro BS allocates less MBSFN sub-frames of eNB-relay link to serve more macro users. In this work, we assumed that low, medium and high resource demand from relay users is associated with one, two, three MBSFN sub-frames in each macro BS frame structure, respectively.

4.3.4 Proposed resource allocation algorithm for a cellular network with shared relays

The resource allocation for downlink is to allocate resource blocks in every transmission time interval slot. The number of available resource blocks depends on the cellular frequency bandwidth assignment, e.g., according to the 3GPP LTE specifications, 50 RBs in a downlink TTI slot for 10 MHz bandwidth.

In a shared relay assisted network, the relay station is shared among three adjacent sectors, it is possible that three corresponding macro BSs transmit a signal to the shared relay simultaneously. That means that transmissions from different macro BSs need to be carefully separated in time, frequency or space. Since the relay station in LTE-A is a low cost device with a fraction of the base station functions, it is not realistic to equip too many antennas at the RS which means spatial separation is not the first choice. In our work, we propose a time division based scheduler to avoid an information collision problem at the shared relay as a frequency reuse factor of one is assumed among the macro BSs and shared RNs in the network. In this work, we assume that the frame structures of all base stations are synchronous.

In the regular hexagonal cellular layout with tri-sectored sites, we index sectors for each site with the number 1 to 3 or mark them with three different colors as illustrated in Figure 4.9. A shared relay and three adjacent macro sectors with different color can be grouped as a joint subsystem, e.g., as the shaded blocks in Figure 4.9. We design a frame structure and resource partition algorithm for this shared relay subsystem as shown in Figure 4.10. The different macro BSs transmit signals to the shared relay at MBSFN sub-frames with unique index in the frame structure, which is to avoid the signal collision problem. As shown in our example: eNB1 transmits the signal to the shared relay in the 2nd and 7th sub-frame; eNB2 and eNB3 to the shared relay transmission happens in 4th

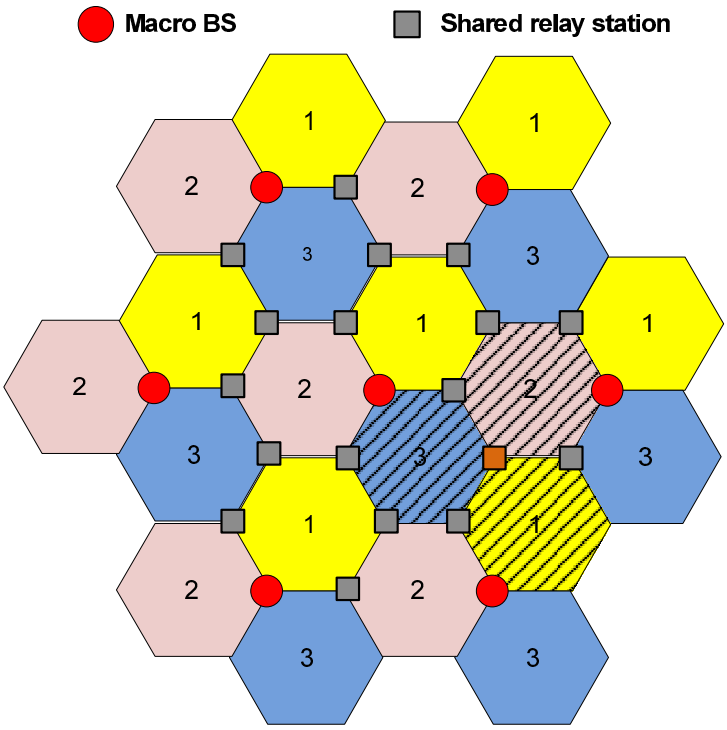

Figure 4.9: The hexagonal cellular layout with shared relays.

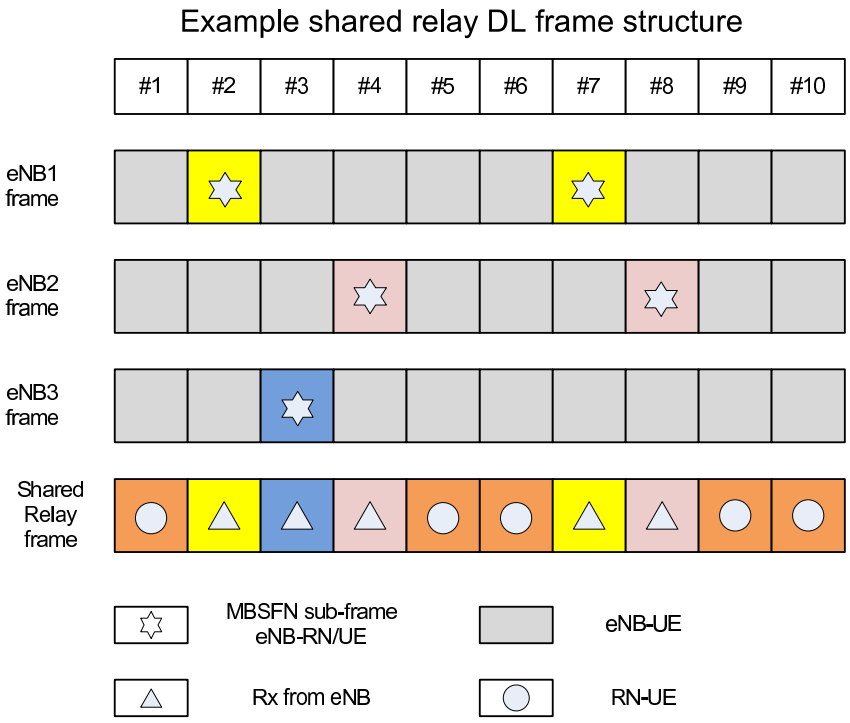

Figure 4.10: An example of frame structure for the shared relay system.

and 8th sub-frame and 3rd sub-frame, respectively. Therefore, in these corresponding MBSFN sub-frames (marked as triangles in Figure 4.10) the shared relay works on the receiving mode since we assume a half-duplex relay strategy. In other sub-frames (marked as circles in Figure 4.10), the shared relay could forward the signal from eNBs to the UEs which are assisted by the shared relay station.

As defined in LTE standard, a basic LTE radio frame has an overall length of 10 ms and comprises 10 sub-frames. It hence is worth to mention that if more than three MBSFN sub-frames exist in each macro BS frame structure, all sub-frames of the shared relay are occupied by MBSFN sub-frames. Therefore, the shared relay will always work in receiving mode. This shortcoming makes that the shared relay cannot work in a situation in which data demand from relay users is huge.

4.3.5 Simulation results and analysis

In this section, the scenario of 3GPP LTE-A Case 1 scenarios (Urban) with inter-site distance of 500 m are carried out. The shared relay station is assumed to utilize decode-and-forward strategy. All simulation parameters follow the latest parameter settings agreed in 3GPP [9] and summarized in Chapter 3.

Table 4.2: Spectral efficiency comparison of different relay scenarios

	No RN	Separate RN			Shared RN
		1 relay	3 relays	5 relays	
Average UE spectral efficiency	2.09	2.07	2.12	2.22	2.71
5%-ile UE spectral efficiency	0.14	0.20	0.28	0.26	0.25

(All values are measured in bit/s/Hz.)

Table 4.2 lists the performances of different relay scenarios in the case of medium resource demand from cell edge users. We compare the performance of both the separated relay scenario and the shared relay scenario as shown in Figure 4.7. The performance metrics include the average user spectral efficiency and the 5%-ile user spectral efficiency, which corresponds to the cell edge user performance. It can be observed that with one relay station deployed in each sector, the average spectral efficiency shows a slight degradation compared with the result from the system without relay station. However, cell edge performance increases around 50%. The reason is that the relay deployment aims at improving the cell edge performance not the capacity of the network and hence the total efficiency improvement is somehow limited. Furthermore, with more relay stations

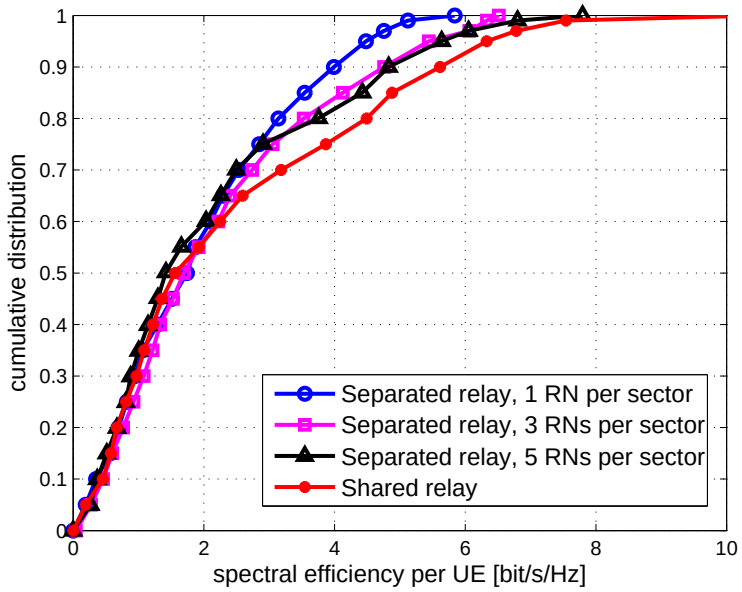

Figure 4.11: Spectral efficiency of different relay networks in the case of medium resource demand from cell edge users.

deployed in each sector, the spectral efficiency of cell edge users is clearly increased (up to 80% increase compared to the system without RN). But the average spectral efficiency in the five relays case is almost the same as in three relays case. The additional relay stations cause additional interference to other cells (other relay cells and all macro cells). As the conventional separated relay node deployment is strongly interference limited, the advantage of shared relaying comes mostly from its interference cancellation ability. Results show that the shared relay deployment significantly improves the system performance compared to separated relay deployments. It achieves 22% increase in average user spectral efficiency over the deployment of five relay nodes and 80% improvement in cell edge UE spectral efficiency over the traditional cellular network without relay station deployment. In addition, the simulation results are also depicted for all approaches as spectral efficiency cumulative distribution functions as shown in Figure 4.11. The CDF results illustrate the consistent trends.

Next, we implement and simulate the shared relay deployment in different cell edge resource demand cases. As mentioned before, when the resource demand from cell edge users is relatively low, we consider there is only one MBSFN subframe in each macro eNB frame. The medium resource demand is associated with two MBSFN subframes existing in each macro eNB frame structure. From Table 4.3, it can be observed that the shared relay deployment shows its advantage over the deployment with five separated

relays in the case of low and medium resource demand from cell edge users. The average user spectral efficiency can achieve up to 8% improvement and the cell edge user spectral efficiency achieves 13.3% $\sim$ 17.9% increase. In high cell edge resource demand case, the shared relay scheme does not have a good performance due to the shortcoming of the time-division scheduler and resource allocation scheme. And the simulation results verify this shortcoming. However, in a realistic case, resource demand from cell edge users is usually relatively low compared to the demand from the cell center. The corresponding spectral efficiency CDF results are illustrated in Figure 4.12, which show the same trends. In our work we assume that the frame structure is configured pre-fixed and synchronous to avoid higher dynamics in interference. An adaptive subframe allocation and scheduling scheme may need to be investigated in future work.

Table 4.3: Spectral efficiency comparison of shared relay system under different resource demand situations

Resource demand	Relay scenario	Average UE efficiency	5%-ile UE efficiency
Low	separate relay	2.42	0.30
	shared relay	2.36	0.34
Medium	separate relay	2.24	0.39
	shared relay	2.41	0.46
High	separate relay	2.17	0.46
	shared relay	2.05	0.30

(All values are measured in bit/s/Hz.)

4.3.6 Conclusion

In this section, we carried out a comprehensive system level simulation of 3GPP LTE-A Case 1 scenarios with relay deployments of separated cell-edge relay stations and shared relay stations. This contribution showed the advantage of the shared relay deployment in the average and cell edge performance from a system level perspective. A time division based resource allocation and scheduling algorithm was proposed to realize more potential of the cellular network with shared relays. Simulation results proved that the shared relay concept is effective in avoiding the inter-cell interference problem. The average and cell edge user spectral efficiencies can be increased by the shared relay deployment in the cases of low and medium resource demand from cell edge users.

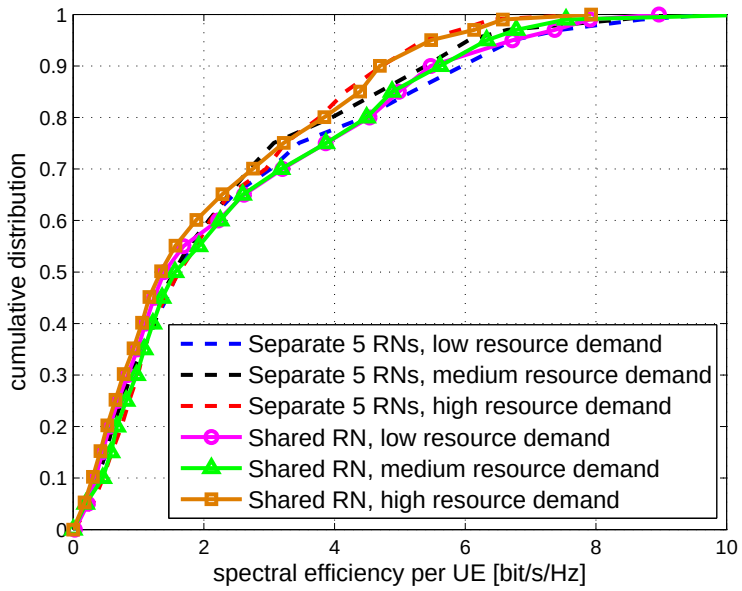

Figure 4.12: Performance comparison of shared relay and five separated relays deployment under different resource demand situations of cell edge users.

4.4 Summary

In this chapter, we have focused on mitigating the inter-cell interference problem in relay-enhanced LTE-A cellular networks. Two potential solutions have been proposed: one is beamforming design for cooperative communication and the other is the deployment of shared relays.

For beamforming design, the work is firstly focused on a two cell scenario (a macro cell with a relay cell). The sum-rate lower bound has been derived under the limited feedback situation, when zero forcing or eigen-beamforming is applied to the macro base station and relay station. With the lower bound, we have optimized the numbers of feedback bits for quantizing the desired and interfering channels and proposed an adaptive beamforming strategy with limited feedback which selects a suitable beamforming scheme from ZF or eigen-beamforming based on the received interference and noise power level of the users. Simulation results show that the bit partitioning algorithm outperforms the equal bit distribution scheme especially when the signal-to-noise ratio is large. In addition, our proposed adaptive beamforming strategy outperforms existing schemes in different interference scenarios. Next, the proposed strategy has been extended to general multi-cell networks. The spectral efficiency performance of different beamforming strategies has been given.

The concept of shared relays is introduced and proved to be an effective solution to avoid inter-cell interference. Next, the resource demand situation and resource competition problem have been discussed. Based on these studies, an efficient and effective resource allocation and scheduling scheme based on the subframe structure has been proposed to maximize the benefit of the shared relay. System level simulations quantify the system performance in different resource demand situations. And simulation results show that the deployment of shared relays can improve significantly the overall system performance and also increase the spectral efficiency of cell edge users compared to the conventional separated cell edge relay station deployment.

Chapter 5

Mobile Relays

5.1 Introduction and motivation

5.1.1 High speed railway scenario

With the progress of globalization, the demand for traveling with a higher speed is increasing. High-speed railway transportation becomes a popular choice and is widely used around the world such as German ICE, French TGV, and China Railways High-speed (CRH). In order to provide continuous wireless communication service for on-board passengers, such as on-board calling or online entertainment, it is necessary to apply mobile broadband communication systems for the high speed railway system.

The high-speed train scenario is a special case for outdoor to indoor communication with a high moving speed and an enclosed body of good sealing property [52]. The major challenges in such scenario are:

- High Doppler spread

  The wireless channel in a high speed railway scenario is rapidly time-varying. In an OFDM system, the fast time variation of the fading channel over one OFDM symbol resulting from severe Doppler frequency shift (DFS) results in a loss of subcarrier orthogonality and thus introduces inter-carrier interference. Inter-carrier interference caused by the Doppler spread cannot be easily compensated because in the multi-path channel the received signal is composed of many incidence waves with different random Doppler frequency shifts due to arriving angles.

- High penetration loss

  The high-speed train carriages are made of aluminum or stainless steel, which leads to a high penetration loss generally between 12 dB and 24 dB [108]. This high penetration loss will directly degrade the communication link quality between UEs inside the carriages and the base stations along the railway and will also degrade the cell coverage.

- Too frequent handover (HO)

Due to the high speed of the train, handover will occur with higher frequency for on-board UEs. The handover process in the current LTE system requires multiple seconds to complete. Frequent handover failures may happen because of unreliable uplink measurement reports and long handover processing time at high mobility. Furthermore, a large group of UEs in a train may perform handover simultaneously, which causes a high call drop rate because of signaling congestion.

- Abrupt change of radio channel attenuation

  Normally, the radio channel attenuates with a slow change of channel variety. However, in the case of high-speed railway scenario, abrupt changes of the radio channel attenuation are expected. Therefore the precise prediction of the channel becomes a problem to be solved in the high-speed railway scenario [70].

5.1.2 Previous works

The existing global wireless communications standard for railway communication and applications is GSM for Railway (GSM-R), which is mainly based on the second generation Global System for Mobile Communications (GSM). Although GSM-R has obtained success in voice communications, its data rate is too low to meet current broadband mobile communication services, such as online video and gaming. And to reduce the call drop rate, conventional GSM-R systems use dedicated base station towers densely located along railway tracks. Adjacent cells therefore have a large overlap area so as to guarantee sufficient handover time [44].

LTE has been chosen as the next generation's evolution of mobile communication for railway by International Union of Railways (UIC) in order to provide high quality services to high speed train passengers. LTE-R requirements include supporting higher data rate and low system latency, several possible solutions have been hence discussed in the LTE-A standard [11].

- Dedicated deployment of macro eNBs

  The solution of dedicated deployment of macro eNBs, such as GSM-R, is naturally being considered. Operators deploy dedicated base station towers with directional antennas along the railway to directly serve the UEs on the train. In GSM-R, the distance between the base stations is 7-15 km. Dedicated path is enabled to handle all traffics generated for the on-board communication. The cell coverage of every macro eNB is generally extended to increase the interval of handovers and therefore reduce UE handover failure rate. Furthermore, a higher degree of redundancy and higher availability and reliability can be achieved.

- Dedicated deployment of macro eNBs with L1 repeaters

  In addition to deploying dedicated macro base stations along the railway, Layer 1 repeaters can be deployed on the train to overcome the high penetration loss caused by train body and windows.

- LTE as backhaul and Wi-Fi as access on-board

  A solution has been brought up that deploying a wireless access point on the train to provide on board communication service. And the mounted wireless node connects to the eNB as a LTE UE. This solution is less complicated and less costly as it can be built based on the current technologies. An optimized outdoor antenna (e.g. a smart antenna mounted on the train roof) can be envisaged to enhance the performance of the backhaul link.

Radio-over-fiber (RoF) systems, in which fully functional base stations are replaced by distributed radio access units (RAU) , are proposed in [60]. The signals from a base station are firstly transmitted to several radio access units, which are located along the rail tracks and are connected to the base station with optical fibers. The signals are transmitted into the air and are received by on-board UEs. The main challenge of RoF system is the fact that it requires frequent band switching since each RAU has a separate fixed radio frequency.

5.2 Overview about mobile relays

Besides the aforementioned possible solutions for high speed railway scenario, another potential idea is to employ mobile relays. As shown in Figure 5.1, the basic idea of a mobile relay is to install the mobile relay node (MRN) on the high speed train. The MRN moves along with the UEs in the carriage, as the train moves. The mobile relay is connected with eNB wirelessly and provides wireless connectivity service to end users inside the vehicle. In addition to the eNB functionality, mobile relays also support a subset of the UE functionality to connect to the DeNB.

Compared to existing solutions, a mobile relay can prove to be beneficial in several ways. In order to reduce the penetration loss, which is caused by well-shielded carriages, the mobile relay can deploy individual transceivers inside and outside the carriage separately. The antenna served for backhaul link is located on the rooftop of the train and the antenna serving UEs is placed inside the train. With more powerful antennas at the mobile relay, the backhaul link (eNB-MRN) will be better than the direct link (eNB-on-board UE). And since the on-board passengers move only with the pedestrian speed with

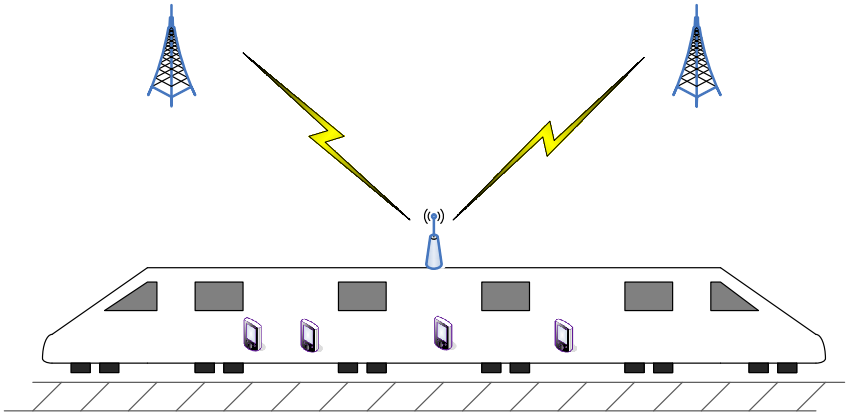

Figure 5.1: A reference scenario for a mobile relay.

respect to the MRN, the access link channel quality can be guaranteed. Therefore, one of contributions of the mobile relay is that it can effectively improve the system capacity. As discussed in [27], with the functionality of radio resource management and mobility measurement reporting, the mobile relay can perform a group handover procedure instead of individual mobility procedures for each UE. Group mobility can significantly reduce the signaling overhead and radio link failures, thus minimizing the latency for all UEs. The problem of high transmit power of UEs can be also partially solved since the MRN is much closer to on-board UEs than macro eNBs. Hence, the UE battery life can be extended.

5.3 Mobile relay handover procedure

In a high speed railway scenario, frequent handovers will happen in a relatively short period because of very high movement speed (300-400 km/h). A UE has very limited time to measure and execute one handover procedure. Furthermore, because UEs in a carriage perform handover almost at the same time, this will certainly increase the system signaling overhead, create channel congestion and result in handover failures. With a mobile relay, group mobility is a possible solution to solve existing handover problems.

5.3.1 Mobile relay architecture

[11] proposes two potential mobile relay architectures, which are based on the architecture Alternative 1 (Full-L3 relay) and architecture Alternative 2 (Proxy S1/X2) of fixed relays [8]. In the architecture Alternative 1, the S-GW/P-GW (Serving Gateway/Packet Data Network Gateway) entity serving the relay is separated from the DeNB and the relay is transparent for DeNB. Whereas, in the architecture Alternative 2 the S-GW/P-GW

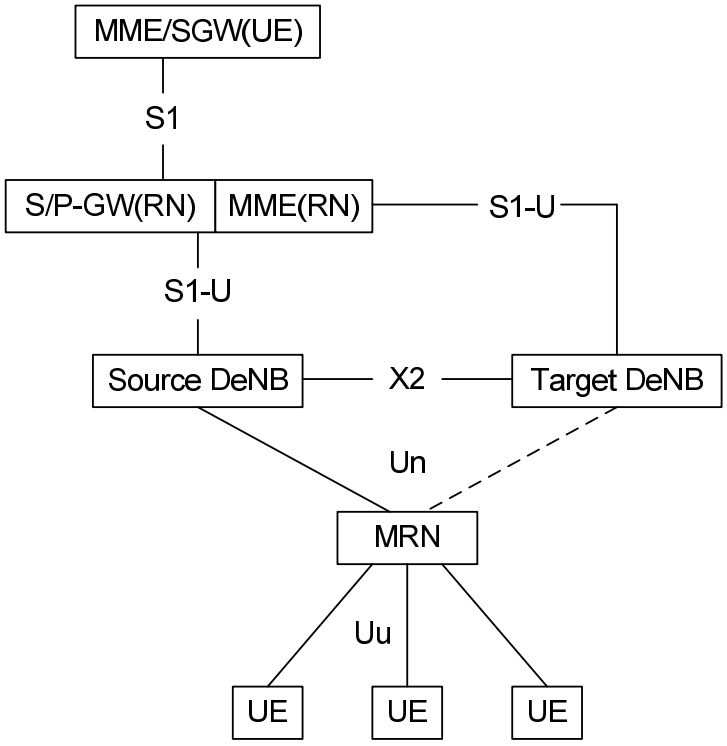

Figure 5.2: Architecture Alternative 1 for mobile relay handover.

functionality serving the relay is embedded in the DeNB and the relay S1/X2 interfaces in the architecture are terminated in the DeNB.

In Figure 5.2 architecture elements involved in moving relay handover for the 3GPP Alternative 1 architecture are presented. In architecture Alternative 1 the mobile relay node is transparent to the DeNB, i.e. the MRN S1/X2 interfaces are not terminated in the DeNB, but are terminated in the S/P-GW of the mobile relay node, which is separated from the DeNB. When the MRN moves from the source DeNB (S-DeNB) to the target DeNB (T-DeNB), the S/P-GW of the MRN, which handles the IP packets, serves as anchor. Therefore, the IP address of the MRN is not changed during the movement and the S1 interface re-establishment is not needed during the handover between MRN and DeNB.

Architecture Alternative 2 was developed as an optimization of alternative 1 to solve the back and forth signaling problem between the relay S/P-GW and the relay during the UEs inbound handover. So, one major feature of alternative 2 is to move the S/P-GW of the relay node into the DeNB and to consider S1/X2 proxy structure in the DeNB, so the back and forth signaling problem between the DeNB and the relay S/P-GW is solved. A simplified view of MRN handover in 3GPP architecture Alternative 2 is described in

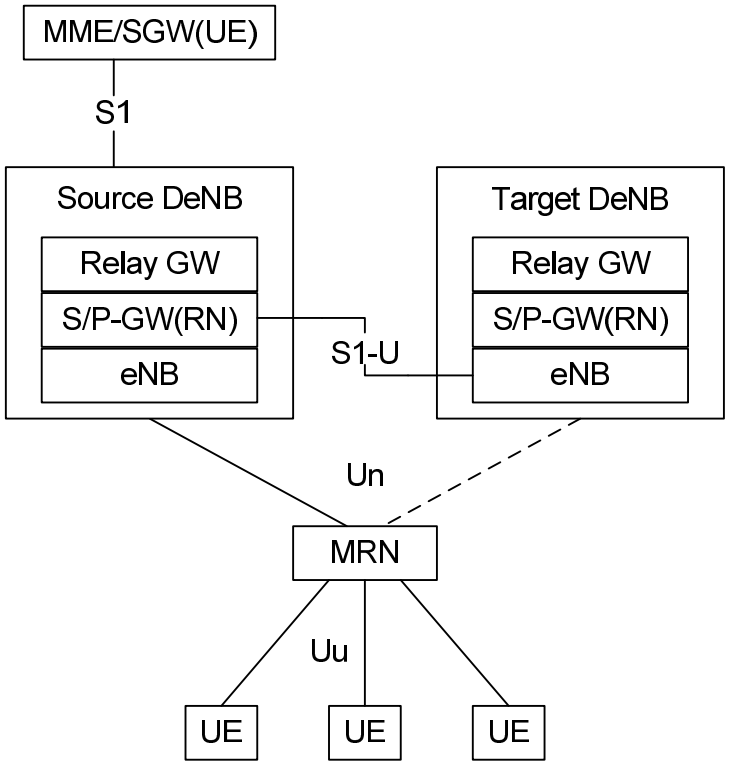

Figure 5.3: Architecture Alternative 2 for mobile relay handover.

Figure 5.3.

5.3.2 Mobile relay handover scheme

The mobile relay supports partial UE functionality [7], the UE handover procedure can be re-used as a basis for the mobile relay handover procedure. It also is necessary to support relay specific functionalities which are listed in [7]. During moving relay handover, three basic procedures are needed in order to maximize the handover success probability. These handover procedures are grouped as for UE handover into handover preparation, handover execution, and handover completion phase. The mobile relay handover procedure for 3GPP architecture Alternative 1 and Alternative 2 are described in Appendix D in detail.

Although mobile relays can help on-board UEs execute group handover procedure as introduced in the 3GPP specification [8], mobile relays still suffer too frequent handover in the high speed railway scenario. More reliable mobile relay handover schemes have been addressed in literature. In [42], authors propose a fast handover scheme based on GPS information for IEEE 802.16e on HSR networks. The idea is that the handover procedure can be automatically triggered in a predefined handover point, in which the scanning operation can be omitted and the operation time of handover procedure can

be greatly shortened. In [15] a handover scheme with adaptive triggering conditions is proposed. The on-board UE can select the suitable triggering condition according to the velocity of the train. [51] introduces a seamless handover strategy, which is based on the cell-array that smartly organizes the cells along a railway, to overcome interrupts during the multimedia streaming. Most of the above schemes are proposed with the help of the location information provided by global positioning system (GPS) devices. Since these GPS based schemes may not be robust when GPS service is not continuous, handover schemes without the help of the location information are proposed. In [103], the authors introduce a handover scheme, in which the front antenna executes handover while the rear antenna is used to communicate with BS, so that the communication can be kept during the handover procedure. The study in [36] offers a novel handover decision algorithm based on the UE relative velocities to the S-DeNB and the T-DeNB. In [75], an enhanced handover scheme is proposed to accelerate the measurement procedure when the train travels in fixed trajectories.

5.4 Performance analysis of the mobile relay

In this section, system level simulations are carried out to evaluate the downlink transmission performance of the mobile relay in terms of on-board user sum rate and handover performance. The cases of high speed train with and without MRN will be considered. And a coordinated MRN algorithm is proposed to optimize the system performance of the mobile relay.

5.4.1 System layout

In our simulation, typical base stations with three transceivers serving three sectors per site are placed on a hexagonal grid with wrap around to avoid border effects. For complexity reasons, simulations use a scaled down network, with 7 cells, 21 sectors, and 5 macro UEs per sector instead of 57 cells as shown in Figure 5.4. A train with a velocity of 350 km/h starts in one cell and travels along the displayed line across multiple cells. The train has 5 carriages of 50 meters long and 5 meters wide. The number of UEs in each car is supposed to be 10, i.e. totally 50 on-board UEs. For each carriage, there is one MRN located on the center of the rooftop. The used relaying method is full-duplex in-band decode-and-forward, since we consider sufficient antenna isolation (The antenna served for the backhaul link is located on the rooftop of train and the antenna served for the UE access link is placed inside the train with wired connection).

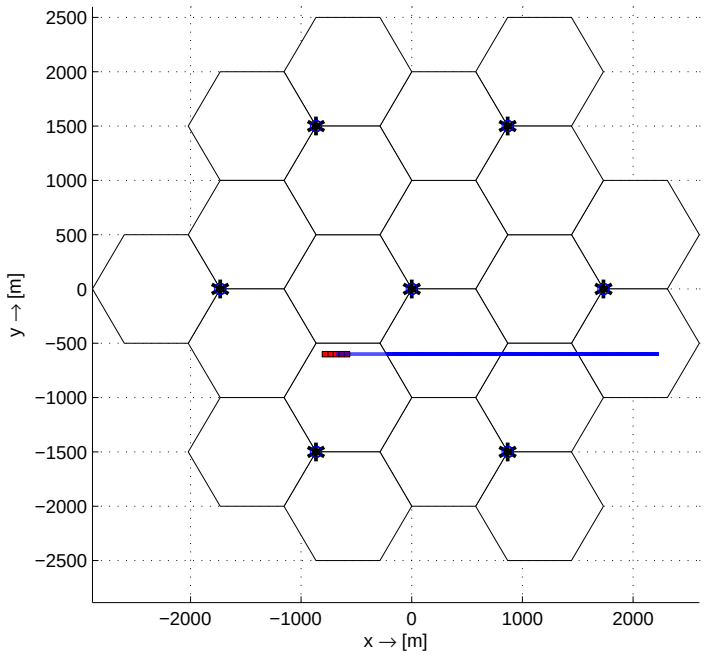

Figure 5.4: Network layout of LTE-A high speed railway scenario with mobile relay.

5.4.2 Simulation parameters

The 3GPP LTE-A Case 3 scenario (suburban) with inter-site distance of 1732 m is used as the baseline for all simulation cases in this section. Propagation case D2a (moving networks) in WINNER II [46] is specially considered to present the radio propagation of the eNB-MRN link. The main simulation parameters are summarized in Table 5.1.

5.4.3 Simulation results and analysis

To evaluate the performance of a MRN, we mainly focus on on-board UE performance. Figure 5.5 shows the instantaneous sum rate of on-board UEs with the movement of the train. In the simulation scenario a train with 50 onboard users is moving across the network on a predefined path, and the on-board user sum rate fluctuates when the train is moving into the cell center or moving out to the cell edge. Here we are interested in investigating the on-board UE performance of HSR scenario with mobile relays deployed, compared to a traditional system with direct and individual service of all on-board UEs in the cells.

As shown in Figure 5.5, we can see that the average total on-board UE sum rate reach 11.44 Mbit/s in the mobile relay case, while it only reaches 6.76 Mbit/s in the scenario without MRN, which means an improvement of about 70%. This illustrates that MRS

Table 5.1: System level simulation parameters of the mobile relay

Parameter	Value
System parameters	
Transmission bandwidth	10 MHz, DL
Carrier frequency	2 GHz
Modulation and coding scheme	CQI1 - CQI16
Number of RBs per sub-frame	50
Traffic model	Full Buffer
Scheduling method	Round Robin
MIMO case	SISO
eNB parameters	
Transmit power level	46 dBm
Antenna gain	14 dBi
Antenna pattern	$A(\theta) = -\min\left\{12\left(\frac{\theta}{\theta_{3\text{dB}}}\right)^2, A_m\right\}$, $\theta_{3\text{dB}} = 65°$ and $A_m = 20$ dB
Penetration loss	22 dB on eNB-onboard UE link
MRN parameters	
Forwarding strategy	decode-and-forward
Transmit power level	30 dBm
Antenna gain	5 dBi
Antenna pattern	Omni-directional
Noise figure	5 dB (RN) / 9 dB (UE)
Path loss setting	
Direct link (eNB-onboard UE) $L(R) = 131.1 + 42.8\log_{10}(R)$ **Access link (RN-onboard UE)** $L(R) = 103.8 + 20.9\log_{10}(R)$ **Backhaul link (eNB-MRN/MRN-MRN)** $L(R) = 10.5 + 40\log_{10}(R) - 18.5\log_{10}(h_{\text{BS}}) - 18.5\log_{10}(h_{\text{Train}}) + 1.5\log_{10}(f/5)$	
Shadowing parameters	
Standard deviation	8 dB on the direct link, 10 dB on the access link, 6 dB on the backhaul link
Correlation factor	0.5 between sites & 1.0 between sectors

where $h_{\text{BS}} = 32$ m, $h_{\text{Train}} = 2.5$ m, R is the distance between links (km), f is the center frequency (GHz).

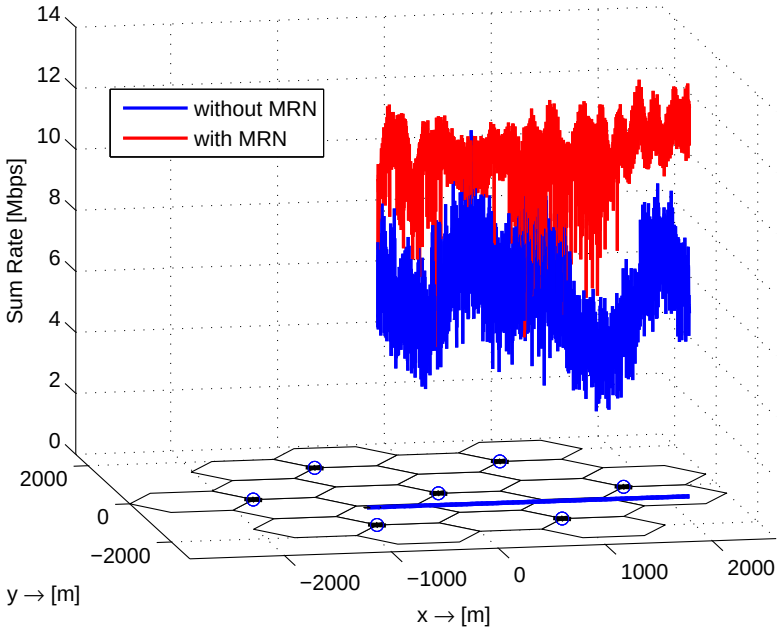

Figure 5.5: Onboard UE sum rate comparison between with and without mobile relay.

can significantly and stably improve the capacity of users in a high speed vehicle, thus providing the possibility to support high data rate services. However, multiple relay nodes will interfere each other, which tremendously affects the on-board UE performance. In the next section, we propose a coordinated MRN algorithm to overcome the interference problem and optimize the handover procedure.

5.5 Coordinated MRN system

5.5.1 Proposed innovation

There are two main challenges in the conventional mobile relay system, which are co-channel interference from multiple relays deployment and on-board UE performance degradation caused by mobile relay handover failures. Since we find that the LTE-A handover procedure is not suitable in the HSR scenario with frequent handover, a coordinated MRN system is proposed. In such system, the train and mobile relay nodes cooperatively coordinated by a relay central controller (RCC) , which consists of two main functions: one is to adjust frequency bands for different mobile relay nodes; another is to perform the group advanced handover procedure. It is assumed that a wired connection is used in the coordinated MRN system, in this case there are no traffic load or delay constraints. An example of a coordinated MRN system is given in Figure 5.6.

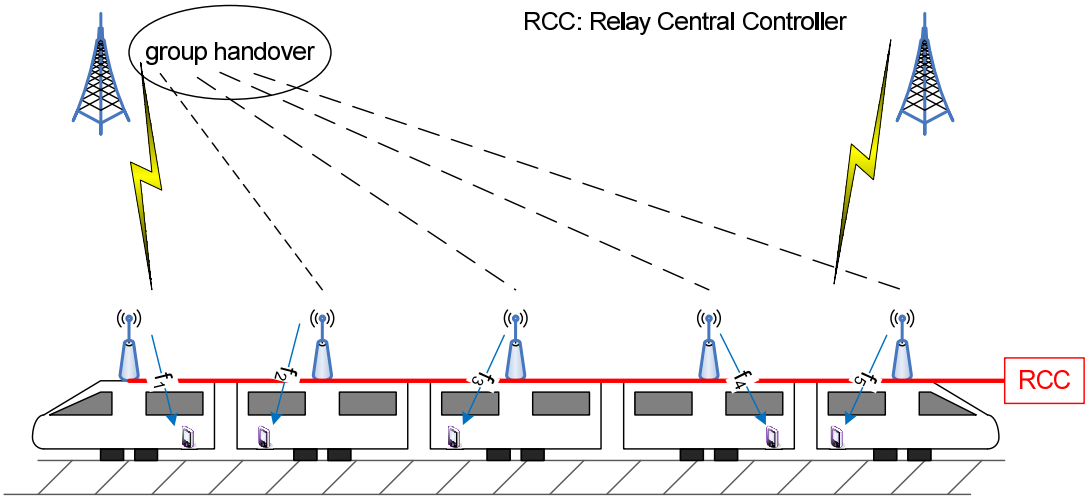

Figure 5.6: Coordinated MRN system in HSR scenario.

In the LTE OFDM system, the co-channel interference from other cells is the main source of interference. Frequency reuse technology is proved to be an efficient way to overcome co-channel interference. In a coordinated MRN system, the whole frequency band is divided into multiple sub-bands determined by the number of mobile relay nodes. With a central controller, it is possible to optimally allocate the access radio resources jointly. An example is shown in Figure 5.6: each relay node works on a different frequency band avoiding inter-cell interference from neighbor mobile relay nodes.

The handover delay caused by hard handover is still relatively large in current mobile relay system. Since the high speed train passes the overlapping areas so fast, the handover procedure cannot finish in time. And it is possible that the mobile relay could miss the optimal handover position because of the high velocity, which degrades the handover success probability. To overcome these problems, we consider a group advanced handover strategy in a coordinated MRN system.

Handover latency for the mobile relay with architecture Alternative 2 is around $105 + N * 42$ ms, where N is the number of attached on-board UEs [58]. And the handover measurement period is normally 200 ms in an FDD LTE-A system [4]. Therefore the total handover delay can be approximated as:

$$\begin{aligned} T_{\text{total delay}} &\approx T_{\text{handover latency}} + T_{\text{max measurement delay}} \\ &= (105 + 50 * 42 + 200)\ \text{ms} = 2405\ \text{ms}, \end{aligned} \tag{5.1}$$

where we consider that 10 UEs are attached to a mobile relay node. The movement speed of high speed train is 350 km/h. The movement distance in handover delay period is hence

around 200 meters, which is larger than the distance between the front mobile relay node and the rear mobile relay node (the length of the train is around 200 meters). We find that when the front mobile relay node finishes the handover procedure the rear mobile relay has already passed the optimal handover position. Based on this investigation we propose a group advanced handover strategy in a coordinated MRN system.

In every measurement period, mobile relay nodes measure the RSRP of the source and the target DeNB. If the RSRP from the target DeNB becomes better than the serving one, the handover procedure will be triggered at all mobile relay nodes. By triggering handover procedure in advance, it provides an efficient solution to overcome the handover delay problem and further improve the reliability of the backhaul link.

5.5.2 Simulation results and analysis

In this sub-section, the advantage of a coordinated MRN system strategy is verified by performance comparison with a traditional mobile relay system.

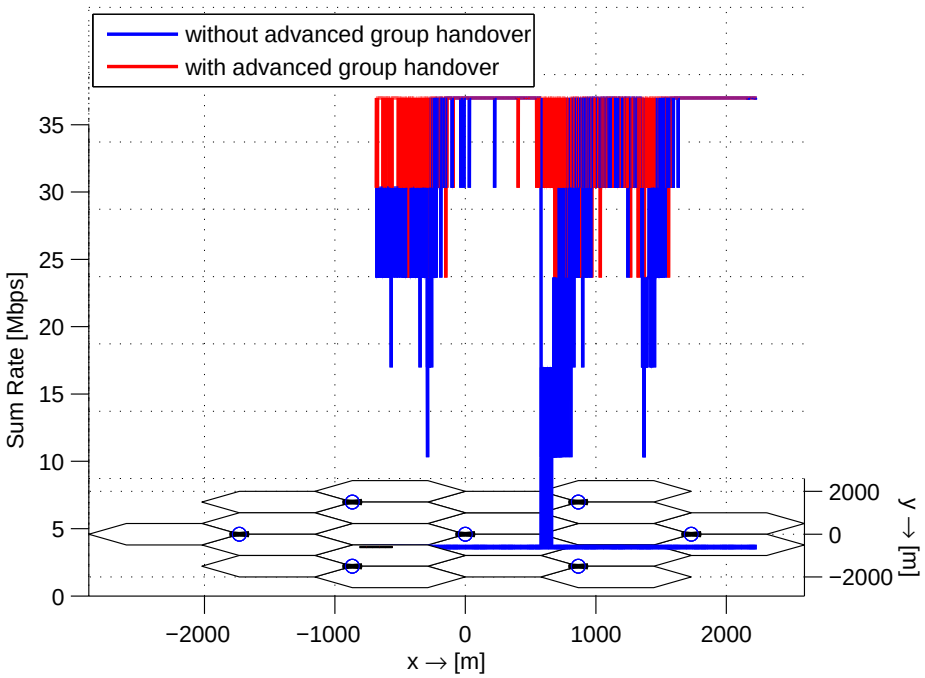

Figure 5.7: Onboard UE sum rate in group advanced handover and traditional handover case.

We firstly focus on the performance gain from the group handover strategy by assuming perfect frequency reuse within different mobile relay nodes. Figure 5.7 shows the instantaneous sum rate of on-board UEs with the movement of the train in the group

advanced handover and the traditional handover case. Since on-board UEs are located close to mobile relays, the channel quality of the relay-UE link is good. With extremely good channel quality, the transmission with maximum number of bits in each frame can be always achieved in the relay-UE link. Without any backhaul link failure, the sum rate will keep in the highest level. In contrast, if a backhaul link of a mobile relay is failed, on-board UEs served by this mobile relay is not served with data. That is why the sum rate suddenly decreases to some level in our simulation results. Hence, the sum rate of on-board UEs represent five quantized levels in our simulation results as shown in Figure 5.7. The backhaul radio link failure mainly happens during mobile relay handover. With optimized handover strategy, the backhaul link failure is less likely than in traditional handover procedure.

Table 5.2 lists the backhaul radio link failure ratio for different mobile relays. It is obvious that the proposed group advanced handover strategy could improve the backhaul link reliability compared with conventional mobile relay handover.

Table 5.2: The backhaul link failure ratio on mobile relay nodes

Handover strategy	1st MRN	2nd MRN	3rd MRN	4th MRN	5th MRN
Traditional	13.3%	12.6%	17.5%	17.2%	8.6%
Proposed	3.3%	2.1%	1.6%	0.7%	2.8%

Furthermore, Figure 5.8 illustrates the instantaneous on-board UE sum rate with the movement of the high speed train in a conventional mobile relay system and the proposed coordinated MRN system. There is a huge performance gap between the two approaches. In the proposed scheme, the maximal sum rate is more than 30 Mbit/s, which means 800 kbit/s average user transmission rate. Whereas, in the conventional scheme, the maximal sum rate can only reach 11 Mbit/s.

Figure 5.9 shows the average user spectral efficiency of on-board UE. With the proposed coordinated MRN system, the average on-board user spectral efficiency increases by 185 % and the 5%-ile user spectral efficiency, which indicates the cell edge user performance, increases up to 678 % compared to the conventional mobile relay system.

5.6 Summary

In this chapter, we have firstly described the high speed railway scenario, which was agreed as a main scenario in a 3GPP Rel. 11 study item. The existing challenges in the

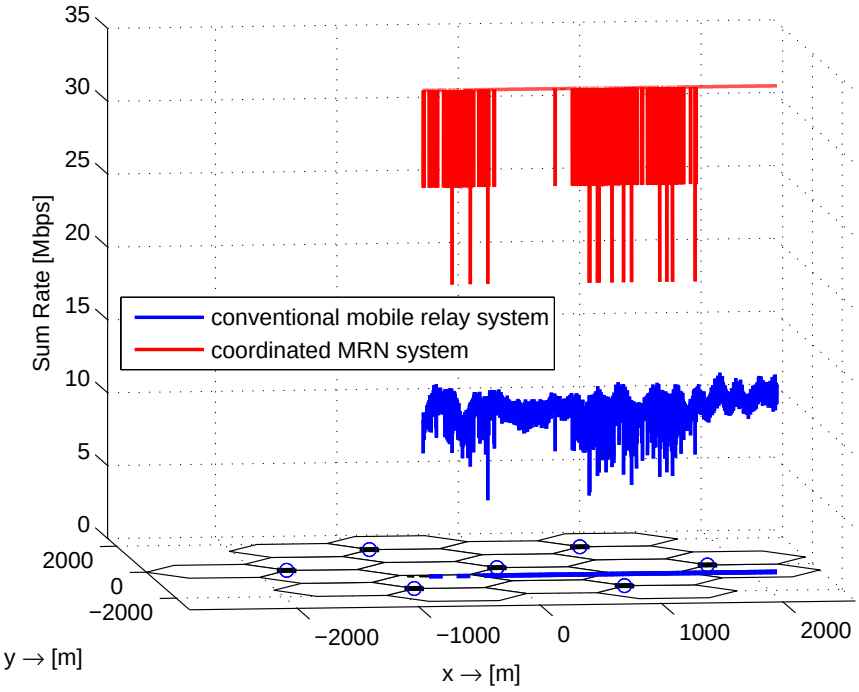

Figure 5.8: Onboard UE sum rate comparison.

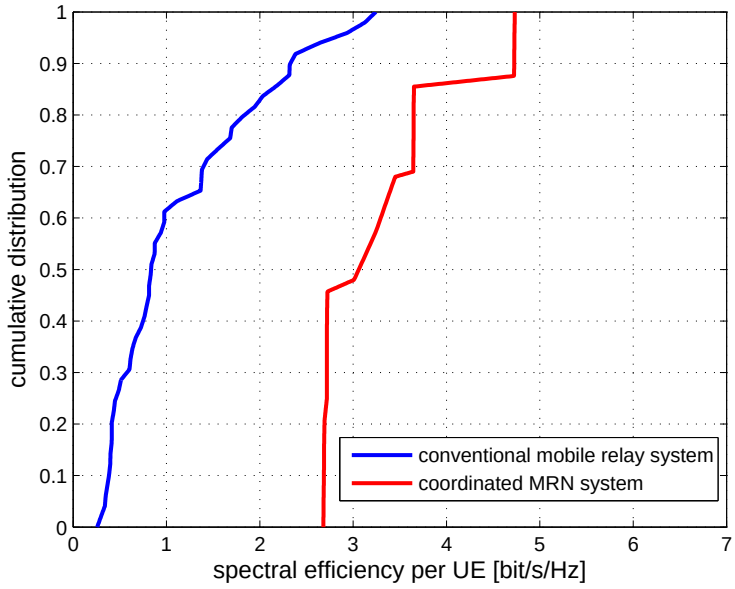

Figure 5.9: Average onboard UE spectral efficiency comparison.

HSR scenario have been briefly discussed. Mobile relay stations are dedicated network nodes equipped on the train, which have been concluded as an efficient solution for a HSR scenario. Furthermore, relay mobility scenarios based on the 3GPP architectures Alternative 1 and Alternative 2 have been discussed and the handover procedures for both alternatives have been described.

A system level simulator has been developed to investigate the capacity and handover performance gain of the mobile relay. Two kinds of scenarios are considered: one is without mobile relays; the other is a train implemented with mobile relays. Simulation results show that mobile relays increase the average on-board user performance by 70 %.

A coordinated MRN strategy has been proposed to combat the co-channel interference and handover delay challenge in the conventional mobile relay system. With the proposed coordinated MRN system, the radio link failure ratio can be enormously decreased. For the average on-board user spectral efficiency, the proposed strategy provides more than 180 % performance gain.

Chapter 6

Conclusion and outlook

6.1 Conclusions

Relay technology as part of cooperative communications fundamentally changes the abstraction of a wireless link and offers significant potential advantages for wireless communication networks. Relay technology has recently been migrated to one of the state-of-the-art features of 3GPP LTE-Advanced. In this thesis, we mainly focus on relay technology implemented in cellular networks.

In the first part of this thesis, the performance of basic cooperation methods are compared by calculating the outage capacity and characterizing diversity gains in a single relay scenario. In a multiple relay scenario, exact novel closed-form expressions for the total SNR at the destination and symbol error rate performance are derived for Rayleigh fading channels. The derived numerical result can be viewed as a performance lower bound for the future research. Furthermore, computer simulation results verified the accuracy and the correctness of the numerical results. Cooperative networks with relay selection have better SER performance and bandwidth efficiency compared with that of regular relay networks. Furthermore, we have investigated the relay selection scheme for a MIMO relay system. An effective joint relay selection and beamforming vector design scheme, which employs a new channel quantization strategy and centralized selection, has been proposed with limited feedback. Simulation results show that our proposed scheme approaches the performance of the theoretical optimal scheme with full CSI assumption and outperforms conventional schemes, while having lower computational complexity and lower feedback delay.

In the second part of this thesis, our aim is to investigate the system level performance of fixed relay-enhanced LTE-A cellular networks. Baseline assumptions for relay technology in LTE-A have been introduced in detail. With the feature of a wireless backhaul, the LTE-A relay offers deployment flexibility and eliminates the high costs of a fixed backhaul link. As defined in the 3GPP LTE-A standard, two basic types of relays are proposed: Type 1 relay and Type 2 relay. We have developed a dynamic system level simulator to evaluate the downlink transmission performance of relay-enhanced LTE-A systems. All simulation parameters follow the latest parameter settings agreed in 3GPP 36.814. An

efficient architecture for relay-assisted cellular networks is analyzed based on a system level simulator. Two different resource allocation schemes (static and dynamic) for in-band relays have been announced and evaluated by system level simulations. Simulation results show that the relay deployment, which is a part of a heterogeneous network, can reduce the extraordinary interference in the cell edge and improve the performance. However, in a dense network, additional interference caused by relays will limit the whole network performance. Therefore, the number of relay nodes in each sector should be determined carefully. From our simulation results, suitable numbers of relay nodes for urban case and suburban case are three and five, respectively.

System level simulations show that with the deployment of a high number of relay nodes inter-cell interference and resource management problems increase. In the third part of this work, potential approaches to mitigate inter-cell interference in relay-enhanced cellular systems have been discussed. We focussed on two contributions: adaptive beamforming design for cooperative communication and the concept of shared relays. For beamforming design, we have analyzed the performance of using ZF and eigen-beamforming with RVQ in a cooperative relay two-cell system. With derived sum-rate lower bound of ZF and eigen-beamforming, we have proposed a bit partitioning algorithm which allocates the feedback bits for quantizing the serving and interfering channels. The simulation results show that a suitable bit partitioning can improve the system sum-rate especially in an OCI-dominated scenario. In addition, an adaptive beamforming strategy has been proposed and proved to outperform the conventional schemes in a two-cell system. The proposed strategy has been extended into multi-cell LTE-A cellular network, and a performance comparison of different beamforming strategies was given.

The concept of shared relays has been introduced and proved to be an effective solution to avoid inter-cell interference. Next, the resource demand situation and resource competition problem have been discussed in the shared relay scenario. Based on these studies, an efficient and effective resource allocation and scheduling scheme based on the subframe structure has been proposed to maximize the benefit of the shared relay. System level simulations quantify the system performance in different resource demand situations. And simulation results show that the deployment of shared relays can improve the overall system performance by 8.4% $\sim$ 14.3% and also increase the throughput of cell edge users by 4.8% $\sim$ 15.9% compared to the conventional separated cell edge relay station deployment.

In the last part of this thesis, the mobile relay, which is another relay application in cellular networks, has been discussed in detail. The high speed railway scenario has been agreed as a main scenario in 3GPP Rel. 11 study item. A system level simulator has

been developed to explore the capacity and handover performance gain by the mobile relay. Two kinds of scenarios are considered: one is without mobile relays; the other is with mobile relays. Simulation results show that mobile relay deployment increases the average on-board user performance by 70 %. In the traditional mobile relay case, multiple relay nodes interfere with each other, what tremendously reduces the on-board UE performance. Therefore, we have proposed a coordinated MRN algorithm to overcome the interference problem and optimize the handover procedure. In a coordinated MRN system, the train and mobile relay nodes are cooperatively coordinated by a central controller, which adjusts frequency bands for different mobile relay nodes and performs the group advanced handover procedure. With the proposed coordinated MRN system, the radio link failure ratio can be enormously decreased. The average on-board user throughput increases by 185 % and the 5%-ile user throughput, which indicates the cell edge user performance, increases up to 678 % compared to a conventional mobile relay system.

6.2 Outlook

In this thesis, our proposed schemes have been analyzed by some practical assumptions, e.g. imperfect channel estimation and transmitter side CSI knowledge. However, the performance evaluation of relay deployments is still based on the common assumptions that perfect inter-cell synchronization is assumed and a network-wide sub-frame configuration is applied. In a relay-enhanced cellular network, the relay-eNB synchronization is done via a wireless backhaul, which is flexible but fragile. Furthermore, the set of backhaul subframes can be independently configured by the eNBs or RNs to adapt to different network variations, e.g. different cell loads or traffic modes. With this configuration, additional relay to relay interference will arise. Hence, there is an urge to investigate the impact of the backhaul subframe misalignment and associated optimization strategies.

Most research activities in cellular systems have placed special emphasis on downlink traffic scenarios, since traffic in the downlink direction dominates communication. However, in LTE-A this situation is changing, since cloud file uploading and social network applications will be supported that require large uplink traffic. In relay-enhanced cellular networks, the uplink transmission becomes more important due to the cooperative communication. Configuration information and feedback delay on uplink may affect the whole system performance. Due to these facts, the uplink performance of a relay-enhanced LTE-A network need to be evaluated and the corresponding resource allocation and scheduling schemes for uplink transmission need to be investigated.

Appendix A

Grassmannian codebook used for OFDM systems

Table A.1: Grassmannian codebook for $N_t = 2$, $N_r = 1$ and 3 bits (8 codewords)[1]

0.8393 - 0.2939j	-0.3427 + 0.9161j	-0.2065 + 0.3371j	0.3478 - 0.3351j
-0.1677 + 0.4256j	0.0498 + 0.2019j	0.9166 + 0.0560j	0.2584 + 0.8366j
0.1049 + 0.6820j	0.0347 - 0.2716j	-0.7457 + 0.1181j	-0.7983 + 0.3232j
0.6537 + 0.3106j	0.0935 - 0.9572j	-0.4553 - 0.4719j	0.5000 + 0.0906j

Table A.2: Grassmannian codebook for $N_t = 3$, $N_r = 1$ and 3 bits (8 codewords)[2]

0.4170 + 0.0350j	-0.5521 + 0.2276j	0.2148 + 0.0059j	0.1814 + 0.3412j
0.2583 + 0.5635j	0.2496 + 0.4156j	-0.4115 - 0.8788j	-0.7407 + 0.0188j
0.4826 + 0.4558j	-0.1060 - 0.6301j	-0.0625 - 0.0911j	0.5024 + 0.2221j
0.9126 + 0.1633j	0.4883 - 0.5125j	0.2020 - 0.4667j	0.4294 - 0.1103j
-0.2865 + 0.0983j	0.4955 - 0.1385j	-0.1941 + 0.2372j	0.1998 - 0.5339j
-0.1510 + 0.1608j	-0.4266 + 0.2284j	-0.7891 - 0.1576j	0.6693 + 0.1747j

[2]https://engineering.purdue.edu/∼djlove/grass.html

Appendix B

Antenna pattern

- eNB-UE link

  A 3-D antenna pattern with 15 degree electrical downtilt for 500 m ISD case and 6 degree for 1732 m ISD case will be used as described in [9] and summarized in Table B.1. The heights of the DeNB and UE antenna are 32 m and 1.5 m, respectively. The minimum distance between UE and DeNB is 35 m.

Table B.1: Antenna configuration for eNB-UE link [9]

Parameter	Assumption
Antenna pattern (horizontal) (For 3-sector cell sites with fixed antenna patterns)	$A_H(\varphi) = -\min\left[12\left(\frac{\varphi}{\varphi_{3\text{dB}}}\right)^2, A_m\right]$ $\varphi_{3\text{dB}} = 70°$ and $A_m = 25$ dB
Antenna pattern (vertical) (For 3-sector cell sites with fixed antenna patterns)	$A_V(\theta) = -\min\left[12\left(\frac{\theta-\theta_{\text{etilt}}}{\theta_{3\text{dB}}}\right)^2, SLA_v\right]$ $\theta_{3\text{dB}} = 10°$ and $SLA_v = 20$ dB θ_{etilt} is the electrical antenna downtilt.
3D Combining method	$A(\varphi,\theta) = -\min\{-[A_H(\varphi) + A_V(\theta)], A_m\}$

Table B.2: Antenna configuration for backhaul link [9]

Parameter	Assumption
Antenna pattern	7 dBi antenna gain, directional $A(\theta) = -\min\left[12\left(\frac{\theta}{\theta_{3\text{dB}}}\right)^2, A_m\right]$ $\theta_{3\text{dB}} = 70°$ and $A_m = 20$ dB

- eNB-RN link(backhaul link)

  A 2-D directional atenna pattern with an RN antenna height of 5 m, as listed in [9] and Table B.2, will be used for the backhaul link.

- RN-UE link(relay access link)

  A 2-D omni-directional antenna pattern with 5 dBi gain is considered. The height of the relay nodes is 5 m. The minimum distance between UE and RN is 10 m. In case of multi-hop relay deployments, the intermediate RN-RN link will be treated in the same way as a relay access link, but assuming same height of transmitter and receiver antenna.

Appendix C

Power delay profiles

The delay profiles are selected to be representative for low, medium and high delay spread environments.

Table C.1: Extended Pedestrian A model (EPA)

Path number	Average path gain (dB)	Path delay (ns)
1	0.0	0
2	-1.0	30
3	-2.0	70
4	-3.0	90
5	-8.0	110
6	-17.2	190
7	-20.8	410

Table C.2: Extended Vehicular A model (EVA)

Path number	Average path gain (dB)	Path delay (ns)
1	0.0	0
2	-1.5	30
3	-1.4	150
4	-3.6	310
5	-0.6	370
6	-9.1	710
7	-7.0	1090
8	-12.0	1730
9	-16.9	2510

Table C.3: Extended Typical Urban model (ETU)

Path number	Average path Gain (dB)	Path delay (ns)
1	-1.0	0
2	-1.0	50
3	-1.0	120
4	0.0	200
5	0.0	230
6	0.0	500
7	-3.0	1600
8	-5.0	2300
9	-7.0	5000

Appendix D

Mobile relay handover procedure

D.1 Mobile relay handover procedure for alternative 1

Figure D.1 illustrates the moving relay handover procedure when the mobile relay moves from S-DeNB to T-DeNB for 3GPP architecture alternative 1. The whole procedure is described in the following:

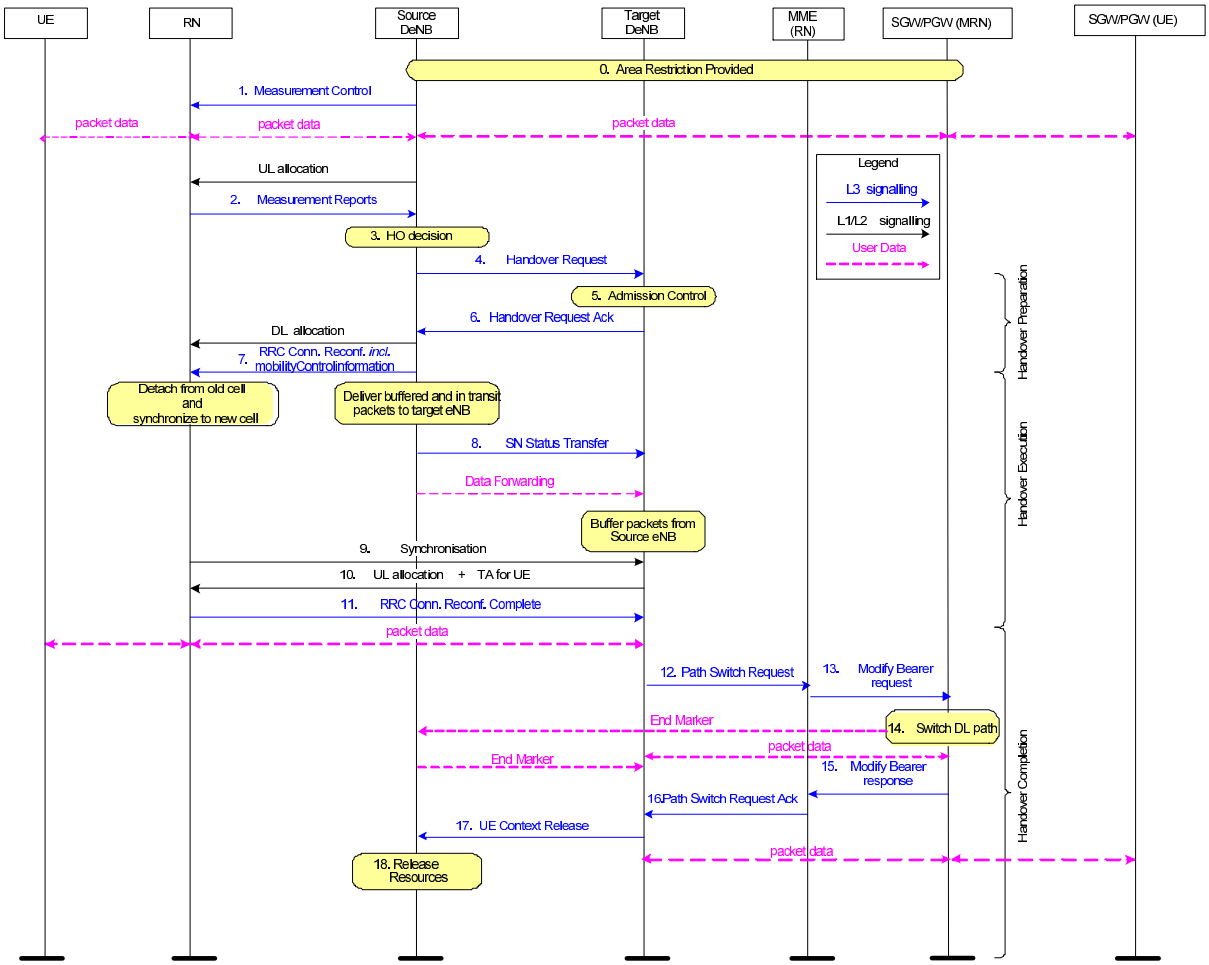

Figure D.1: Mobile relay handover procedure for Alternative 1 [11].

Handover preparation phase

During the mobile relay handover preparation phase, the following steps may be performed at the S-DeNB and T-DeNB:

- The mobile relay sends a measurement report to the S-DeNB. The reports contain all necessary information for handover including the ID of T-DeNB and radio resource management information.
- The S-DeNB makes the handover decision based on measurement reports.
- The S-DeNB sends a handover request to the target DeNB. Information about S1/X2 signalling references for MRN and LTE radio access bearer (E-RAB) attributes for MRN will be included in the request message.
- Admission control is performed at the T-DeNB dependent on the transmitted E-RAB attributes of MRN. The target DeNB configures the necessary resources for the MRN operation.
- The T-DeNB sends a handover request acknowledgment (ACK) message to the S-DeNB after resources to support the mobile relay with attached UEs are guaranteed.

Handover execution phase

- The radio resource control (RRC) contains the RRC Connection Reconfiguration and Mobility Control information to be sent to MRN by the S-DeNB for backhaul link reconfiguration.
- The S-DeNB sends the SN status transfer message to the T-DeNB to ensure packet forwarding from the S-DeNB to the T-DeNB.
- The mobile relay performs synchronization and backhaul reconfiguration to the T-DeNB. The T-DeNB performs UL allocation towards the mobile relay.
- The mobile relay sends RRC Connection Reconfiguration Complete message to the T-DeNB to confirm handover and the packet data can be transferred between the T-DeNB and the mobile relay.

Handover completion phase

- A Path Switch Request message is sent from the T-DeNB to the mobility management entity (MME) of the MRN to inform that the MRN has changed the cell.
- The MME of the MRN sends a Modified Bearer request message to the S/P-GW of MRN.

- The S/P-GW of MRN switches the downlink data path to the T-DeNB and sends the end marker on the old path to S-DeNB to release user plane resources.
- The S/P-GW of MRN sends a Modified Bearer response message to the MME of MRN.
- The MME of MRN confirms the T-DeNB Path Switch message with a Path Switch Request ACK message.
- The handover success is informed by sending the UE Context Release message to the S-DeNB from the T-DeNB.

In architecture Alternative 1, the user plane packets and the corresponding path switches are naturally grouped in the S/P-GW of the mobile relay node, which allows a group handover procedure.

D.2 Mobile relay handover procedure for alternative 2

Figure D.2 illustrates the moving relay handover procedure when the mobile relay moves from S-DeNB to T-DeNB for 3GPP architecture alternative 1. The whole procedure is described in the following:

Handover preparation phase

During the mobile relay handover preparation phase, the following steps may be performed at the S-DeNB and T-DeNB:

- The mobile relay sends a measurement report to the S-DeNB. The reports contain all necessary information for handover including the ID of T-DeNB and radio resource management information.
- The S-DeNB makes the handover decision based on measurement reports.
- The S-DeNB sends a handover request to the target DeNB. The information about S1/X2 signalling references for MRN and E-RAB attributes for MRN will be included in the request message.
- Admission control is performed at the T-DeNB dependent on the transmitted E-RAB attributes of MRN. The target DeNB configures the necessary resources for the MRN operation.
- The T-DeNB sends a handover request ACK message to the S-DeNB after resources to support mobile relay with attached UEs are guaranteed.

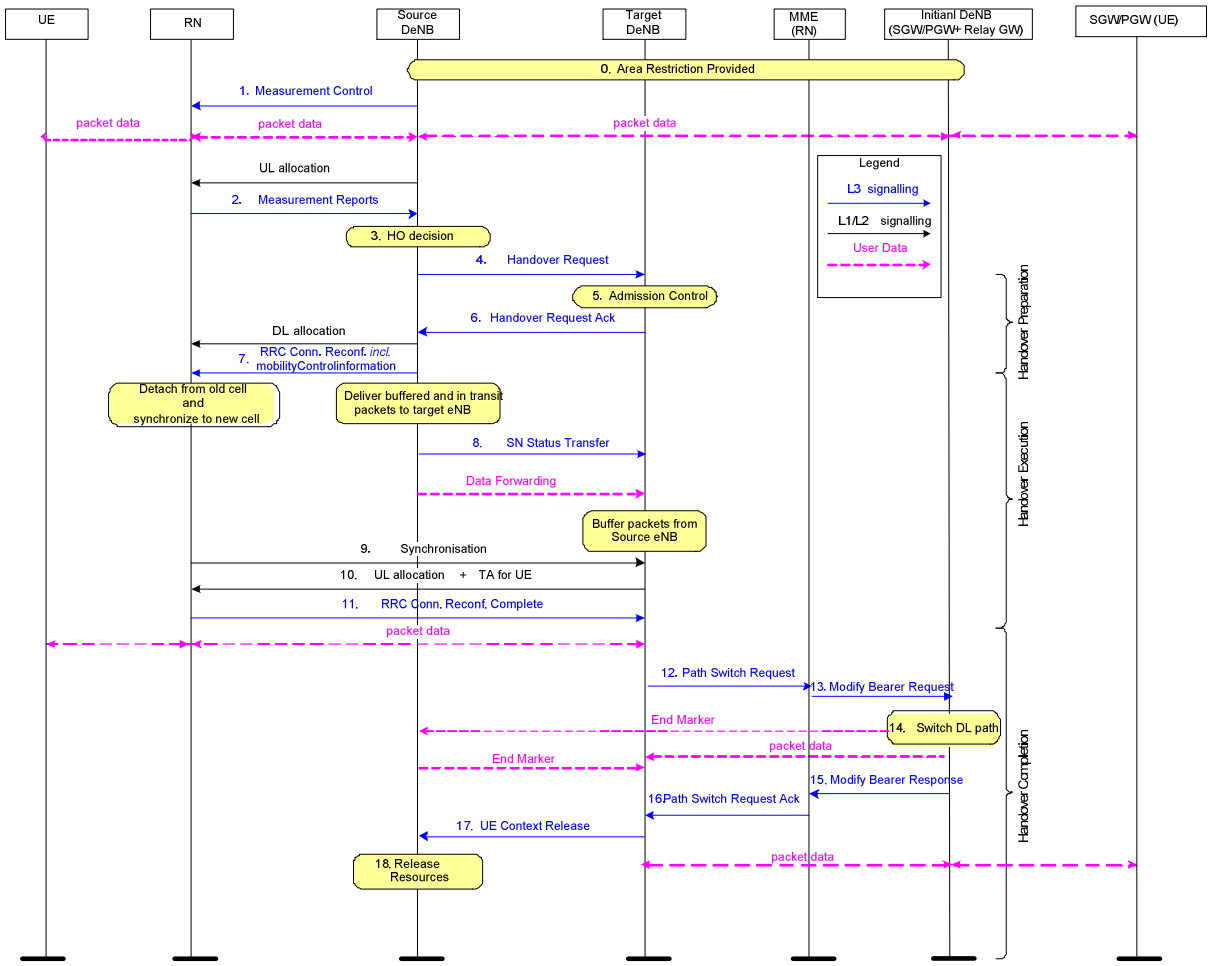

Figure D.2: Mobile relay handover procedure for Alt 2 [11].

Handover execution phase

- The radio resource control contains the RRC Connection Reconfiguration and Mobility Control information to be sent to MRN by the S-DeNB for backhaul link reconfiguration.
- The S-DeNB sends the SN status transfer message to the T-DeNB to ensure packet forwarding from the S-DeNB to the T-DeNB.
- The mobile relay performs synchronization and backhaul reconfiguration to the T-DeNB. The T-DeNB performs UL allocation towards the mobile relay.
- The mobile relay sends RRC Connection Reconfiguration Complete message to the T-DeNB to confirm handover and the packet data can be transferred between the T-DeNB and the mobile relay.

Handover completion phase

- A Path Switch Request message is sent form the T-DeNB to the MME of the MRN to inform that the MRN has changed cell.
- The MME of the MRN sends an Modified Bearer request message to the S/P-GW of the initial DeNB.
- The S/P-GW of the initial DeNB switches the downlink data path to the T-DeNB and sends end marker on the old path to S-DeNB to release user plane resources.
- The S/P-GW of the initial DeNB sends an Modified Bearer response message to the MME of MRN.
- The MME of MRN confirms the T-DeNB Path Switch message with a Path Switch Request ACK message.
- The handover success is informed by sending the UE Context Release message to the S-DeNB from the T-DeNB.

The handover procedure for Alternative 2 is basically the same as the procedure under Alternative 1, except the RN P/S-GW is always located in the initial DeNB where the mobile relay is attached for normal operation. There is no additional signaling for UE handover in both radio access network (RAN) and core network side during the RN mobility, i.e., the RN HO is transparent to the UE in both the RAN and core network.

Bibliography

[1] 3GPP TR 25.814. Physical layer aspect for evolved Universal Terrestrial Radio Access (UTRA). Technical report, October 2006.

[2] 3GPP TR 25.996. Spacial channel model for Multiple Input Multiple Output (MIMO) simulations. Technical report, June 2007.

[3] 3GPP TS 36.101. Evolved Universal Terrestrial Radio Access (E-UTRA); User Equipment (UE) radio transmission and reception (Release 9). Technical report, December 2010.

[4] 3GPP TS 36.133. Evolved Universal Terrestrial Radio Access (E-UTRA); Requirements for support of radio resource management (Release 11). Technical report, March 2014.

[5] 3GPP TS 36.211. Evolved Universal Terrestrial Radio Access (E-UTRA); Physical channels and modulation (Release 12). Technical report, March 2014.

[6] 3GPP TS 36.216. Evolved Universal Terrestrial Radio Access (E-UTRA); Physical layer for relaying operation (Release 11). Technical report, September 2012.

[7] 3GPP TS 36.300. Evolved Universal Terrestrial Radio Access (E-UTRA) and Evolved Universal Terrestrial Radio Access Network (E-UTRAN); Overall description (Release 11). Technical report, March 2014.

[8] 3GPP TR 36.806. Evolved Universal Terrestrial Radio Access (E-UTRA); Relay architectures for E-UTRA (LTE-Advanced) (Release 9). Technical report, March 2010.

[9] 3GPP TR 36.814. Evolved Universal Terrestrial Radio Access (E-UTRA); Further advancements for E-UTRA physical layer aspects (Release 9). Technical report, 2010.

[10] 3GPP TR 36.826. Evolved Universal Terrestrial Radio Access (E-UTRA); Relay radio transmission and reception (Release 11). Technical report, July 2013.

[11] 3GPP TR 36.836. Study on Mobile Relay for Evolved Universal Terrestrial Radio Access (E-UTRA) (Release 12). Technical report, July 2013.

[12] 3GPP TR 36.912. Feasibility study for Further Advancements for E-UTRA (LTE-Advanced) (Release 11). Technical report, September 2012.

[13] 3GPP. Future Radio in 3GPP. `http://www.3gpp.org/news-events/3gpp-news/1266-Future-Radio-in-3GPP`.

[14] A. Adinoyi, Yijia Fan, H. Yanikomeroglu, and H.V. Poor. On the performance of selection relaying. In *IEEE 68th Vehicular Technology Conference, 2008. VTC 2008-Fall.*, pages 1 –5, Sept. 2008.

[15] Marina Aguado, Eduardo Jacob, Jasone Astorga, Nerea Toledo, and Marion Berbineau. The cross layer rmpa handover: a reliable mobility pattern aware handover strategy for broadband wireless communication in a high-speed railway domain. *EURASIP Journal on Wireless Communications and Networking*, 2012(1):1–29, 2012.

[16] J.G. Andrews, Wan Choi, and R.W. Heath. Overcoming interference in spatial multiplexing MIMO cellular networks. *IEEE Transactions on Wireless Communications*, 14(6):95–104, Dec. 2007.

[17] C. K. Au-Yeung and D. J. Love. On the performance of random vector quantization limited feedback beamforming in a MISO system. *IEEE Transactions on Wireless Communications*, 6(2):458–462, Feb. 2007.

[18] Norman C. Beaulieu and Jeremiah Hu. A closed-form expression for the outage probability of decode-and-forward relaying in dissimilar rayleigh fading channels. *IEEE Communications Letters*, 10(12):813 –815, December 2006.

[19] T. Beniero, S. Redana, J. Hamalainen, and B. Raaf. Effect of relaying on coverage in 3gpp lte-advanced. In *IEEE 69th Vehicular Technology Conference, 2009, VTC Spring 2009.*, pages 1–5, April 2009.

[20] E. Beres and R. Adve. Outage probability of selection cooperation in the low to medium snr regime. *IEEE Communications Letters*, 11(7):589 –597, July 2007.

[21] E. Beres and R. Adve. Selection cooperation in multi-source cooperative networks. *IEEE Transactions on Wireless Communications*, 7(1):118 –127, Jan. 2008.

[22] P Bergmans and Thomas M Cover. Cooperative broadcasting. *IEEE Transactions on Information Theory*, 20(3):317–324, 1974.

[23] Abdallah Bou Saleh, Omer Bulakci, Zhe Ren, Simone Redana, Bernhard Raaf, and Jyri Haemaelaeinen. Resource sharing in relay-enhanced 4G networks. In *11th European Wireless Conference 2011 - Sustainable Wireless Technologies (European Wireless)*, pages 1–8, 2011.

[24] D. G. Brennan. Linear diversity combining techniques. *Proceedings of the IEEE*, 91(2):331–356, Feb. 2003.

[25] K. Brueninghaus, D. Astely, T. Salzer, S. Visuri, A. Alexiou, S. Karger, and G.-A. Seraji. Link performance models for system level simulations of broadband radio access systems. In *IEEE 16th International Symposium on Personal, Indoor and Mobile Radio Communications, 2005. PIMRC 2005.*, volume 4, pages 2306–2311 Vol. 4, Sept 2005.

[26] G. Caire and D. Tuninetti. The throughput of hybrid-arq protocols for the gaussian collision channel. *IEEE Transactions on Information Theory*, 47(5):1971–1988, Jul 2001.

[27] CATT. Analysis on mobile relay functionalities, 3GPP TSG RAN WG3 #74, R3-112821. November 2011.

[28] Jae-Hwan Chang and L. Tassiulas. Energy conserving routing in wireless ad-hoc networks. In *Proceedings of IEEE INFOCOM 2000. Nineteenth Annual Joint Conference of the IEEE Computer and Communications Societies.*, volume 1, pages 22–31 vol.1, 2000.

[29] Jung-Fu Cheng. Coding performance of hybrid arq schemes. *IEEE Transactions on Communications*, 54(6):1017–1029, June 2006.

[30] Huawei China Mobile, Vodafone. Application scenarios for LTE-Advanced relay, 3GPP TSG-RAN WG1 #54 RAN1, R1-082975. August 2008.

[31] H. Claussen. Efficient modelling of channel maps with correlated shadow fading in mobile radio systems. In *IEEE 16th International Symposium on Personal, Indoor and Mobile Radio Communications, 2005. PIMRC 2005.*, volume 1, pages 512–516, Sept 2005.

[32] T. Cover and A.E. Gamal. Capacity theorems for the relay channel. *IEEE Transactions on Information Theory*, 25(5):572–584, Sep. 1979.

[33] Ericsson. Considerations on the system-performance evaluation of HSDPA using OFDM modulation, 3GPP TSG-RAN WG1 #34, R1-030999. October 2003.

[34] Ericsson. System-level evaluation of OFDM - further considerations, 3GPP TSG-RAN WG1 #35, R1-031303. November 2003.

[35] M. Fadel, A. Hindy, A. El-Keyi, M. Nafie, O.O. Koyluoglu, and A.M. Tulino. Resource allocation for throughput enhancement in cellular shared relay networks. In *2012 35th IEEE Sarnoff Symposium (SARNOFF)*, pages 1–6, 2012.

[36] Junwei Feng, Mugen Peng, Jian Li, Xiang Zhang, Yihai Xing, and Wei Hu. Optimal resource allocation for time sharing relaying system. In *2012 1st IEEE International Conference on Communications in China (ICCC)*, pages 492–496, Aug 2012.

[37] A.E. Gamal and M. Aref. The capacity of the semideterministic relay channel (corresp.). *IEEE Transactions on Information Theory*, 28(3):536–536, May 1982.

[38] S.A. Ghorashi, E. Homayounvala, F. Said, and A.H. Aghvami. Dynamic simulator for studying wcdma based hierarchical cell structures. In *2001 12th IEEE International Symposium on Personal, Indoor and Mobile Radio Communications*, volume 1, pages D–32–D–37 vol.1, Sep 2001.

[39] Gene H Golub and Charles F Van Loan. *Matrix computations*, volume 3. JHU Press, 2012.

[40] Wei Guan and Hanwen Luo. Joint mmse transceiver design in non-regenerative mimo relay systems. *IEEE Communications Letters*, 12(7):517 –519, july 2008.

[41] V. Havary-Nassab, S. Shahbazpanahi, and A. Grami. Joint receive-transmit beamforming for multi-antenna relaying schemes. *IEEE Transactions on Signal Processing*, 58(9):4966–4972, Sept 2010.

[42] Huan Huang and Wenjiang Hu. A fast handover scheme based on gps information for ieee 802.16e on high-speed railway. In *2011 International Conference on Electronics, Communications and Control (ICECC)*, pages 2408–2412, Sept 2011.

[43] Yongming Huang, Luxi Yang, M. Bengtsson, and B. Ottersten. A limited feedback joint precoding for amplify-and-forward relaying. *IEEE Transactions on Signal Processing*, 58(3):1347 –1357, march 2010.

[44] Guo Hui, Wu Hao, and Zhang Yushu. Gsm-r network planning for high speed railway. In *IET 3rd International Conference on Wireless, Mobile and Multimedia Networks (ICWMNN 2010)*, pages 10–13, Sept 2010.

[45] S.S. Ikki and M.H. Ahmed. Performance analysis of adaptive decode-and-forward cooperative diversity networks with best-relay selection. *IEEE Transactions on Communications*, 58(1):68 –72, January 2010.

[46] IST-WINNER II Deliverable 1.1.2 v1.2. WINNER II Channel Models. Technical report, 2007.

[47] REC. ITU-R M.1225. Guidelines for evaluation of radio transmission technologies for IMT-2000. ITU-R M.1225, 1997.

[48] Mikio Iwamura, Hideaki Takahashi, and Satoshi Nagata. Relay technology in lte-advanced. *NTT DoCoMo Technical Journal*, 12(2):29–36, 2010.

[49] N. Jindal. MIMO broadcast channels with finite-rate feedback. *IEEE Transactions on Information Theory*, 52(11):5045–5060, Nov. 2006.

[50] N. Jindal, J.G. Andrews, and S. Weber. Rethinking MIMO for wireless networks: Linear throughput increases with multiple receive antennas. In *2009 IEEE International Conference on Communications, ICC '09.*, pages 1–6, June.

[51] O.B. Karimi, Jiangchuan Liu, and Chonggang Wang. Seamless wireless connectivity for multimedia services in high speed trains. *IEEE Journal on Selected Areas in Communications*, 30(4):729–739, May 2012.

[52] K. Kastell. Challenges and improvements in communication with vehicles and devices moving with high-speed. In *2011 13th International Conference on Transparent Optical Networks (ICTON)*, pages 1–4, June 2011.

[53] B. Khoshnevis, Wei Yu, and R. Adve. Grassmannian beamforming for mimo amplify-and-forward relaying. *IEEE Journal on Selected Areas in Communications*, 26(8):1397 –1407, october 2008.

[54] Dongwook Kim, Bang Chul Jung, Hanjin Lee, Dan Keun Sung, and Hyunsoo Yoon. Optimal modulation and coding scheme selection in cellular networks with hybrid-arq error control. *IEEE Transactions on Wireless Communications*, 7(12):5195–5201, December 2008.

[55] Junhyeong Kim, Jin-Yup Hwang, and Youngnam Han. Joint processing in multi-cell coordinated shared relay network. In *2010 IEEE 21st International Symposium on Personal Indoor and Mobile Radio Communications (PIMRC)*, pages 702–706, 2010.

[56] Young-Han Kim. Capacity of a class of deterministic relay channels. *IEEE Transactions on Information Theory*, 54(3):1328–1329, March 2008.

[57] G. Kramer, M. Gastpar, and P. Gupta. Cooperative strategies and capacity theorems for relay networks. *IEEE Transactions on Information Theory*, 51(9):3037–3063, Sept. 2005.

[58] Andrey Krendzel. Lte-a mobile relay handling: Architecture aspects. In *Proceedings of the 2013 19th European Wireless Conference (EW)*, pages 1–6, April 2013.

[59] J.N. Laneman, D.N.C. Tse, and Gregory W. Wornell. Cooperative diversity in wireless networks: Efficient protocols and outage behavior. *IEEE Transactions on Information Theory*, 50(12):3062–3080, Dec. 2004.

[60] B. Lannoo, D. Colle, M. Pickavet, and P. Demeester. Radio-over-fiber-based solution to provide broadband internet access to train passengers. *IEEE Communications Magazine*, 45(2):56–62, Feb 2007.

[61] N. Lee and W. Shin. Adaptive feedback scheme on k-cell MISO interfering broadcast channel with limited feedback. *IEEE Transactions on Wireless Communications*, 10(2):401–406, Feb. 2011.

[62] Namyoon Lee, Wonjae Shin, Young-Jun Hong, and B. Clerckx. Two-cell MISO interfering broadcast channel with limited feedback: Adaptive feedback strategy and multiplexing gains. In *2011 IEEE International Conference on Communications (ICC)*, pages 1–5, June.

[63] W.C.Y. Lee. *Mobile communications engineering.* McGraw-Hill, 1982.

[64] G. Liebl, T.M. de Moraes, A. Soysal, and E. Seidel. Fair resource allocation for inband relaying in lte-advanced. In *2011 8th International Workshop on Multi-Carrier Systems Solutions (MC-SS)*, pages 1–5, May 2011.

[65] Yicheng Lin and Wei Yu. Fair scheduling and resource allocation for wireless cellular network with shared relays. *IEEE Journal on Selected Areas in Communications*, 30(8):1530–1540, 2012.

[66] Martin Liu, Xin Chang, Yi Lu, and Hongjie Si. A novel network structure based on multi cell coordinated relay. In *IEEE C802.16m-08/029*, Jan. 2008.

[67] T. K Y Lo. Maximum ratio transmission. *IEEE Transactions on Communications*, 47(10):1458–1461, Oct 1999.

[68] D.J. Love. Personal Webpage on Grassmannian Subspace Packing. `https://engineering.purdue.edu/~djlove/grass.html`.

[69] D.J. Love, Jr. Heath, R.W., and T. Strohmer. Grassmannian beamforming for multiple-input multiple-output wireless systems. *IEEE Transactions on Information Theory*, 49(10):2735 – 2747, oct. 2003.

[70] Changwei Lv, Shujuan Hou, and Wenbo Mei. Dual-adaptive linear prediction for radio channel with abrupt change. In *2012 IEEE Vehicular Technology Conference (VTC Fall)*, pages 1–4, Sept 2012.

[71] A.F. Molisch. *Wireless Communications*. Wiley - IEEE. Wiley, 2005.

[72] S. M. Moser. Some expectations of a non-central chi-square distribution with an even number of degrees of freedom. In *TENCON 2007 - 2007 IEEE Region 10 Conference*, pages 1–4, Oct. 30-Nov. 2 2007.

[73] NGMN. NGMN Radio Access Performance Evaluation Methodology, NGMN White Paper. July 2008.

[74] Nokia Nokia Siemens Networks. Selection criteria for relay site planning, 3GPP TSG RAN WG1 #57, R1-091764. May 2009.

[75] M. Pan, T. Lin, and W. Chen. An enhanced handover scheme for mobile relays in lte-a high-speed rail networks. *IEEE Transactions on Vehicular Technology*, PP(99):1–1, 2014.

[76] Ali Y Panah, Kien T Truong, Steven W Peters, and Robert W Heath. Interference management schemes for the shared relay concept. *EURASIP Journal on Advances in Signal Processing*, 2011:1, 2011.

[77] A. Papoulis. *Probability, Random Variables, and Stochastic Processes*. Mc-Graw Hill, 1984.

[78] R. Pawula, S. Rice, and J. Roberts. Distribution of the phase angle between two vectors perturbed by gaussian noise. *IEEE Transactions on Communications*, 30(8):1828 – 1841, Aug. 1982.

[79] C. B. Peel, B. M. Hochwald, and A. L. Swindlehurst. A vector-perturbation technique for near-capacity multiantenna multiuser communication-part I: channel inversion and regularization. *IEEE Transactions on Communications*, 53(1):195–202, Jan. 2005.

[80] Fei Peng, Jinyun Zhang, and W.E. Ryan. Adaptive modulation and coding for ieee 802.11n. In *IEEE Wireless Communications and Networking Conference, 2007. WCNC 2007.*, pages 656–661, March 2007.

[81] Yu Qian, Zhiheng Guo, Rui Fan, Hai Wang, Jianjun Liu, Yuan Yan, Xiaodong Shen, and Zhenping Hu. Improving outdoor to indoor coverage by use of td-lte in-band relay. In *Personal Indoor and Mobile Radio Communications (PIMRC), 2013 IEEE 24th International Symposium on*, pages 2658–2662, Sept 2013.

[82] K.J. Ray Liu, Ahmed K. Sadek, Weifeng Su, and Andres Kwasinski. *Cooperative Communications and Networking*. Cambridge University Press, December 2008.

[83] A.K. Sadek, Zhu Han, and K.J.R. Liu. A distributed relay-assignment algorithm for cooperative communications in wireless networks. In *IEEE International Conference on Communications, 2006. ICC '06.*, volume 4, pages 1592–1597, June 2006.

[84] Hiroshi Sato. *Information transmission through a channel with relay*. 1976.

[85] A. Sendonaris, E. Erkip, and B. Aazhang. Increasing uplink capacity via user cooperation diversity. In *Proceedings IEEE International Symposium on Information Theory(ISIT)*, pages 156–, Aug. 1998.

[86] Andrew Sendonaris, Elza Erkip, and Behnaam Aazhang. User cooperation diversity. part i. system description. *Communications, IEEE Transactions on*, 51(11):1927–1938, 2003.

[87] Yi Shi, Jiaheng Wang, K. Letaief, and R.K. Mallik. A game-theoretic approach for distributed power control in interference relay channels. *IEEE Transactions on Wireless Communications*, 8(6):3151–3161, June 2009.

[88] S. Simoens and D. Bartolome. Optimum performance of link adaptation in hiperlan/2 networks. In *IEEE VTS 53rd Vehicular Technology Conference, 2001. VTC 2001 Spring.*, volume 2, pages 1129–1133 vol.2, 2001.

[89] Marvin K. Simon and M.-S. Alouini. A unified approach to the performance analysis of digital communication over generalized fading channels. *Proceedings of the IEEE*, 86(9):1860–1877, Sep. 1998.

[90] M. Simsek, T. Akbudak, Bo Zhao, and A. Czylwik. An lte-femtocell dynamic system level simulator. In *2010 International ITG Workshop on Smart Antennas (WSA)*, pages 66–71, Feb 2010.

[91] Quentin H Spencer, A Lee Swindlehurst, and Martin Haardt. Zero-forcing methods for downlink spatial multiplexing in multiuser mimo channels. *IEEE Transactions on Signal Processing*, 52(2):461–471, 2004.

[92] V. Sreng, H. Yanikomeroglu, and D.D. Falconer. Relayer selection strategies in cellular networks with peer-to-peer relaying. In *2003 IEEE 58th Vehicular Technology Conference, 2003. VTC 2003-Fall.*, volume 3, pages 1949–1953 Vol.3, Oct. 2003.

[93] V. Srinivasan, P. Nuggehalli, C. F Chiasserini, and R.R. Rao. Cooperation in wireless ad hoc networks. In *IEEE Societies INFOCOM 2003. Twenty-Second Annual Joint Conference of the IEEE Computer and Communications.*, volume 2, pages 808–817 vol.2, March 2003.

[94] A. Stefanov and E. Erkip. Cooperative coding for wireless networks. *IEEE Transactions on Communications*, 52(9):1470–1476, Sept 2004.

[95] Peters Steven W, Panah Ali Y, Truong Kien T, et al. Relay architectures for 3GPP LTE-advanced. *EURASIP Journal on Wireless Communications and Networking*, 2009, 2009.

[96] X. Tang and Y. Hua. Optimal design of non-regenerative mimo wireless relays. *IEEE Transactions on Wireless Communications*, 6(4):1398 –1407, april 2007.

[97] Tao Tao and A. Czylwik. Combined fast link adaptation algorithm in lte systems. In *2011 6th International ICST Conference on Communications and Networking in China (CHINACOM)*, pages 415–420, Aug 2011.

[98] Tao Tao and A. Czylwik. Performance analysis of link adaptation in lte systems. In *Smart Antennas (WSA), 2011 International ITG Workshop on*, pages 1–5, Feb 2011.

[99] Tao Tao and A. Czylwik. Beamforming design and relay selection for multiple mimo af relay systems with limited feedback. In *2013 IEEE 77th Vehicular Technology Conference (VTC Spring)*, pages 1–5, June 2013.

[100] Tao Tao and A. Czylwik. System performance of an lte-a cellular network with shared relays under different resource demands. In *2014 IEEE 79th Vehicular Technology Conference (VTC Spring)*, May 2014.

[101] Tao Tao, Bo Zhao, and Andreas Czylwik. Beamforming design for a cooperative relay system with limited feedback. In *2013 IEEE 24th International Symposium on Personal Indoor and Mobile Radio Communications (PIMRC)*, pages 2616–2620. IEEE, 2013.

[102] Emre Telatar. Capacity of multi-antenna gaussian channels. *European transactions on telecommunications*, 10(6):585–595, 1999.

[103] Lin Tian, Juan Li, Yi Huang, Jinglin Shi, and Jihua Zhou. Seamless dual-link handover scheme in broadband wireless communication systems for high-speed rail. *IEEE Journal on Selected Areas in Communications*, 30(4):708–718, May 2012.

[104] Edward C Van Der Meulen. Three-terminal communication channels. *Advances in applied Probability*, pages 120–154, 1971.

[105] H. Wu, Chunming Qiao, S. De, and O. Tonguz. Integrated cellular and ad hoc relaying systems: icar. *IEEE Journal on Selected Areas in Communications*, 19(10):2105–2115, Oct 2001.

[106] Yikang Xiang, Jijun Luo, and Christian Hartmann. Inter-cell interference mitigation through flexible resource reuse in ofdma based communication networks. In *European wireless*, pages 1–4, 2007.

[107] Mochan Yang, Oh-Soon Shin, Yoan Shin, and Hakseong Kim. Inter-cell interference management using multi-cell shared relay nodes in 3GPP LTE-Advanced networks. In *2013 IEEE Wireless Communications and Networking Conference (WCNC)*, pages 3579–3584, 2013.

[108] Jia You, Zhangdui Zhong, Rongtao Xu, and Gongpu Wang. Transmission schemes for high-speed railway: Direct or relay? In *2012 8th International Wireless Communications and Mobile Computing Conference (IWCMC)*, pages 1103–1107, Aug 2012.

[109] Yifei Yuan. *LTE-Advanced Relay Technology and Standardization*. Springer, 2013.

[110] Bin Zhang, Zhiqiang He, Kai Niu, and Li Zhang. Robust linear beamforming for mimo relay broadcast channel with limited feedback. *IEEE Signal Processing Letters*, 17(2):209 –212, feb. 2010.

[111] J. Zhang and J. G. Andrews. Adaptive spatial intercell interference cancellation in multicell wireless networks. *IEEE Journal on Selected Areas in Communications*, 28(9):1455–1468, Dec. 2010.

[112] Yi Zhao, R. Adve, and Teng Joon Lim. Symbol error rate of selection amplify-and-forward relay systems. *IEEE Communications Letters*, 10(11):757 –759, November 2006.